5-2012

Metabolic Regulation of mTOR Activation and Endoplasmic Reticulum Stress in the Heart

Shiraj Sen

METABOLIC REGULATION OF mTOR ACTIVATION AND ENDOPLASMIC RETICULUM STRESS IN THE HEART

by

Shiraj Sen, B.A.

APPROVED:

_____

Heinrich Taegtmeyer, M.D., D.Phil.

Supervisory Professor

_____

Michael Gambello, M.D., Ph.D.

_____

Teresa Davis, Ph.D.

_____

Russell Broaddus, M.D., Ph.D.

_____

Sandeep Agarwal, M.D., Ph.D.

_____

Aarif Khakoo, M.D., M.B.A.

APPROVED:

_____

George Stancel, Ph.D.

Dean, The University of Texas

Graduate School of Biomedical Sciences

METABOLIC REGULATION OF mTOR ACTIVATION AND ENDOPLASMIC RETICULUM STRESS IN THE HEART

A DISSERTATION

Presented to the Faculty of The University of Texas Health Science Center at Houston and University of Texas M.D. Anderson Cancer Center

Graduate School of Biomedical Sciences

in Partial Fulfillment

of the Requirements

for the Degree of

DOCTOR OF PHILOSOPHY

by

Shiraj Sen, B.A.

Houston, Texas

May, 2012

DEDICATION

This thesis is dedicated to my parents, whose love, guidance and sacrifice have provided me the opportunity to pursue every one my dreams.

ACKNOWLEDGMENTS

I would like to express my utmost gratitude to my research advisor Dr. Heinrich Taegtmeyer for the last ten years of mentorship. The summer after my sophomore year of college he first introduced me to both translational research and clinical cardiology and my excitement for both continues to grow even today. I thank the members of the lab, both past and present, for creating a friendly lab environment and sharing my excitement for cardiac metabolism. I am especially grateful to Patrick Guthrie for helping with experiments and providing endless laughter, without which I would not have pushed forward after each failed experiment 'bright eyed and bushy tailed'.

I thank the faculty of my advisory, examining and supervisory committees for their encouragement and constructive criticism throughout the duration of my project - Dr. Russell Broaddus, Dr. Sandeep Agarwal, Dr. Teresa Davis, Dr. Michael Gambello, Dr. Aarif Khakoo, Dr. Dos Sarbassov, and Dr. Ambro Van Hoof.

The work would have also not been possible without our lab's funding from the National Institute of Health (NIH) and American Medical Association (AMA) Foundation. I am also grateful to the Center for Clinical and Translational Sciences (CCTS) T32 training grant for both financial support as well as for guidance with professional development.

I am also grateful for the support I have received from my classmates and faculty mentors in the MD/PhD Program. I would like to especially thank the director of our program, Dr. Dianna Milewicz, for her leadership of the program as well as co-director

Dr. Russell Broaddus for his support and guidance throughout my training in the program.

Finally, I would not be the person I am today without the unconditional love and support of my parents, Subrata and Pramila Sen. Thank you for always believing in me, even during times when I did not believe in myself, and for teaching me the importance of passion, dedication, and sacrifice in order to achieve your goals. I am especially grateful to my younger sister, Parnali, whose friendship and warm, lively nature serves as a constant reminder of what life is really about no matter how much stress I am under.

METABOLIC REGULATION OF mTOR ACTIVATION AND ENDOPLASMIC RETICULUM STRESS IN THE HEART

Publication No. _____

Shiraj Sen, B.A.

Supervisory Professor: Heinrich Taegtmeyer, M.D., D.Phil

When subjected to increased workload, the heart responds metabolically by increasing its reliance on glucose and structurally by increasing the size of myocytes. Whether changes in metabolism regulate the structural remodeling process is unknown. A likely candidate for a link between metabolism and growth in the heart is the mammalian target of rapamycin (mTOR), which couples energy and nutrient metabolism to cell growth. Recently, sustained mTOR activation has also been implicated in the development of endoplasmic reticulum (ER) stress. We explored possible mechanisms by which acute metabolic changes in the hemodynamically stressed heart regulate mTOR activation, ER stress and cardiac function in the *ex vivo* isolated working rat heart. Doubling the heart's workload acutely increased rates of glucose uptake beyond rates of glucose oxidation. The concomitant increase in glucose 6-phosphate (G6P) was associated with mTOR activation, endoplasmic reticulum (ER) stress and impaired

contractile function. Both rapamycin and metformin restored glycolytic homeostasis, relieved ER stress and rescued contractile function. G6P and ER stress were also downregulated with mechanical unloading of failing human hearts. Taken together, the data support the hypothesis that metabolic remodeling precedes, triggers, and sustains structural remodeling of the heart and implicate a critical role for G6P in load-induced contractile dysfunction, mTOR activation and ER stress. In general terms, the intermediary metabolism of energy providing substrates provides signals for the onset and progression of hypertrophy and heart failure.

TABLE OF CONTENTS

DEDICATION…….…….....iii

ACKNOWLEDGMENTS…….……...…iv

ABSTRACT…….....vi

LIST OF FIGURES…….....xiii

LIST OF TABLES…….…….....xvi

LIST OF ABBREVIATIONS…….....xvii

CHAPTER 1: INTRODUCTION

1.1. Scope Of The Dissertation…….…….....2

1.2. Regulation Of Cardiac Metabolism……4

1.3. Structural and Functional Responses To Altered Hemodynamic Load…12

1.4. mTOR Signaling Pathway…….....18

1.5. Endoplasmic Reticulum Stress…….....23

CHAPTER 2: MATERIALS AND METHODS

2.1 Rationale For Methods Used…….....29

2.2 Materials…….....……30

2.2.1. Rodent Experiments

2.2.1.1. Mice…….....30

2.2.1.2. Rats……..….....31

2.2.2. Left Ventricular Tissue Samples From Heart Failure Patients…...33

2.2.3. Perfusion Apparatus For The Isolated Working Heart……...34

2.2.4. Liquid Scintillation Counter For Determination Of Radioactivity 35

2.2.5. Spectrophotometer For Assessment Of Intracellular Metabolite Content…….....37

2.2.6. Western Blotting Apparatus And Sources Of Antibodies….....37

2.2.7. Sequence Analyzer For Quantitatve RT-PCR……....38

2.2.8. Miscellaneous Equipment……...……38

2.3 Methods…….....39

2.3.1. PET And MRI Imaging…….....39

2.3.2. Isolated Working Rat Heart Perfusions……..……...…41

2.3.2.1. Perfusion Buffers And Protocols…..……..…….43

2.3.2.2. Determination Of Cardiac Power, Rates Of Glucose Uptake, Rates Of Glucose Oxidation…….…….…..46

2.3.3. Spectrophotometric Enzymatic Metabolite Analyses…….48

2.3.4. Western Immunoblotting……51

2.3.5. QRTPCR…….....52

2.3.6. Statistical Analysis……..….....55

CHAPTER 3: LOAD-INDUCED mTOR ACTIVATION IS MEDIATED BY CHANGES IN GLUCOSE METABOLISM

3.1 Introduction…….....57

3.2 Results…….....61

3.2.1. Metabolic Remodeling Precedes Structural Remodeling In Response to Increased Workload *In Vivo*…….61

3.2.2. Load-Induced mTOR Activation Requires Glucose……64

3.2.3. mTOR Activation Impairs Contractile Function At High Workload…….....68

3.2.4 Workload-dependent Mismatch Between Rates Of Glucose Uptake And Oxidation At High Workload……..…….70

3.2.5. Glucose 6-Phosphate Accumulates At High Workload as a Consequence of a Mismatch Between Rates of Glucose Uptake and Oxidation.....72

3.2.6. Accumulation Of Glucose 6-Phosphate Analogue 2-Deoxy-Glucose 6-Phosphate Activates mTOR……...….74

3.2.7. Glucose 6-Phosphate-dependent mTOR Activation is Mediated By Downregulation of AMPK…….…….76

3.2.8 Metformin Inhibits mTOR Activation and Rescues Contractile Function at High Workload…….…….78

3.2.9 Glucose Phosphorylation Modulates mTOR Activation *in vivo* (TAC and ACSL-/- mice) ……..……..…83

3.2.10 Mechanically unloading failing human hearts with LVAD reduces Glucose 6-Phosphate levels and mTOR Activation……86

3.3 Discussion…….....88

CHAPTER 4: SUSTAINED mTOR ACTIVATION INDUCES ER STRESS

4.1 Introduction…….....98

4.2 Results…….....100

4.2.1 Load-induced ER Stress Requires Glucose and mTOR Activation…….....100

4.2.2 Pretreatment with Rapamycin or Metformin Inhibits ER Stress and Prevents Contractile Dysfunction at High Workload…..…104

4.2.3 Markers of ER Stress are Downregulated in Failing Human Hearts Following Mechanical Unloading with LVAD……..…108

4.2.4 Role of Autophagy in G6P-mediated mTOR activation…..…..109

4.3 Discussion…….....110

4.4 Limitations of the Isolated Working Heart as a Model…….…….114

CHAPTER 5: CONCLUSIONS AND PERSPECTIVE……..……..…....116

BIBLIOGRAPHY…….…125

VITA……..……....…154

LIST OF FIGURES

Figure 1.1 Multiple metabolic fates of glucose……..……...…..8

Figure 1.2 Changes in glucose metabolism in the hypertrophied heart. ……...…11

Figure 1.3 Plasticity of the Heart. ……....…13

Figure 1.4 Components of an LVAD…….17

Figure 1.5 mTORC Signaling Pathway…….……21

Figure 1.6 Endoplasmic Reticulum (ER) Stress Response. ……..25

Figure 2.1 Modification of perfusion apparatus developed by Taegtmeyer, Hems and Krebs. ……36

Figure 2.2 Cannulation of the left atrium and aorta. ……..…43

Figure 2.3 Sample Standard Curve Used to Quantify mRNA Transcript levels of ER stress markers. ……...……55

Figure 3.1 Proposed activation of the mTOR signaling pathway by glucose……58

Figure 3.2 Metabolic remodeling precedes structural remodeling in hearts subjected to high workload *in vivo*. ……..…62

Figure 3.3 Functional changes accompany metabolic changes in response to high workload. ……..…64

Figure 3.4 In hearts subjected to high workload, glucose activates mTOR……...66

Figure 3.5 In the presence of mixed substrates, mTOR signaling is activated and G6P levels are elevated at high workload…….……...67

Figure 3.6 In hearts subjected to high workload, cardiac power is impaired when glucose is the only substrate. Rapamycin rescues contractile function…….69

Figure 3.7 Rates of glucose uptake exceed rates of glucose oxidation in response to high workload. Rapamycin corrects this mismatch……..71

Figure 3.8 G6P accumulates in response to high workload……...……73

Figure 3.9 Glucose analogues used in isolated working heart perfusions…….75

Figure 3.10 Increased phosphorylation of mTOR and p70S6K is associated with increased hexose 6-phosphate levels in hearts perfused with 2DG…….75

Figure 3.11 G6P-dependent mTOR activation is mediated by AMPK downregulation. …….……...…77

Figure 3.12 G6P-dependent mTOR activation is inhibited by metformin….……..79

Figure 3.13 Metformin treatment corrects the mismatch between rates of glucose uptake and oxidation at high workload and blunts G6P accumulation…80

Figure 3.14 Metformin treatment improves cardiac power at high workload…….81

Figure 3.15 Early metabolic changes are associated with G6P accumulation in hearts subjected to high workload *in vivo*…….....84

Figure 3.16 Early metabolic changes are associated with mTOR activation in hearts subjected to high workload *in vivo*……..….84

Figure 3.17 G6P accumulation correlates with mTOR activation in the ACSL -/- mouse. ……85

Figure 3.18 Mechanical Unloading of Failing Human Hearts Reduces G6P accumulation and mTOR activation……87

Figure 4.1 Hearts perfused with glucose at high workload show evidence for ER stress. ……102

Figure 4.2 Lactate release is unchanged with workload or rapamycin treatment in isolated working hearts perfused with glucose……..103

Figure 4.3 ER Stress is relieved with rapamyin, metformin, and PBA. Relief of ER stress improves contractile function in hearts perfused with glucose at high workload. ……..……105

Figure 4.4 Transcriptome analysis of stressed hearts treated with rapamycin, metformin, and phenylbutyrate……...…107

Figure 4.5 Mechanically unloading failing human hearts reduces markers of ER stress. ……108

Figure 4.6 Markers of autophagy are unchanged with rapamycin treatment in hearts stressed with an acute increase in workload……109

LIST OF TABLES

Table 1.1 Comparison of energy yields from various fuels per molecule oxidized. ……..…6

Table 2.1 Clinical Data for 11 Patients with Idiopathic Dilated Cardiomyopathy placed on Left Ventricular Assist Device (LVAD)……..…34

Table 2.2 *Ex vivo* perfusion protocols used to study glucose activation of mTOR signaling at high workload……45

Table 3.1 Levels of ATP, ADP, and AMP in *ex vivo* perfused hearts……..…82

LIST OF ABBREVIATIONS

2DG	2-Deoxy-Glucose
3OMG	3-O-Methyl-Glucose
4EBP1	4E-Binding Protein 1
AcAc+P	Acetoacetate + Propionate
ACC	Acetyl-CoA Carboxylase
ACE	Angiotensin Converting Enzyme
ACSL	Long-Chain Acyl Coenzyme A Synthetase
AMPK	5’ Adenosine Monophosphate Activated Kinase
ATF6	Activating Transcription Factor 6
ATP	Adenosine Triphosphate
BSL	Baseline
CHOP	CCAAT/Enhancer-Binding Protein Homologous Protein
DEPTOR	DEP-Domain-Containing mTOR-Interacting Protein
ECG	Electrocardigraphy
ECL	Enhanced Chemiluminescence

EDTA	Ethylenediaminetetraacetic acid
EDV	End Diastolic Volume
EGTA	Ethylene Glycol Tetraacetic Acid
EIF2	Eukaryotic Initiation Factor 2
ER	Endoplasmic Reticulum
ERP72	Endoplasmic Reticulum Protein 72
ESV	End Systolic Volume
G6P	Glucose 6-Phosphate
G6PD	Glucose 6-Phosphate Dehydrogenase
GAP	GTPase Activating Protein
GAPDH	Glyceraldehyde 3-Phosphate Dehydrogenase
GFAT	Glutamine:Fructose-6-Phosphate-Amidotransferase
Glc	Glucose
GLUT	Glucose Transporter
GRP	Glucose Regulated Protein
GS	Glutathione Synthase
GSH	Glutathione (reduced)

GSK	Glycogen Synthase Kinase
GSSG	Glutathione Disulfide (oxidized)
GTP	Guanosine Triphosphate
HK	Hexokinase
HOPE	Heart Outcomes Prevention Evaluation
HW/BW	Heart Weight/Body Weight
IGF	Insulin-like Growth Factor
IP	Intraperitoneal
IRE-1	Inositol Requiring Enzyme-1
JNK	c-Jun N-terminal Kinase
LDH	Lactate Dehydrogenase
LVAD	Left Ventricular Assist Device
LVEDD	Left Ventricular End Diastolic Dimension
LVEDV	Left Ventricular End Diastolic Volume
LVEF	Left Ventricular Ejection Fraction
LVESV	Left Ventricular End Systolic Volume
MCAD	Medium Chain Acyl Dehydrogenase

ME	Malic Enzyme
MF	Metformin
MK	Myokinase
MLST8	Mammalian Lethal with Sec13 Protein 8
MRI	Magnetic Resonance Imaging
mSIN1	mammalian Stress-Activated Protein Kinase-Interacting Protein
mTOR	mammalian Target Of Rapamycin
mW	Milliwatt
NADP	Nicotinamide Adenine Dinucleotide Phosphate
NCS	Noncarbohydrate Substrates
OGT	O-linked N-acetylglucosamine Transferase
OMC	Oxoglutarate-Malate Carrier
PBA	Phenylbutyrate
PCr	Phosphocreatine
PCR	Polymerase Chain Reaction
PDI	Protein Disulfide Isomerase
PDK	Pyruvate Dehydrogenase Kinase

PERK	PKR-like ER Kinase
PET	Positron Emission Tomography
PGI	Phosphoglucoisomerase
PI3K	Phosphotidylinositol 3-kinase
PK	Pyruvate Kinase
PKC	Protein Kinase C
PPAR	Peroxisome Proliferator Activated Receptor
PRAS40	Proline-Rich Akt Substrate 40 kDa
RAPTOR	Regulatory-Associated Protein Of mTOR
REMATCH	Randomized Evaluation of Mechanical Assistance for the Treatment of Congestive Heart Failure
RHEB	Ras Homolog Enriched in Brain
RICTOR	Raptor-Independent Companion of TOR
RNA	Ribonucleic Acid
SEM	Standard Error of the Mean
SERCA	Sarcoendoplasmic Reticulum Calcium ATPase
SGK	Serum Glucocorticoid Regulated Kinase
TAC	Transverse Aortic Constriction

TSC	Tuberous Sclerosis Complex
U	Units
XBP1	X-box Binding Protein

CHAPTER 1: INTRODUCTION

1.1 Scope of the Dissertation

This thesis addresses molecular mechanisms of heart failure. Why is this important?

First, heart failure is a leading cause of death in the United States (Roger, Go et al. 2011). While there is a decline in the incidence of coronary artery disease, we observe a relentless increase in mortality from heart failure. Nearly 5 million Americans suffer from heart failure. Each year over a million patients are hospitalized because of it and nearly 300,000 die from heart failure in the United States alone. Moreover, death from heart failure exceeds death from all forms of cancer combined (Roger, Go et al. 2011).

Secondly, despite many advances in cardiovascular medicine, current treatment has not seen a major drug since the advent of diuretics and neurohormonal antagonists. It is expected that the number of heart failure patients will double in the next five years. The development of heart failure is often preceded by cardiac growth manifested as the hypertrophy of the cardiomyocyte. Decompensated systolic heart failure is a loss of functional heart muscle in response to increased hemodynamic stress on the heart from hypertension, valvular heart disease, anemia, or prior myocardial infarction. However, the molecular mechanisms that drive the stressed heart to hypertrophy and ultimately fail or die remain incompletely understood.

Before the stressed heart progresses into failure, it undergoes a series of characteristic changes. The heart ‘remodels’ both metabolically and structurally. Metabolically, hearts augment glucose uptake and oxidation, and structurally, hearts

grow by underdoing hypertrophy. When stressed, the heart can increase its mass by up to 100% through hypertrophic remodeling (Hill and Olson 2008). Modulation of the remodeling process is recognized as a potentially auspicious approach in the prevention and treatment of heart failure.

The structural remodeling process has been studied extensively in an unbiased approach using microarray gene expression profiling. With this technology, key gene clusters involved in calcium handling proteins, sarcomeric proteins, mitochondrial proteins, cell death, inflammation, and the extracellular matrix have been identified (Steenman, Chen et al. 2003; Asakura and Kitakaze 2009). Unfortunately, strategies designed to prevent apoptotic cell death, inflammation, (Sandler and Dodge 1963) and excessive degradation of the extracellular matrix (Mann 1999) have yielded little therapeutic benefit. Therefore, a better understanding of the remodeling process is necessary to develop more effective treatment for heart failure.

The lab has previously demonstrated that metabolic remodeling precedes structural remodeling in the heart (Taegtmeyer and Overturf 1988) and proposed that, when stressed, metabolic remodeling (which is potentially reversible) regulates functional and structural remodeling (which may be irreversible) (Taegtmeyer, Golfman et al. 2004). I therefore set out to investigate whether the metabolic remodeling process regulates functional and structural changes that accompany cardiac growth and explore whether these changes are preventable.

The work presented in my dissertation provides evidence in support of the hypothesis that metabolic remodeling precedes, triggers, and sustains structural

remodeling of the heart. The rationale is based on the foundation that in all eukaryotic cells the target of rapamycin (TOR) signaling pathway couples energy and nutrient metabolism to the execution of cell growth (Sandler, Dodge et al. 1963). Specifically, I identify dysregulated glucose metabolism and subsequent G6P accumulation as mediators of load-induced mTOR activation, ER stress, and contractile dysfunction. The study highlights the importance of intermediary metabolism as a source of signals for cardiac growth and demonstrates the potential to reduce internal work and improve cardiac efficiency by targeting the metabolic axis in load-induced heart disease.

Understanding the mechanism and consequences of G6P-mediated mTOR activation will help identify novel metabolic targets to reverse contractile dysfunction in the hemodynamically stressed heart. Given the limitations of current heart failure treatment there is an urgent need for a more targeted approach to treating the early metabolic changes in the stressed heart. I propose that my project has taken an important step in this direction.

1.2 Regulation of Cardiac Metabolism

In order to fully appreciate the ability for metabolic signals to activate cardiac growth pathways, a brief review of the regulation of cardiac metabolism is needed. Like any organ in a living organism, the mammalian heart liberates energy contained in organic molecules to support its physiologic function (Holmes 1992). Critical steps are phosphorylation of ADP and subsequent hydrolysis of ATP. Rates of ATP turnover in

the heart are greater than rates of ATP turnover in any other organ, and so are the rates of substrate utilization and oxygen consumption (Taegtmeyer 1994). Hence, the need for early restoration of coronary blood flow in acute coronary syndrome and myocardial infarction.

Research on the metabolism of energy providing substrates for the heart began in a major way when Bing performed the first coronary sinus catheterization and identified fatty acids, glucose, and lactate as the major sources of fuel for the heart (Bing, Vandam et al. 1947). It was appreciated early on that the heart is a metabolic 'omnivore', i.e. an organ with that has the capacity to utilize multiple substrates in combination to support contractile function (Taegtmeyer 1994). Initially, by calculating oxygen extraction ratios and respiratory quotients (the ratio of the number of molecules of carbon dioxide produced per oxygen taken up for a given substrate), Bing showed that the heart in the fasted and unstressed state of the body oxidizes primarily fatty acids. Later, it was confirmed more precisely that indeed the normal mammalian heart generates 60-90% of its ATP from the oxidation of fatty acids and 10-40% from the oxidation of pyruvate by glycolysis and lactate oxidation (Bing, Siegel et al. 1954; Wisneski, Gertz et al. 1987). It has been reasoned that the healthy, unstressed heart preferentially metabolizes fatty acids because each molecule yields significantly more reducing equivalents (H), and hence ATP compared to glucose, lactate, or pyruvate **(Table 1.1)**.

Molecule	C per molecule	H per molecule	ATP yield per molecule	ATP yield per carbon atom	ATP yield per oxygen atom taken up (P/O ratio)
Glucose	6	12	38	6.3	3.17
Lactate	5	6	18	6.0	3.00
Pyruvate	5	4	15	5.0	3.00
Palmitate	16	32	130	8.1	2.83
Oleate	18	34	136	8.0	2.81

Table 1.1 Comparison of energy yields from various fuels per molecule oxidized. Adapted and expanded from The Heart: Physiology and Metabolism (Opie 1991, page 211).

While the unstressed heart primarily oxidizes fatty acids, the increased energy requirements of hearts subjected to high workload are met by the oxidation of carbohydrates (Goodwin, Taylor et al. 1998). A classic explanation for this phenomenon is based on the fact that the heart oxidizes the most efficient substrate for a given situation (Taegtmeyer, Hems et al. 1980). Despite the higher number of reducing equivalents per molecule, fatty acids are less oxygen-efficient (lower P/O ratio, see Table 1.1) and require up to 40% more oxygen to produce the same amount of ATP (Korvald, Elvenes et al. 2000). Because oxygen consumption increases linearly with workload in the heart, when oxygen becomes a limiting factor at high workload the heart preferentially oxidizes glycogen, glucose, and lactate (Goodwin, Taylor et al. 1998). Similarly, it has been proposed that the poorly oxygenated fetal heart also preferentially oxidizing glucose and lactate for this reason.

Our fundamental understanding of intermediary glucose metabolism started in 1860 with the identification of glycolysis by Pasteur (Holmes 1992). By 1937, the details of the glycolytic pathway were discovered by Embden and Meyerhof. Later that year,

Krebs and Johnson demonstrated that pyruvate formed succinate and closed the loop of the citric acid cycle (Krebs and Johnson 1937). Since then, investigators have discovered more and more of the complexity of intermediary glucose metabolism, the multiple metabolic fates of glucose, as well as the potential involvement of glucose in pathways that regulate intracellular signaling in the heart. These topics will now be briefly reviewed.

Glucose enters the cardiomyocyte down its concentration gradient from the coronary circulation by facilitated (or carrier-mediated) diffusion through glucose transporters (GLUT). The two major GLUTs in the heart include the insulin-independent GLUT1 transporter found on the sarcolemma and the insulin-dependent GLUT4 transporter, which is translocated to the sarcolemma in the presence of insulin. Increases in workload also promote glucose transporter translocation to the plasma membrane (Wheeler, Fell et al. 1994).

The bulk of glucose taken up by the cardiomyocyte and phosphorylated enters the glycolytic pathway and generates pyruvate, which is oxidized in the mitochondria via the Krebs cycle. The Krebs cycle provides the reducing equivalents for the formation of ATP under aerobic conditions. Glucose 6-phosphate can potentially enter a number of other pathways, as well, including glycolysis, glycogen synthesis pathway, pentose phosphate pathway, hexosamine biosynthetic pathway, and aldose reductase/polyol pathway **(Fig. 1.1)**. Glucose metabolism through these accessory pathways provides some energy, maintains the biological functions of the cardiomyocyte, and plays a role in intracellular cardiac growth signaling, as described below.

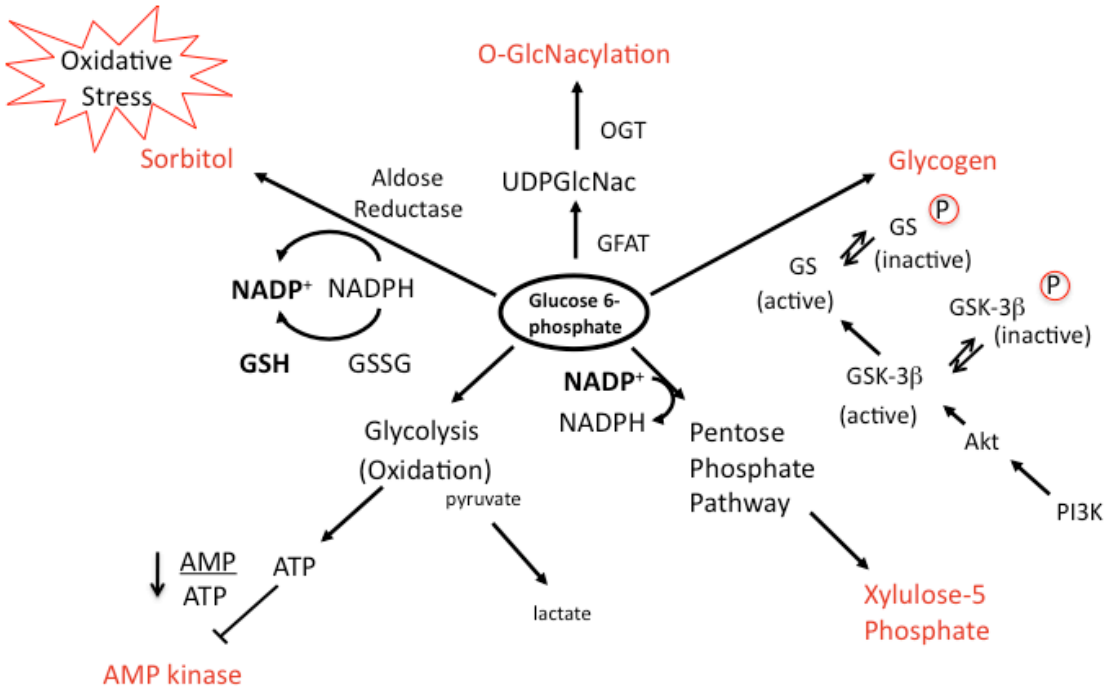

Figure 1.1 Multiple metabolic fates of glucose 6-phosphate. Upon entry into the cardiomyocyte, glucose can be metabolized through a number of different pathways. Many of these pathways have been demonstrated to regulate intracellular growth signaling either in the heart or in other organs.

Changes in the rate of glycolysis and glucose oxidation can modulate intracellular signaling pathways by altering levels of free ADP, AMP, and the PCr:ATP ratio in both the rodent and human heart (Neubauer 2007) (Nascimben, Ingwall et al. 2004). A hallmark of the failing heart is a reduction in the PCr:ATP ratio (Neubauer 2007), which is thought to contribute to the decline in contractile function accompanying heart failure. On a molecular level, a reduction of the [ATP]/[AMP] ratio is known to modulate the activity of AMP Kinase (AMPK), the 'metabolic fuel gauge' of the cell, which regulates metabolic enzymes, ion channels, gene expression, and intracellular signaling pathways of protein turnover through various phosphorylation events. Most

notably, AMPK phosphorylates ACC, reduces malonyl CoA, and increases fatty acid oxidation. AMPK phosphorylation also promotes glucose transporter translocation to the plasma membrane (Young, Li et al. 2005).

Although heart muscle lacks the enzyme glucose 6-phosphatase, glucose 6-phosphate (G6P) can undergo multiple metabolic fates **(Fig. 1.1)**. G6P can be converted into UDP-N-acetylglucosamine (UDPGlcNac) by the enzyme glutamine:fructose-6-phosphate-amidotransferase (GFAT), the rate-limiting enzyme of the *hexosamine biosynthetic pathway*. UDPGlcNac serves as the substrate for O-GlcNacylation of proteins by the enzyme O-GlcNac transferase (OGT). Like phosphorylation reactions, post-translational modification of proteins and transcription factors by O-GlcNacylation holds potential to regulate a number of intracellular signaling pathways (McClain 2002). Indeed, both gene expression of the rate limiting enzyme GFAT (Young, Yan et al. 2007) and O-linked –N-acetylglucosamine transferase are known to be elevated in mouse models of heart failure (Watson, Facundo et al. 2010).

The *pentose phosphate pathway* provides an additional avenue for glucose upon entry into the cardiomyocyte **(Fig 1.1)**. Our laboratory has previously demonstrated that up to 20% of glucose taken up by the heart enters the pentose phosphate pathway (Goodwin, Cohen et al. 2001). The pathway is divided into the oxidative and non-oxidative arms (Horecker and Mehler 1955). The oxidative arm consumes G 6-P using glucose 6-phosphate dehydrogenase (G6PD). The non-oxidative arm of the pentose phosphate pathway produces xylulose-5-phosphate, an important building block for nucleic acid synthesis but less well appreciated for its ability to induce the expression of metabolic genes in the liver such as pyruvate kinase (Nishimura and Uyeda 1995;

Doiron, Cuif et al. 1996). G6PD enzyme activity is upregulated in cardiac hypertrophy (Zimmer 1992). The significance of this may relate to increased ribose formation and/or modulation of oxidative stress.

G6P can also be enzymatically converted to *sorbitol* by aldose reductase with a concomitant decrease in NADPH, as well (Hwang, Kaneko et al. 2004). NADPH is a required cofactor for the regeneration of the reduced form of the anti-oxidant glutathione, and its depletion would exacerbate intracellular oxidative stress. Intracellular oxidative stress triggers a number of intracellular signaling pathways including those involved in growth signaling (Alexander, Cai et al. 2010). When present in excess, glucose is also converted to glycogen by the enzyme glycogen synthase. Glycogen synthase is phosphorylated by glycogen synthase kinase 3β (GSK-3β) which itself is a regulatory kinase that modulates cardiac growth (Haq, Choukroun et al. 2000). It is conceivable that this kinase plays a dual role in modulating both glucose metabolism in the heart and cardiac growth, as well. I will explore the role of intermediary glucose metabolites and assess whether these accessory pathways regulate cardiac growth in the stressed heart. Changes in glucose metabolism known to occur with cardiac hypertrophy are summarized in (**Fig. 1.2)**. Interestingly, the same changes are present in the unloaded, atrophied heart (Depre, Shipley et al. 1998) (Doenst, Goodwin et al. 2001).

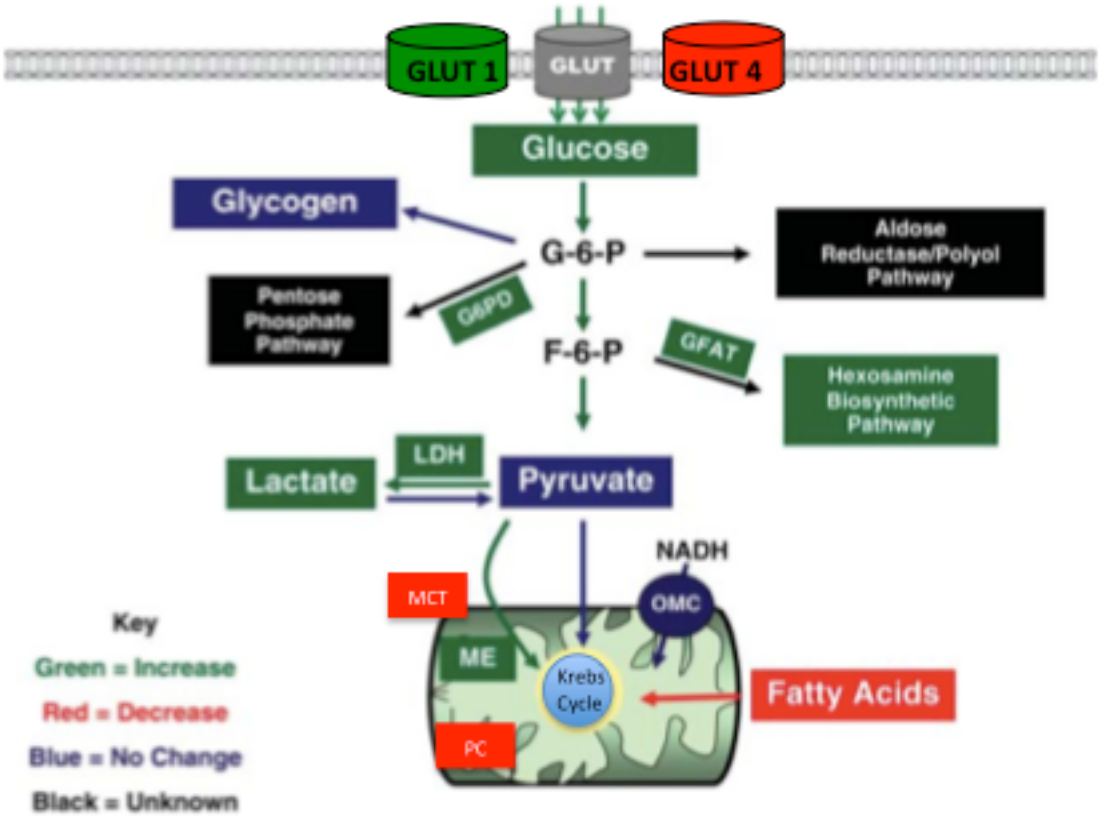

Figure 1.2 Changes in glucose metabolism in the pressure-overload induced hypertrophied heart. Pathways marked in green have been shown to increase, pathways marked in red have been shown to decrease, and pathways marked in blue have been shown to not change in the hypertrophied heart. Black arrows, boxes, and text represent pathways that have yet to be extensively studied in the hypertrophied heart. GFAT, glutamine fructose-6-phosphate amidotransferase; GLUT, glucose transporter; LDH, lactate dehydrogenase; ME, malic enzyme; NADH, reduced nicotinamide adenine dinucleotide; OMC, oxoglutarate-malate carrier; PC, pyruvate carboxylase; MCT, monocarboxylate transporter. Modified from Kolwicz and Tian *Cardiovascular Research* 2011. Reprinted with permission from Oxford University Press.

1.3 Structural and Functional Responses of the Heart to Altered Hemodynamic Load

Development of Cardiac Hypertrophy:

A wide variety of both physiological and pathological stimuli can promote cardiac growth. Physiological cardiac hypertrophy (growth) occurs during postnatal growth, pregnancy, and with prolonged vigorous exercise. Pathological cardiac hypertrophy is induced by cardiac injury, hypertension, or neurohormal stimulation **(Fig. 1.3)**. In the nineteenth century, cardiac growth was first thought to merely represent a step in the development of heart failure when Sir William Osler characterized it as a phenomenon that *"takes place slowly and results from degeneration and weakening of the heart muscle"* (page 98). (Osler W. The Principles and Practice of Medicine. New York: Appleton, 1892.)

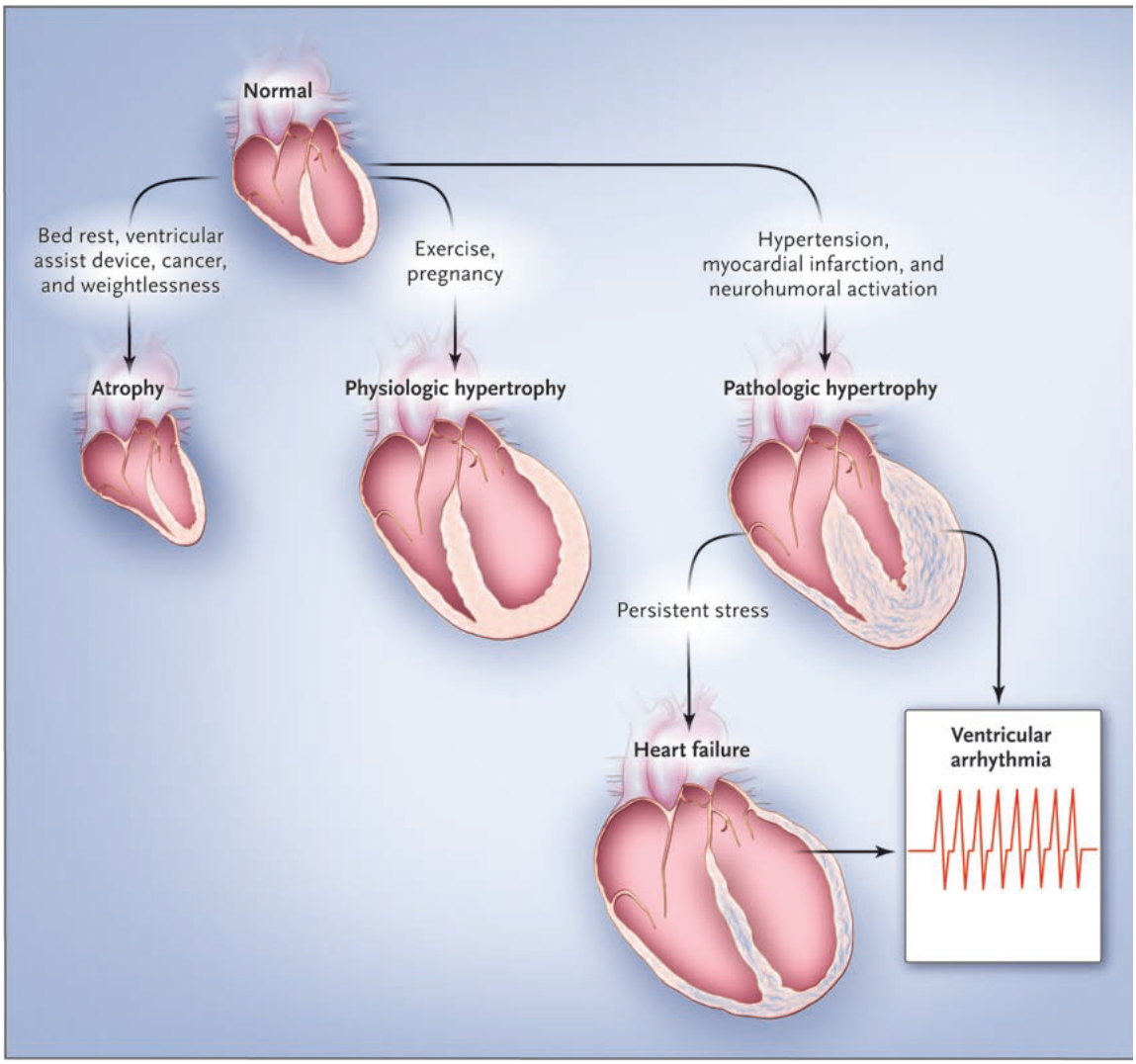

Figure 1.3 Plasticity of the Heart. The healthy human heart structurally remodels in response to both increases and decreases in load. A reduction in load leads to atrophy and an increase in load leads to hypertrophy. Sustained increases in pathological load are known to lead to heart failure and ventricular arrythmias (Hill and Olsen, NEJM 2008). Reprinted with permission from Massachusetts Medical Society.

Nearly a century later, data from the Framingham Heart Study recognized left ventricular hypertrophy as a true risk factor for heart failure and arrhythmias (Levy, Garrison et al. 1990; Koren, Devereux et al. 1991). Why does it occur? According to the law of LaPlace:

wall tension = (pressure) x (radius)/(wall thickness)

Accordingly, increased wall thickness in the heart reduces ventricular wall tension in hearts subjected to high workload (Sandler and Dodge 1963; Grossman, Jones et al. 1975). However, cardiac hypertrophy secondary to valvular heart disease is associated with contractile dysfunction irrespective of the degree of valvular damage (Gunther and Grossman 1979) (Huber, Grimm et al. 1981) (Krayenbuehl, Hess et al. 1988) suggesting that its development may not follow as linear of a pattern as the law of LaPlace would suggest. Is hypertrophy necessary to compensate for increased cardiac work? In preclinical studies, contractile function is preserved in hearts subjected to high workload and treated with small molecular inhibitors of intracellular growth signaling pathways (Hill, Karimi et al. 2000), suggesting that cardiac growth may not be necessary. It remains difficult to ascertain whether cardiac growth is initially a necessary adaptive response in the stressed heart or not.

On a molecular level, the heart has different mechanisms to respond to acute and sustained increases in hemodynamic load. When subjected to an acute increase in workload, changes in cardiac metabolism occur instantaneously, as discussed above. Similarly, even acute changes in workload trigger changes in the post-translational modification of proteins, as well. Most notably, increased workload regulates the activation of membrane-bound receptors such as G-protein coupled receptors leading to downstream changes in the protein phosphorylation and activation of growth signaling pathways (Molkentin and Dorn 2001). Ultimately, sustained increases in workload and activation of these signaling pathways lead to changes in gene expression. Previous members of the lab have reviewed the transcriptional changes in metabolic genes

(GLUT1, GLUT4, PPAR-alpha,PDK2, MCAD, ACC) and contractile protein (myosin heavy chain) isoforms, in the stressed heart (Rajabi, Kassiotis et al. 2007).

Modulation of myocardial growth and hypertrophy without adversely affecting contractile function is increasingly recognized as a potentially auspicious approach in the prevention and treatment of heart failure. A better understanding of the intracellular signaling cascades that drive the hypertrophic process are necessary before this will be possible. This begs the question: which signals and intracellular signaling pathways drive the normal heart to hypertrophy and ultimately fail? Can they be targeted? Molkentin *et al* have extensively reviewed the highly coordinated manner by which a number of signaling cascades interact to regulate cardiac growth signaling (Molkentin and Dorn 2001; Dorn and Force 2005). However, only the mammalian target of rapamycin (mTOR) signaling pathway is known to be both activated in the heart in response to increased workload and responsive to changes in a cell's metabolic milieu. I, therefore, focused our attention on studying whether the metabolic changes known to occur in hearts subjected to increased workload regulate mTOR activation in the stressed heart.

Regression of Cardiac Hypertrophy:

A number of studies have demonstrated that regression of left ventricular hypertrophy improves outcome in patients with cardiovascular disease. In the Heart Outcomes Prevention Evaluation (HOPE) trial, patients with either known high-risk vascular disease or diabetes and at least one additional cardiovascular risk factor

(hypertension, dyslipidemia, cigarette use, microalbuminuria) were randomly assigned to receive either an angiotensin converting enzyme (ACE) inhibitor or placebo daily for 2.5 years (Yusuf, Sleight et al. 2000). Up to a decade later, analyses from the study identified that inhibition or even regression of cardiac hypertrophy by ACE inhibitor therapy lowered the risk for several cardiovascular endpoints including death and progression to heart failure, whereas persistence of cardiac hypertrophy (despite similar blood pressure changes) predicted an adverse outcome (Mathew, Sleight et al. 2001).

Mechanical reduction of load in patients with heart failure also improves cardiovascular hemodynamics, functional status, and quality of life. In the Randomized Evaluation of Mechanical Assistance for the Treatment of Congestive Heart Failure (REMATCH) study, patients with New York Heart Association Class III or IV heart failure were randomized to either optimal medical management or implantation of a left ventricular device (Rose, Gelijns et al. 2001) **(Fig. 1.4)**. At the time of final analysis, LVAD implantation was associated with a forty eight percent reduction in the risk of death from any cause and improvement in quality of life compared to optimal medical therapy.

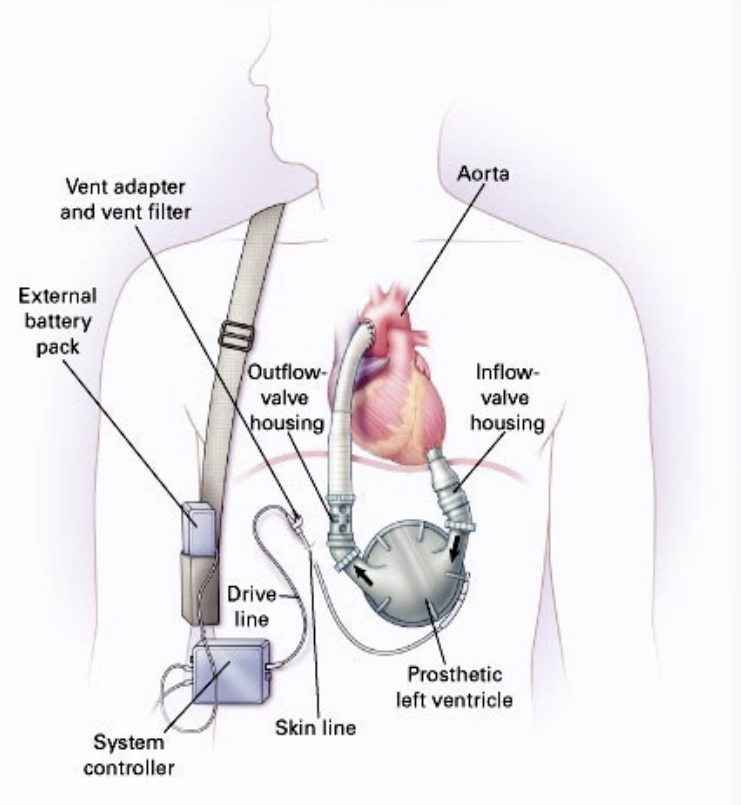

Figure 1.4 Components of an LVAD. The LVAD mechanically reduces the load on failing heart. Circulating blood enters the LVAD from the left ventricle through the inflow cannula. The prosthetic left ventricular then pumps the blood through the outflow cannula and into the (ascending) aorta. The pumping chamber is placed within the abdominal wall or peritoneal cavity. A percutaneous drive exits the skin and connects the device to external battery packs worn on shoulder holsters and a system controller worn on the belt. Image reprinted with permission from Massachusetts Medical Society (Rose, Gelijns et al. 2001).

The effects of LVAD implantation on cardiac metabolism have been investigated extensively at the transcriptional and post-translatoinal levels (Razeghi, Myers et al. 2002) (Margulies, Matiwala et al. 2005). Previous studies in our lab have observed a trend for decreased myocardial glycogen content in failing human hearts after mechanical unloading (Razeghi and Taegtmeyer 2004) and more recently, proteomic analysis has revealed an upregulation of proteins involved in glycolysis, energy, and

oxidative metabolism in LVAD supported patients.(de Weger, Schipper et al. 2011) Taken together, these data suggest improved metabolic capacity with mechanical unloading with LVAD implantation. This conclusion is supported by reports that have suggested improvements in respiratory capacity in mitochondrial isolated from hearts of patients supported by an LVAD (Lee, Doliba et al. 1998).

1.4 mTOR Signaling Pathway

In mammalian tissue, mTOR links nutrient availability to growth in muscle, adipose, liver, and hypothalamus (Howell and Manning 2011). Cardiac growth can occur directly in response to nutrient availability in the Burmese python, which exhibits a 40% increase in ventricular mass within 48 hours of consuming a large meal (Andersen, Rourke et al. 2005; Riquelme, Magida et al. 2011) and I therefore wondered whether it occurs in the stressed heart in an mTOR-dependent manner, as well.

Load-induced protein synthesis and cardiac growth is regulated mTOR, a highly conserved member of the phosphatidylinositol 3 kinase (PI3 kinase) superfamily that regulates cell growth by initiating protein translation and by inducing ribosomal biogenesis (Crespo and Hall 2002) (Rohde, Heitman et al. 2001). Research on mTOR began when the drug rapamycin, an inhibitor of T cell proliferation and potent immunosuppressant, was serendipitously isolated from a strain of *Streptomyces hygroscopius* from soil collected in Rapa-Nui (Easter Island) in the 1970's (Crespo and Hall 2002). Rapamycin is now an FDA-approved immunosuppressant for preventing

graft rejection or re-stenosis after angioplasty, and rapamycin is actively being used in a number of cancer clinical trials to reduce tumor growth (Garza, Aude et al. 2002) (Huang and Houghton 2003). Whether in fungi, T-cells, vascular smooth muscle or cancer cells, the primary action of rapamycin is inhibition of cell growth. The protein responsible for rapamycin action was first identified in yeast and called TOR (target of rapamycin) (Kunz, Henriquez et al. 1993). By analyzing gene expression in yeast cells exposed to rapamycin, it was discovered that TOR mediates protein synthesis and was regulated by nutrient availability in yeast (Cardenas, Cutler et al. 1999). Indeed, in eukaryotic organisms the ability to alter growth according to nutrient availability is essential for survival.

Studies undertaken to elucidate the mechanism by which rapamycin inhibits mTOR revealed that the mTOR kinase actually nucleates two major protein complexes – mTOR complex 1 (mTORC1) and mTOR complex 2 (mTORC2) (Schmelzle and Hall 2000). mTOR complex 1 (mTORC1) contains the scaffolding protein regulatory-associated protein of mTOR (raptor) as well as mammalian lethal with Sec13 protein 8 (mLST8), the proline-rich Akt substrate 40 kDa (PRAS40), and DEP-domain-containing mTOR-interacting protein (Deptor) and regulates cell growth. mTOR complex (mTORC2) consists of mLST8, the scaffolding protein raptor-independent companion of TOR (rictor), mSIN1 proteins, and the protein observed with rictor (Protor) and cytoskeleton regulation and cell survival (Laplante and Sabatini 2009). The components of each respective protein complex are necessary for either upstream regulation, complex formation, or downstream signal activation and function. Most notably, however, mTORC2 is distinguished from mTORC1 by its resistance to inhibition with

acute rapamycin treatment (Sarbassov, Ali et al. 2006). In fact, only prolonged rapamycin treatment (an important consideration for my experiments, see Chapter 3) inhibits mTORC2 complex assembly and reduces the levels of mTORC2 below those needed to maintain downstream Akt signaling both *in vitro* (Sarbassov, Ali et al. 2006), and in samples from patients with acute myeloid leukemia (Zeng, Sarbassov dos et al. 2007) **(Fig. 1.5)**. mTORC2 is also known to activate PKCalpha to regulate actin reorganization and SGK1 to regulate FOXO (Powell and Delgoffe 2010), however the regulation of these proteins by rapamycin has yet to be studied. Our insight into upstream activators of mTORC2 is limited, as well. However, a wealth of information exists on both upstream activators of mTORC1 and downstream consequences, which will now be reviewed.

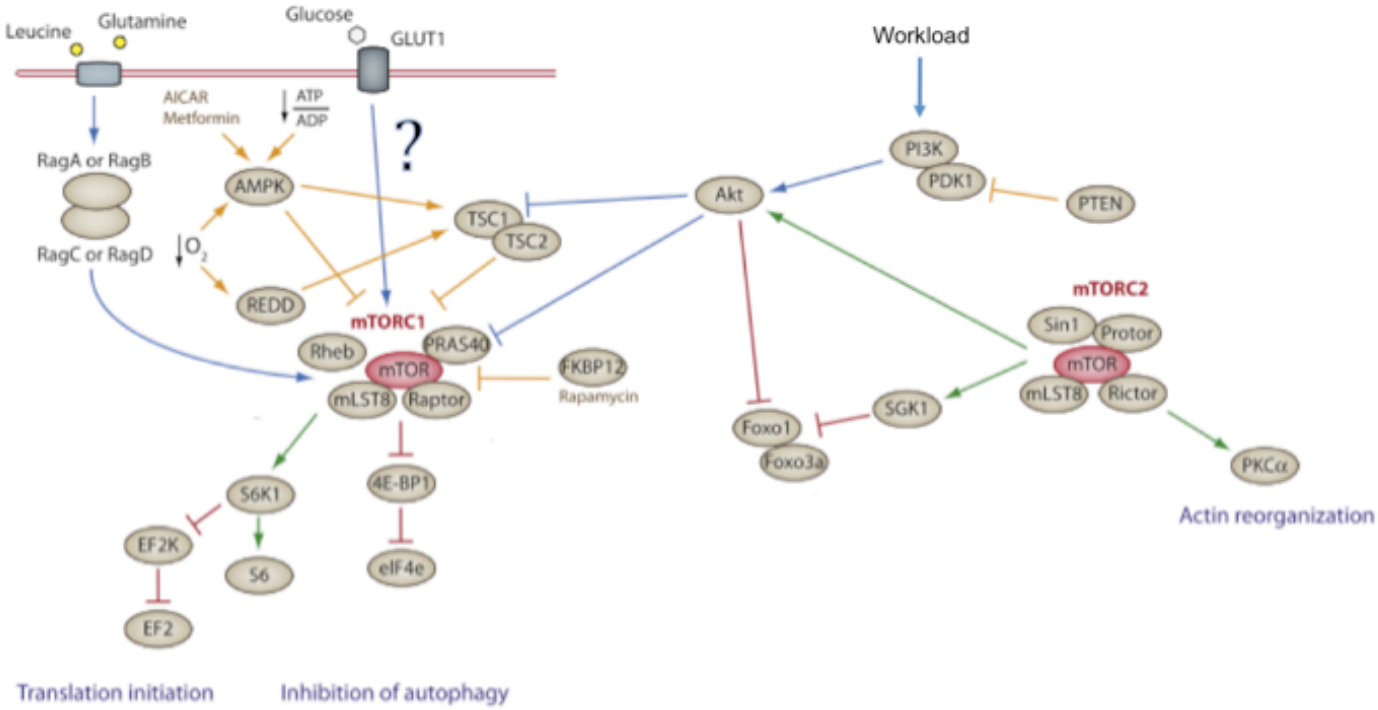

Figure 1.5 mTORC Signaling Pathway. mTORC1 is activated by a number of upstream activators (leucine, glutamine, glucose, workload). Adapted from Powell, Delgoffe *et al.* Immunity 2010. Reprinted with permission from Elsevier Publishing Company.

In the unstressed heart, mTOR and its downstream targets, 4EBP1 and p70S6K (S6K1), are inhibited by the upstream protein Ras homolog enriched in brain (Rheb). Rheb is a small GTPase that requires binding of GTP to interact with and activate mTOR (Long, Ortiz-Vega et al. 2005). Upstream of Rheb is the tuberous sclerosis complex (TSC), which is composed of the proteins TSC1 and TSC2 (Inoki, Corradetti et al. 2005). TSC2 is the GTPase-activating protein (GAP) for Rheb and when bound by TSC1, it promotes the conversion of Rheb-GTP to Rheb-GDP, thereby inhibiting mTOR (Inoki, Li et al. 2003). Therefore, differential phosphorylation of TSC2 regulates mTORC1 activation (Huang and Manning 2008).

Growth factors, branched chain amino acids, reactive oxygen species (ROS), and genotoxic stress are all upstream regulators of mTORC1 (Sengupta, Peterson et al. 2010). Growth factors such as insulin and IGF-1 activate mTORC1 by differentially phosphorylating TSC2 to suppress its GAP activity on Rheb in a PI3K-dependent manner (Tee, Anjum et al. 2003) and amino acids activate mTORC1 by promoting mTOR interaction with lysosomal Rheb-GTP (Sancak, Peterson et al. 2008) (Sancak, Bar-Peled et al. 2010) whereas ROS and genotoxic stress inhibit mTOR by stabilizing the TSC complex and TSC2's GAP activity on Rheb (Budanov and Karin 2008; Alexander, Cai et al. 2010). I, therefore, felt it was plausible that metabolic regulation of mTOR activation in the heart also occurred in a TSC or Rheb-dependent manner.

1.5 Endoplasmic Reticulum Stress

A consequence of sustained activation of mTOR is increased and uncontrolled protein synthesis leading to endoplasmic reticulum (ER) stress. In the unstressed cardiomyocyte, proteins synthesized in the rough endoplasmic reticulum are efficiently folded. Molecular chaperones located within the ER facilitate this process by identifying hydrophobic regions of misfolded or unfolded proteins and refolding them into functioning proteins in order to prevent toxic protein aggregate formation (Ron and Walter 2007). The chaperone protein glucose-regulated protein 78 (GRP78) also serves as a gauge for sensing protein homeostasis within the endoplasmic reticulum. When the concentration of misfolded or unfolded proteins is low, GRP78 remains bound to the three ER proximal effectors – PKR-like ER kinase (PERK), insolitol-requiring enzyme-1 (IRE-1), and activating transcription factor-6 (ATF6). When bound by GRP78, these proximal effectors remain inactive. When subjected to hemodynamic stress (continued pumping against high workload), mTOR activation promotes cardiac growth by increasing rates of protein synthesis. Up to one third of all proteins synthesized in the cardiomyocyte are shuttled through the endoplasmic reticulum (Blobel 2000). When hypertrophic stimuli are sustained, rates of protein synthesis exceed the protein folding capacity of the ER leading to the accumulation of unfolded and misfolded proteins beyond the ER's capacity to cope with the load (Okada, Minamino et al. 2004; Glembotski 2008). The hydrophobic regions of unfolded and misfolded proteins attract GRP78. GRP78 translocation from the luminal surface of IRE-1, ATF6, and PERK activates all three proximal effectors. One of the earliest consequences of proximal

effector activation is the transcriptional activation of ER stress-response genes including chaperone proteins (GRP78, GRP94), disulfide isomerases (ER protein 72, ERp72), and calcium binding proteins (calreticulin). Interestingly, the promoter site of most ER stress response genes has an ER stress response element, suggesting that transcriptional induction is highly conserved (Thuerauf, Hoover et al. 2001). Increased expression of these genes enhances the protein folding capacity of the ER. Moreover, if its transcriptional activation is sufficient to alleviate the acute increase in ER stress, excess GRP78 once again binds the proximal effectors and signals the resolution of the ER stress response.

In both human and animal studies, contractile dysfunction in the hypertrophic and failing heart has been linked to elevated glucose uptake (Taegtmeyer and Overturf 1988) (Zhang, Duncker et al. 1995) (Bishop and Altschuld 1970) in an insulin-independent manner (Allard, Wambolt et al. 2000). It is also known that normal contractile function of the cardiomyocyte requires proper protein folding. However, whether elevated glucose uptake is associated with contractile dysfunction in hearts subjected to high workload as a result of improper protein folding has yet to be studied.

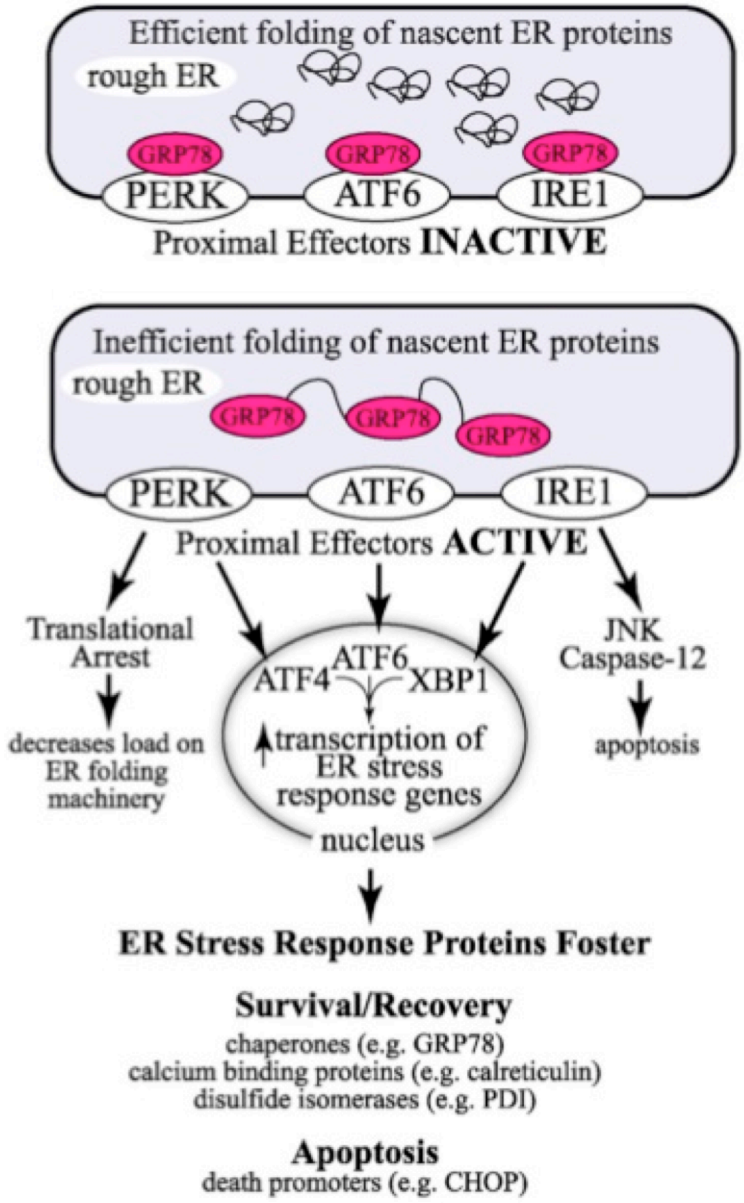

Figure 1.6 Endoplasmic Reticulum (ER) Stress Response. When the protein folding capacity of the ER is exceeded, the ER stress response is activated. Adapted from Glembotski JMCC 2008. Reprinted with permission from Elsevier Publishing Company.

If the ER stress response is sustained, PERK activation inhibits the activation of the protein translational machinery via the phosphorylation of eukaryotic initiation factor 2 α (eIF2α) and IRE1 activation ultimately leads to apoptosis via the activation of JNK and caspase-12.

Ischemia is a known activator of the ER stress response. Mouse hearts subjected to ischemia and reperfusion *ex vivo* demonstrate increased GRP78 expression as do myocytes surrounding the infarct zone in mice subjected to myocardial infarction *in vivo* (Thuerauf, Marcinko et al. 2006). The mechanism is thought to involve AMPK activation (Terai, Hiramoto et al. 2005) and lead to the activation of autophagy-mediated cell death (Takagi, Matsui et al. 2007). The ER stress response is also activated in hypertrophied and failing mouse hearts that have been subjected to increased workload by transverse aortic constriction (Okada, Minamino et al. 2004). Whether load-induced mTOR activation, ER stress and contractile dysfunction are metabolically regulated in the heart remains unknown.

Systemic metabolic disorders such as diabetes are associated with ER stress in skeletal muscle, liver, and adipocytes (Hotamisligil 2010) (Eizirik, Cardozo et al. 2008). Indeed, changes in glucose or fatty acid metabolism *in vitro* regulate the ER stress response. Whether changes in cardiac metabolism regulate (or are regulated by) ER stress remain to be investigated. Because chemical chaperone treatment has been shown to alleviate ER stress and correct glucose homeostasis in mouse models of diabetes

(Ozcan, Yilmaz et al. 2006), it is plausible that it holds great promise in targeting heart disease, as well.

The consequences of ER stress on cardiac function and metabolism form the second part of my thesis. They have led us to speculate that relief of ER stress improves metabolism and efficiency of the heart.

CHAPTER 2: MATERIALS AND METHODS

2.1 Rationale for Methods Used and Overall Strategy

The structural and functional response to increased workload has been extensively studied in the murine transverse aortic constriction (TAC) model (Rockman, Ross et al. 1991). How the metabolic responses to increased workload may regulate these changes has yet to be investigated. In order to answer this question systematically we used three different models – C57BL/6J mouse hearts subjected to increased workload *in vivo* by TAC, Sprague-Dawley rat hearts subjected to increased workload *ex vivo* using the isolated working heart apparatus, and left ventricular tissue samples from human heart failure patients before and after implantation of a left ventricular assist device (LVAD).

First, in studies initiated in the laboratory of our collaborator Bijoy Kundu at the University of Virginia Medical School, *in vivo* FDG-PET and MRI were performed simultaneously in mice subjected to TAC for upto four weeks to serially image changes in metabolism, structure and function in response to increased cardiac workload. Using this model, it was established that metabolic remodeling (enhanced glucose uptake) and contractile dysfunction precede structural remodeling (growth and dilation of the left ventricle) of the heart when subjected to increased workload. Second, we systematically manipulated workload and substrate supply individually used the isolated working rat heart *ex vivo* to elucidate the mechanisms for the observed phenomena *in vivo*. The isolated working rat heart permitted a dynamic minute-by-minute assessment of metabolism and function and allowed for assessment of intracellular metabolites and activation of relevant signaling pathways at the end of the perfusion. The *ex vivo* isolated

working heart model was also chosen because it gave us complete control over workload, substrate concentration and hormone supply. Third, we analyzed left ventricular tissue from failing human heart muscle before and after mechanical unloading with a left ventricular assist device to correlate our findings to the failing human heart, as well. Thus, in contrast to the prevailing strategies (from the bedside to the bench) we went from the bench to the bedside to test whether findings in *ex vivo* models are relevant for the failing heart *in vivo*. The following materials and methods were required to carry out these studies.

2.2 Materials

2.2.1 Rodent Experiments

2.2.1.1 Mice

For our *in vivo* imaging studies, male C57BL/6J mice (8-9 weeks of age) obtained from Charles River Laboratories (Raleigh, NC) were subjected to sham operation or transverse aortic constriction (TAC) to induce pressure-overload hypertrophy by our collaborators at The University of Virginia Medical School using methods previously described (Liao, Takashima et al. 2003). During each imaging protocol, left ventricular pressure measurements were performed using a Mikro-tip Catheter Transducer (Model SPR-671, Size 1.4F, Millar Instruments Inc., Houston, TX) connected to Millar and PowerLab hardware and ADI Software (AD Instruments Inc.,

Colorado Springs, CO). Throughout the experiment heart rate, respiration, and body temperature were recorded with a physiological recorder (SA Instruments, Inc., model 1025L, Stony Brook, NY), and the ECG were monitored (Blue Sensor, Ambu Inc., Glen Burnie, MD) and stored for further analysis later. The SAI 1025L was also used to maintain the animal's core body temperature at 37^{o}C. Positron Emission Tomography (PET) with the fluorinated glucose tracer analogue 2-deoxy-2-[^{18}F] fluoro-D-glucose and Magnetic Resonance Imaging (MRI) were sequentially performed in anesthetized animals. PET imaging was performed in a Focus 120 micro PET scanner (Siemens Molecular Imaging Inc., Knoxville, TN) to assess changes in metabolism. 150-200 μL of 18.5-37 MBq FDG solution (IBA Molecular, Sterling VA) was injected intravenously into the mice over a period of one minute prior to imaging. Arterial blood samples were used for input function estimation. Mice were also imaged using a 7T Bruker-Siemens Clinscan MRI system for structural and functional analyses of the heart. The MR images were analyzed using the ARGUS software package (Siemens Medical Systems, Erlangen, Germany) for left ventricular end systolic volume (LVESV) and left ventricular end diastolic volume (LVEDV) while left ventricular ejection fraction (LVEF) was computed from the traced borders.

2.2.1.2 Rats

For our *ex vivo* studies, male Sprague-Dawley rats (387 ± 11g) were obtained from Harlan Laboratories (Indianapolis, IN) and housed in the Animal Care Center of The University of Texas Medical School at Houston under controlled conditions (23 ±

1°C; 12-h light/12-h dark cycle) prior to experimentation. The animals received standard laboratory chow (LabDiet® Rodent Diet 5001 containing as a percentage of total calories: 28 % protein, 60 % carbohydrate and 12 % fats) and water *ad libitum* and were given at least 48 hours to acclimatize to the facility before they were used in experiments.

Through the course of this project, two subsets of rats received pharmacological agents before they were sacrificed. The first subset of rats received either the mTOR inhibitor rapamycin (4 mg/kg/d) or vehicle control (propylene glycol) by oral gavage for 7 days prior to the experiments. We have previously shown that the timing, dose, and delivery of the drug is effective in inhibiting mTOR in the heart (Sharma, Guthrie et al. 2007). The second subset received either metformin (250 mg/kg/day or 500 mg/kg/day) or vehicle control (saline) intraperitoneally for 7 days prior to sacrifice. Others have shown before us that the delivery of metformin by IP injection activates AMPK in the heart (Gundewar, Calvert et al. 2009; Benes, Kazdova et al. 2011). Prior to perfusion, all animals were anesthetized with chloral hydrate (300 mg/kg/kg).

Reflexes were tested in all four limbs prior to incision to ensure sufficient sedation. A midline incision was then made to each animal and heparin (200U) was injected directly into the inferior vena cava immediately before opening the thoracic cavity to ensure proper anticoagulation. Hearts were then quickly removed and transferred into ice-cold saline. After cannulation, hearts were perfused in the working mode as described before (Taegtmeyer, Hems et al. 1980) and as will be described later.

At the conclusion of each perfusion protocol, hearts were freeze-clamped while

still beating with aluminum tongs cooled in liquid nitrogen (Wollenberger and Schulze 1961). A portion of frozen heart tissue was used for dry weight calculations and the remainder used for molecular analyses.

2.2.2. Left Ventricular Tissue Samples from Heart Failure Patients

Myocardial biopsy samples were obtained from the hearts of 11 non-diabetic patients with idiopathic dilated cardiomyopathy referred to the Texas Heart Institute (Dr. O.H. Frazier) for heart transplantation at the time of placement of left ventricular assist device (LVAD) and at the time of removal after a mean duration of 254±63 days on mechanical support. **Table 2.1** provides further details on the patients assessed in this study. Because mTOR is known to be activated by insulin and many diabetic patients are hyperinsulinemic, only non-diabetic patients were studied. A reduction in LVEDD in each patient was used to confirm unloading.

Tissue from the left ventricular apex was obtained during LVAD implantation and again *from the same heart* during explantation when each patient received a heart transplant. Tissue samples were immediately frozen in liquid nitrogen and stored at -80^{o}C for metabolic and molecular analyses.

Gender	10 males, 1 female
Ethnicity	5 Caucasian, 5 African-American, 1 Hispanic
Age	48±4 years (range, 19-67)
LVEDD before LVAD	75.33±4.40 mm
LVEDD after LVAD	55.67+±3.22 mm
EF before LVAD	19%
Duration of LVAD	254±63 days

Table 2.1 Clinical Data for 11 Patients with Idiopathic Dilated Cardiomyopathy. Abbreviations: LVAD = left ventricular assist device, LVEDD = left ventricular end diastolic dimension, EF = ejection fraction. Data are presented as the mean ± SEM.

2.2.3. Perfusion Apparatus for the Isolated Working Heart

The perfusion apparatus used in this project was nearly identical to the one previously described (Taegtmeyer, Hems et al. 1980). In a modification of the method developed by Taegtmeyer *et al*., in this project the apparatus was assembled in the non-recirculating mode to prevent the accumulation of lactate, the end product of glycolysis and a carbohydrate substrate that would confound our data.

The glassware used to assemble the perfusion apparatus was designed by Dr. Heinrich Taegtmeyer and made by Mr. Peter Brooks (Ducklington, Oxon, England). The apparatus **(Fig. 2.1)** consisted of (a) A reservoir containing fresh perfusate, (b) Watson Marlow 505S peristaltic pump (Watson Marlow Wilmington, MA), which circulated the perfusate through the apparatus, (c) 5 μm Millipore filter (Millipore Billerica, MA),

which filtered out any debris that may have precipitated out of the perfusate, (d) multi-bulb oxygenator (connected to an external oxygen tank) (e) oxygen sensor, (f) perfusion chamber, which housed the cannulated heart, (g) compliance chamber, (h) aortic overflow reservoir, (i) coronary overflow reservoir, (j) Langendorff reservoir, and (k) reservoir for metabolized perfusate. Each piece of glassware was taken down, disconnected from its tubing and submerged in Chromerge (Sigma Aldrich, St Louis, MO) at the end of the day daily to prevent protein and bacterial contamination of the glassware (Fanburg, Posner Biochim Biophys Acta1969) **(Fig. 2.1)**.

The glassware was water-jacketed and circulated with water in the opposite direction of the perfusate at a constant temperature of 37^{o} by a C10 immersion circulator (Haake GmbH, Karlsruhe, Germany). The water temperature was measured using a YSI Tele-thermometer (YSI, Yellow Springs, Ohio). The perfusate circulated between pieces of glassware through PVC tubing (VWR, West Chester, PA), which was replaced daily. The PVC tubing and glassware were flushed out with 4L of ddH_2O in between experiments.

Aortic pressures were continuously registered throughout each perfusion with a Millar Mikro-Tip Catheter Transducer (Model #SPR-524, size 2.5F) attached to a Millar Transducer Balance, model TBC-500 (Millar Instruments Co, Houston, TX). The signal was transmitted to a MacLab/4e AD instrument and recorded, stored, and analyzed using MacLab software, chart v3.3.5 (AD Instruments Inc., Colorado Springs, CO). The following parameters were recorded: heart rate, systolic and diastolic pressures, and mean aortic pressure.

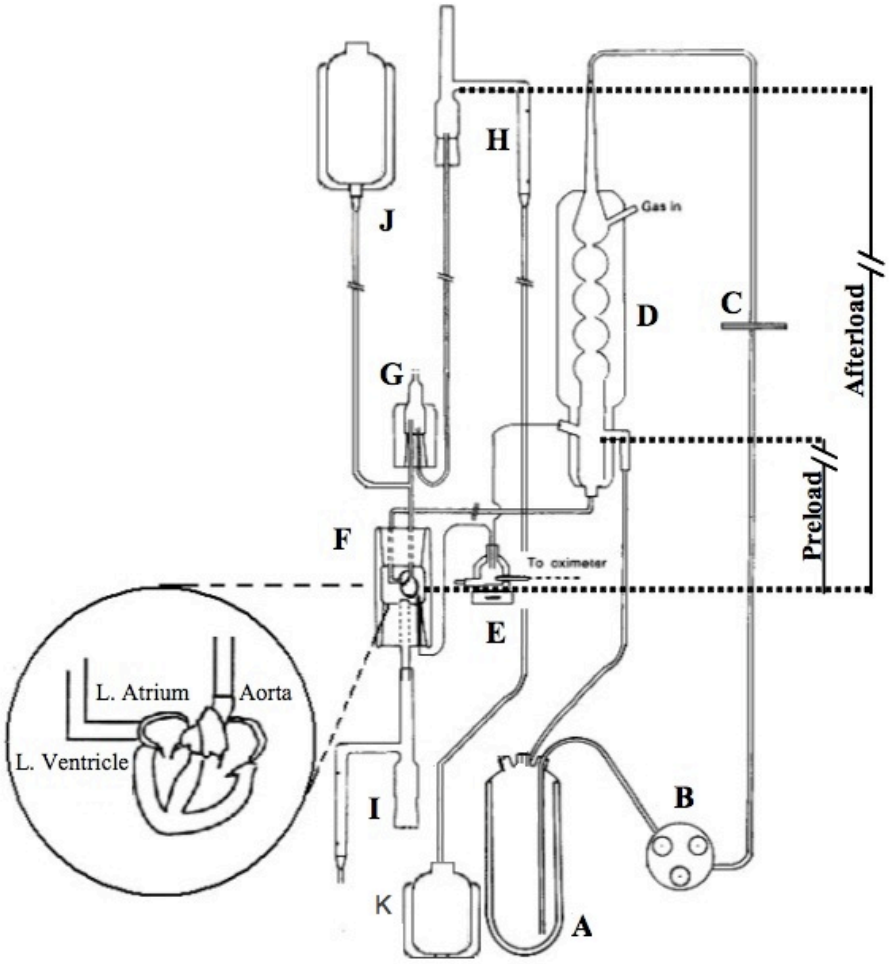

Figure 2.1 Modification of perfusion apparatus developed by Taegtmeyer, Hems and Krebs. The apparatus consisted of a (a) reservoir containing fresh perfusate, (b) Watson Marlow 505S peristaltic pump, (c) 5 µm Millipore filter, (d) multi-bulb oxygenator, (e) oxygen sensor, (f) perfusion chamber, (g) compliance chamber, (h) aortic overflow reservoir, (i) coronary overflow reservoir, (j) Langendorff reservoir, and (k) reservoir for metabolized perfusate.

2.2.4 Liquid Scintillation Counter for Determination of Radioactivity

Ultima Gold liquid scintillation cocktail (Perkin Elmer, Waltham, MA) was added to coronary effluent samples in a 25 mL glass or PVC scintillation vial and read in

a Packard Model 2200 liquid scintillation counter (Packard Instruments, Warrenville, IL) to measure radioactivity. Radioactive decay was measured by the scintillation counter in counts per minute, which was then converted into disintegrations per minute. Samples were stored in the dark overnight prior to reading to correct for liquid sctintillation cocktail autoilluminescence. Both [U-^{14}C]glucose and [2-^{3}H]glucose were obtained from Perkin Elmer (Waltham, MA).

2.2.5 Spectrophotometer for Assessment of Intracellular Metabolite Content

All metabolite analyses were performed on a Shimadzu UV1600 UV-visible Spectrophotometer (Tokyo, Japan). Enzymes necessary for metabolite analyses, including hexokinase and glucose 6-phosphate dehydrogenase used for measuring glucose 6-phosphate, were purchased from Sigma Aldrich (St. Louis, MO).

2.2.6 Western Blotting Apparatus and Sources of Antibodies

Mini-PROTEAN Tetra Cell electrophoresis system and Trans-Blot SD Semi-Dry Transfer Cell (Bio-Rad, Hercules, CA) were used to separate proteins from heart lysates and transfer them onto a nitrocellulose membrane (GE Healthcare Life Sciences, Pittsburgh, PA). Proteins were detected using Amersham ECL Plus, also purchased from GE Healthcare Life Sciences.

Antibodies for PI3K, AKT 1/2, TSC2, mTOR, RAPTOR, p70S6K1, 4EBP1, AMP kinase, Acetyl CoA Carboxylase (ACC), phospho-PI3K p85 (Tyr458)/p55 (Tyr199)

phospho-Akt1/2 (Ser473), phospho-mTOR (Ser2448), phospho-p70S6K (Thr389), phospho-4EBP1 (Thr70), (phospho-AMPKinase (Thr172), phospho-ACC (Ser79), phospho-TSC2 (Ser 939), and phospho-RAPTOR (Ser 792) were obtained from Cell Signaling (Beverly, MA). Antibody for glucose-regulated protein 78 (GRP78), glucose-regulated protein 94 (GRP94), and ER protein 72 (ERp72) were purchased from Enzo Life Sciences (Plymouth Meeting, PA) and GADD153 was purchased from Santa Cruz Biotechnology (Santa Cruz, CA). GAPDH was used to normalize for protein loading (Research Diagnostics, NJ).

2.2.7 Sequence Analyzer for Quantitatve RT-PCR

Absolute quantification of gene expression was completed using an ABI Prism 7000 Sequence Detection System (Foster City, CA). The ABI 7000 calculates absolute transcript numbers by comparing the number of cycles necessary to meet a fluorescence threshold in the sample to the number of cycles needed in standard amounts of RNA over a 10^5 range (standard curve method). Taqman probe chemistry was utilized to generate fluorescence by uncoupling the fluorogenic dye molecule and the quencher moeity found on a nucleic acid probe by Taq polymerase during each PCR cycle.

2.2.8 Miscellaneous Equipment

Revco -80^{o}C freezer (Thermo Scientific, Asheville, NC) and -20^{o}C freezer (Sanyo Scientific, Bensenville, IL) for sample and reagent storage, NanoDrop ND-1000

spectrophotometer (Nanodrop Technologies, Wilmington, DE) for RNA concentration assessment, Polytron tissue homogenizer (Brinkman Instruments, Westbury, NY), Ohaus AS120 scale (Florham Park, NJ), Eppendorf desktop centrifuge Model 5415C (Hamburg, Germany), Isotemp shaking water bath (Fisher Scientific, Waltham, MA), and 2EG gravity convection oven (Precision Scientific, Chicago, IL) for dry heart sample preparation.

2.3 Methods

2.3.1 PET and MRI Imaging

Male C57BL/6J mice (8-9 weeks of age) were subjected to sham operation or transverse aortic constriction (TAC) to induce pressure-overload hypertrophy and housed in a 12 h light/12 h dark cycle and given standard laboratory chow and water *ad libitum* at The University of Virginia Medical School. Mice were serially imaged 1 day, 2 weeks, and 4 weeks after either sham or TAC surgery by the Kundu lab at the University of Virginia Medical School. Prior to imaging, animals were fasted overnight with access to water. All experiments were performed in compliance with the Guide for the Care and Use of Laboratory Animals, published by the National Institutes of Health and were conducted under protocols approved by the Animal Care and Use Committee at the University of Virginia. On the day of imaging, each mouse was anesthetized with 3% Isoflurane and maintained at 1-2% Isolflurane. A Mikro-tip Catheter Transducer was then placed in the right carotid artery under stereo-magnification and advanced through

the aorta until the tip was positioned in the left ventricle to make left ventricular pressure measurements. Heart rate and cardiac pressure were continuously monitored throughout. Body temperature was maintained at 37^{o}C with a warming blanket.

Positron Emission Tomography (PET) with [^{18}F] FDG and Magnetic Resonance Imaging (MRI) were sequentially performed in anesthetized animals. PET imaging was performed in a Focus 120 micro PET scanner (Siemens Molecular Imaging Inc., Knoxville, TN) to assess changes in metabolism. The protocol was initiated by injecting 150-200 μL of 18.5-37 MBq FDG solution intravenously over a period of one minute. The net FDG influx constant, *Ki (1/min)*, was measured over a period of 4 weeks. Determination of *Ki* is considered a robust index of glucose transport and phosphorylation (Nguyen, Mossberg et al. 1990). Throughout the procedure heart rate, respiration, and body temperature were recorded with a physiological recorder (SA Instruments, Inc., model 1025L, Stony Brook, NY), and the ECG was monitored (Blue Sensor, Ambu Inc., Glen Burnie, MD). All of the signals were sent to a single SA Instruments software interface, which was configured to trigger data acquisition based on the ECG. The SAI 1025L was also used to maintain the animal's core body temperature at 37^{o}C.

Mice were also imaged using a 7T Bruker-Siemens Clinscan MRI system for structural and functional analyses of the heart. After once again being anesthetized, the mouse was placed prone inside the radiofrequency coil, and the ECG leads were connected to an ECG monitoring module (SA Instruments, Inc., Stony Brook, NY). An ECG-triggered, 2D cine gradient echo pulse sequence was used (Berr, Roy et al. 2005) with a slice thickness of 1 mm and a zero-filled, in-plane resolution of 100x100 μm^2.

During each session, the entire LV was imaged with 6-7 contiguous short-axis slices. The MR images were analyzed using the ARGUS software package (Siemens Medical Systems, Erlangen, Germany) for LVESV, LVEDV, and LVEF was computed from the traced borders. Epicardial contours were also traced at the end-diastolic and end-systolic phases to compute LV mass (Vinnakota and Bassingthwaighte 2004). This was divided by the body weight to obtain the HW/BW ratios.

2.3.2. Isolated Working Rat Heart Perfusions

Isolated hearts were perfused using the isolated working heart apparatus, as described previously (Taegtmeyer, Hems et al. 1980; Goodwin, Taylor et al. 1998). Hearts were removed from the thoracic cavity and placed in ice-cold Krebs-Henseleit buffer (25 mM $NaHCO_3$, 2.54 mM $CaCl_2$, 1.18 mM $MgSO_4$, 1.18 mM KH_2PO_4, 4.75 mM KCl, 118.5 mM NaCl). Upon isolation and cannulation of the aorta onto the apparatus, hearts were initially perfused in the Langendorff mode with Krebs-Henseleit buffer equilibrated with 95:5% O_2:CO_2 to flush residual blood out of the ventricles and allow the heart to resume regular contraction. Following cannulation of the left atrium, hearts were switched to the non-recirculating working mode and perfused for 60 minutes.

The afterload against which each heart pumped is proportional to the height of the aortic overflow reservoir. Under steady state conditions, hearts were perfused at a physiological workload (afterload set to 100 cm) for 60 minutes. Hearts subjected to a high workload were perfused for 30 minutes at a physiological workload followed by 30

minutes at an increased workload (afterload raised to 140 cm H_2O, plus 1μM epinephrine bitartrate added to the perfusate). The preload, determined by the height of the oxygenator's overflow above the left atrium, was set to 15 cm H_2O for all perfusions. At the end of each 60 minute perfusion, hearts were freeze-clamped while still beating with aluminum tongs cooled in liquid nitrogen (Wollenberger and Schulze 1961).

The isolated working heart apparatus was selected as a model because it provides numerous advantages over *in vivo, in vitro,* and other *ex vivo* approaches available. A number of *in vivo* models have manipulated glucose entry into the heart by overexpressing a transporter (Liao, Jain et al. 2002) or knocking out a receptor (Belke, Betuing et al. 2002) necessary for glucose transport in the heart. However, in each instance, the insult to the animal is both supraphysiological and accompanied by compensatory changes in the heart that make it difficult to delineate the role of glucose in cardiac growth signaling in a heart stressed in a physiological manner. *In vitro* systems simply do now allow for modulating workload in the cardiomyocyte nor to accurately measure contractile function. In other *ex vivo* models such as the Langendorff preparation, the amount of perfusate pumped by the ventricles is far less than physiological and contractile function cannot accurately assessed (Neely, Liebermeister et al. 1967). On the other hand, there is a near-physiologic level of work performed by the heart in the *ex vivo* working perfusion system (Taegtmeyer, Hems et al. 1980). Moreover, hemodynamic stress can be applied to hearts using our system by subjecting hearts to an *ex vivo* increase in workload, and both contractile function and changes in substrate flux can be assessed in real time, as well.

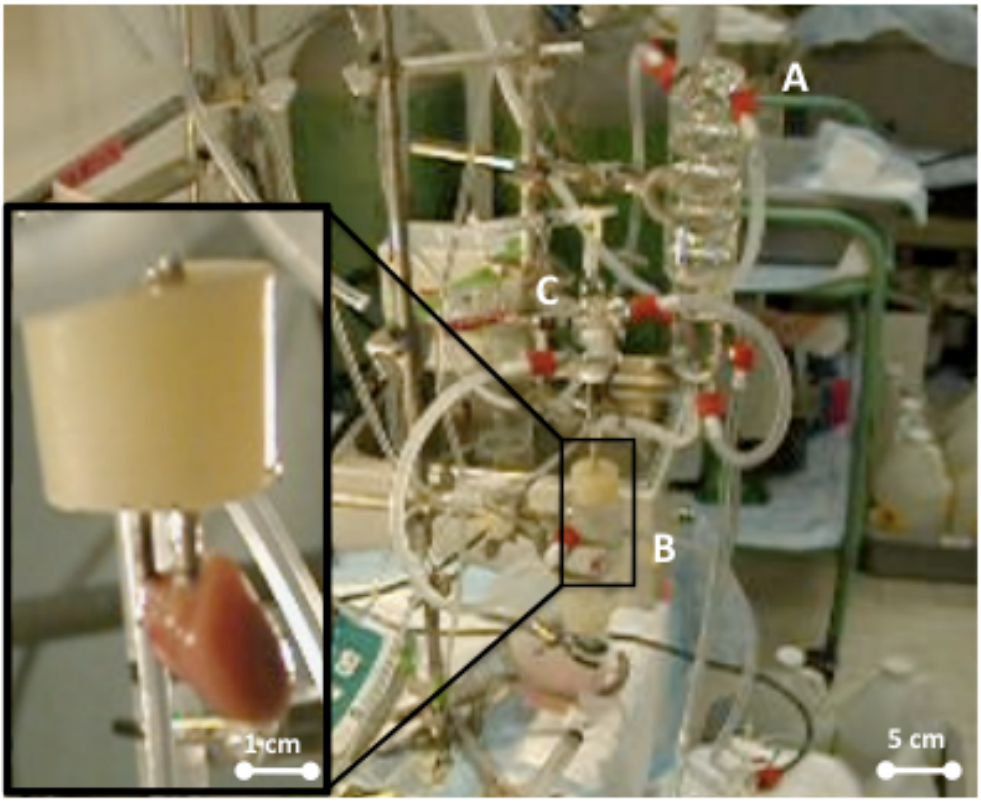

Figure 2.2 Cannulation of the left atrium and aorta. This photograph of the perfusion apparatus highlights the placement of the isolated rat heart within the perfusion chamber and its cannulation both at the left atrium and the aorta. Perfusate flows in a retrograde manner from the left atrium, into the left ventricle, and then pumped out through the aorta. The coronary effluent is collected from perfusate that flows out the coronary arteries proximal to where the aorta is cannulated. For orientation purposes, the oxygenator (A), perfusion chamber (B), and compliance chamber (C) are labeled, as well.

2.3.2.1. Perfusion Protocols and Buffers

Fresh buffer was made daily. All perfusion buffers included Krebs Henseleit buffer (25 mM $NaHCO_3$, 2.54 mM $CaCl_2$, 1.18 mM $MgSO_4$, 1.18 mM KH_2PO_4, 4.75 mM KCl, 118.5 mM NaCl). Buffer was prepared by adding a 20X stock solution containing all electrolytes with the exception of $CaCl_2$ and $NaHCO_3$ to double distilled

H_2O and $NaHCO_3$. The mixture was then oxygenated with 95:5% O_2:CO_2 for 15 minutes before $CaCl_2$ was added. In order to determine the effect of glucose on growth signaling in the stressed heart, substrates were then added to the buffer to make up the perfusate, as indicated in **Table 2.2**. Both metformin (Sigma Aldrich, St. Louis, MO) and 4-phenylbutyrate (Calbiochem, San Diego, CA) were dissolved in H_2O prior to being added to the perfusate.

Group	Perfusate	Workload	Time
Noncarbohydrate Substrates (NCS)	Propionate (2mM) + Acetoacetate (5mM)	Normal	0-60 min
	Substrate-free (Glycogen Depletion)	Normal	0-15 min
	Propionate (2mM) + Acetoacetate (5mM)		15-30 min
	+ Epinephrine (1μM)	High	30-60 min
Glucose	Glucose (5 mM)	Normal	0-60 min
	*Glucose (5 mM)	Normal	0-30 min
	+ Epinephrine (1μM)	High	30-60 min
Glucose Analogues	2 Deoxy-D-glucose (5 mM)	Normal	0-60 min
	2 Deoxy-D-glucose (5 mM)	Normal	0-30 min
	+ Epinephrine (1μM)	High	30-60 min
	3-O-methylglucose (5 mM)	Normal	0-60 min
	3-O-methylglucose (5 mM)	Normal	0-30 min
	+ Epinephrine (1μM)	High	30-60 min
Mixed	Glucose (5 mM) + Oleate (.4 mM) + Propionate (2mM) + Acetoacetate (5mM)	Normal	0-60 min
	Glucose (5 mM) + Oleate (.4 mM) + Propionate (2mM) + Acetoacetate (5mM)	Normal High	0-30 min 30-60 min

Table 2.2 *Ex vivo* perfusion protocols used to study glucose activation of mTOR signaling at high workload.*note: Four different sets of rats were perfused with glucose and subjected to high workload. (1) The first set were untreated prior to perfusion. (2) The second set received mTOR inhibitor rapamycin (PO, 4 mg/kg/day) for 7 days prior to perfusion (or vehicle control). (3) The third set received metformin (IP, 250 mg/kg/day or 500 mg/kg/day) for 7 days prior to perfusion (or vehicle control). (4) The last set of hearts were perfused with either metformin (5 mM, 7.5 mM, or 10 mM) or 4-phenylbutyrate (PBA, 10 mM) added directly to the buffer.

2.3.2.2. Determination of Cardiac Power, Rates of Glucose Uptake and Oxidation

Determination of Cardiac Power:

Cardiac power was used as a marker for contractile function in this project. Cardiac power (mW) was calculated as the product of mean arterial pressure, estimated as the height of the afterload (in cm H_2O) times the cardiac output (sum of the aortic output and coronary flow). Aortic output and coronary flows were derived by measuring the number of seconds needed to collect 10 mL of perfusate in the aortic and coronary overflow reservoirs, respectively, every five minutes throughout each perfusion protocol. These measurements were then converted into mL/min by multiplying by a factor of 60.

Determination of Rates of Glucose Uptake:

Rates of glucose uptake (and subsequent phosphorylation) were determined by adding 2-**[^{3}H]**-glucose to the perfusion buffer and measuring the release of **[^{3}H]**$_2$O in the coronary effluent. When glucose is taken up by the cardiomyocyte, it is immediately acted upon by hexokinase and converted into glucose 6-phosphate. When glucose 6-phosphate is then reversibly converted into fructose 6-phosphate by phosphoglucoisomerase, **[^{3}H]**$_2$O is released into the coronary effluent (Katz and Dunn 1967). The overall reaction is:

2-**[^{3}H]** glucose + 2 NAD^+ + 2 ADP → 2 pyruvate + 2 **[^{3}H]**$_2$O + 2 NADH + 2 ATP + 2H^+

We collected 2 mL of coronary effluent every 5 minutes in order to assess rates of glucose uptake throughout each 60 minute perfusion. A sample of unused perfusate was collected at the end of each perfusion for background radioactivity measurements.

[^{3}H]$_2$O was separated from unmetabolized 2-**[^{3}H]** glucose and other **[^{3}H]** labeled compounds by retention and elution in an ion exchange column. Columns were packed with glass wool and filled with 1.5 mL of AG1-X8 anion exchange resin (BioRad, Hercules, CA). After washing the resin with 6 mL of H_2O, aliquots (.5 mL) of sample were added and eluted into scintillation vials with 3.5 mL H_2O plus 13 mL Ultima Gold liquid scintillation cocktail and radioactivity was measured by a Packard scintillation counter, as described earlier. Specific activity, the amount of radioactivity of the particular radionuclide (SA=tracer (dpm)/tracee (umol)), in the perfusate was concurrently measured by adding .5 mL of unused perfusate directly to 13 mL of scintillation cocktail.

Determination of Rates of Glucose Oxidation:

Rates of glucose oxidation were determined by adding U-**[^{14}C]** glucose to the perfusion buffer and measuring the release of **[^{14}C]**O_2 in the coronary effluent. **[^{14}C]**O_2 is released in the Krebs Cycle when isocitrate (6C) is converted to α-ketoglutarate (5C) by isocitrate dehydrogenase and when α-ketoglutarate (5C) is converted to succinyl CoA (4C) by α-ketoglutarate dehydrogenase. The overall reaction is:

U-**[^{14}C]** glucose → U-[^{14}C] acetyl CoA → **[^{14}C]**O_2

[^{14}C]O_2 release into the coronary effluent is therefore proportional to the rate of glucose oxidation under the given perfusion conditions and can be calculated. In each coronary effluent sample, **[^{14}C]**O_2 was separated from unmetabolized U-**[^{14}C]** glucose and other **[^{14}C]** labeled compounds by acidification and CO_2 trapping by hyamine hydroxide (Goodwin *et al* JBC 1998). Specifically, 1 mL of Hyamine Hydroxide (Perkin Elmer,

Waltham, MA) was added to the bottom of a scintillation vial. An open eppendorf tube containing .5 mL of coronary effluent was then placed in the scintillation vial and closed with a subaseal rubber bung. 200 mL of 60% perchloric acid (v:v) was then injected into each Eppendorf tube to trigger release of **[^{14}C]**O_2 and trapping by hyamine hydroxide. Each scintillation vial was stored overnight to allow the reaction to occur to completion. 13 mL Ultima Gold liquid scintillation cocktail was added the next morning and radioactivity was measured by a Packard scintillation counter, as described earlier.

2.3.3. Spectrophotometric enzymatic metabolite analysis

Using heart tissue that had been stored at -80^{o}C, approximately 500 mg of pulverized frozen heart tissue was added to .5 mL 6% perchloric acid on ice to precipitate out proteins and halt all metabolic activity (Wiliamson, Corkey 1967). Tissue was then homogenized for roughly 30 seconds with a Polytron® homogenizer. The suspension was then neutralized by the addition of KIK (6M KOH, .4M imidazole, .4M KCl), vortexed, and centrifuged at 13,000 rpm to isolate out metabolites. Metabolite concentrations were then determined by enzymatic spectrophotometric analysis, as detailed below. In each instance, absorbance at 340 nm was read in samples placed in plastic cuvettes (10 mm light path) before and after addition of enzyme. Incremental changes in absorbance with time indicated when each reaction was completed.

Metabolite concentrations of glucose 6-phosphate, fructose 6-phosphate, and adenosine-5'-triphosphate (ATP) were measured by a spectrophotometric enzymatic

analysis using glucose-6-phosphate dehydrogenase coupled to NADPH production with extinction at 340 nm.

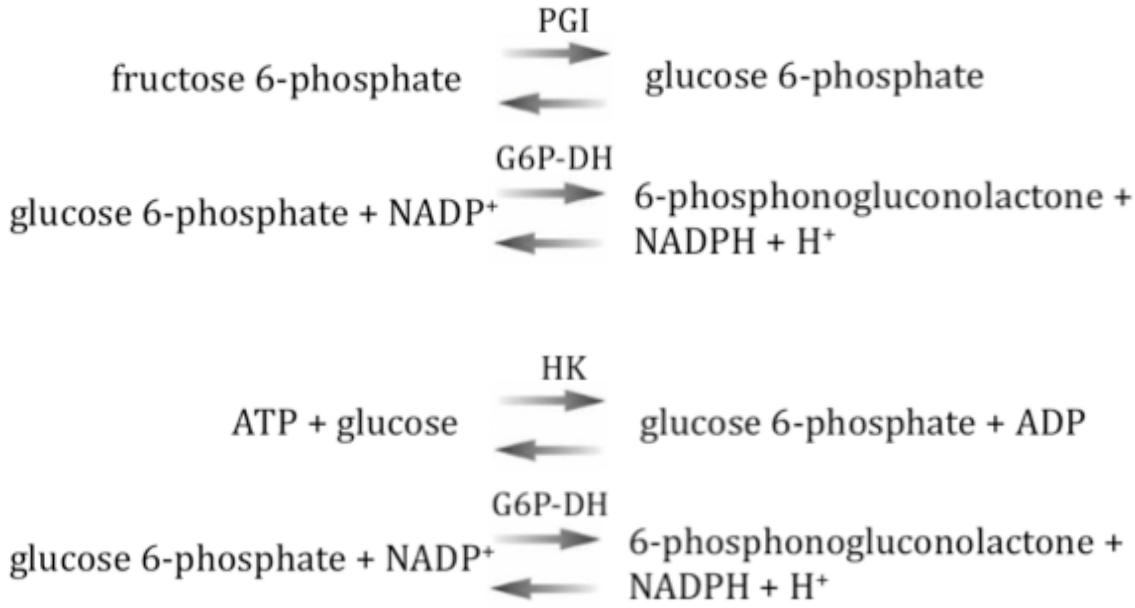

Similarly, conentrations of adenosine-5'-diphosphate (ADP) and adenosine-5'-triphosphate (ATP) were measured using lactate dehydrogenase coupled to the oxidation of NADH to NAD^+ with extinction at 340 nm (Bergmeyer 3rd edition) in a three-step reaction.

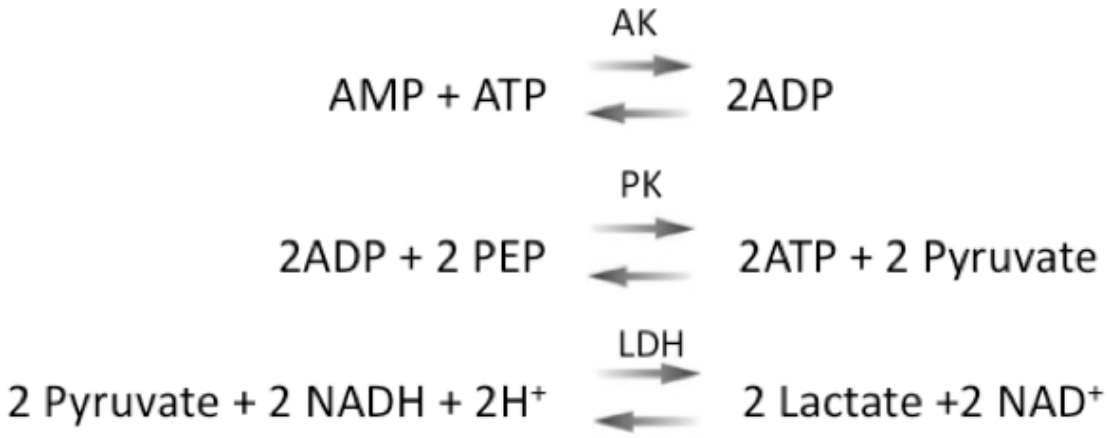

A colorimetric Bradford assay was completed to determine the total protein concentration in each sample (Bradford 1976). Metabolite concentrations were normalized to total protein content in each sample.

2.3.4. Western Immunoblotting

Protein Extraction

Total protein was extracted from frozen heart tissue by homogenizing 100 mg left ventricular tissue at maximum speed for 30 seconds in extraction buffer (30 mM Hepes, 2.5 mM EGTA, 2.5 mM EDTA, 20 mM Kcl, 40 mM glycerophosphate, 40 mM NaF, 4 mM $NaPP_i$ 10% glycerol, .1% non-idet P40) using a Polytron® homogenizer. The suspension was then centrifuged for 30 minutes at 13,000 rpm and the supernatant (protein) was recovered. A colorimetric Bradford assay was completed to determine the protein concentration in each sample (Bradford Anal Biochem. 1976). Aliquots of 25 ug were prepared in 2X protein loading buffer (1M Tris HCl, glycerol, 10% SDS, .1% Bromophenol Blue, 2-mercaptoethanol) and stored at -80^{o}C.

Western blotting

Protein lysates were separated by SDS-PAGE (polyacrylamide gel electrophoresis) and transferred onto a nitrocellulose membrane using a Trans-Blot SD Semi-Dry Electrophoretic Transfer Cell (BioRad, Hercules, CA). Ponceau staining of the membrane was used to confirm uniform transfer of proteins throughout the membrane. Membranes were destained with .4% TBS-T (Tris base in NaCl, in .4% tween-20 detergent) then washed in 5% nonfat milk in TBS-T for two hours at room temperature to block non-specific sites on the membrane. Membranes were then incubated at 4^{o}C in

primary antibody solution (in 5% BSA in TBS-T) overnight. After unbound primary antibody was washed off with TBS-T the next morning and the membrane was incubated in horseradish peroxidase (HRP)-conjugated secondary antibody for one hour at room temperature. Subsequent addition of a chemiluminescent luminol reagent produced light that was captured on film and developed in a dark room. Changes in the phosphorylated protein to total protein ratio by Western immunoblotting is uniformly accepted as an indicator of protein activation/inactivation along the mTOR signaling cascade and was therefore assessed in all hearts.

2.3.5. Quantitative Reverse Transcription Polymerase Chain Reaction (qRTPCR)

RNA Extraction

Total RNA was extracted from frozen heart tissue by first homogenizing 100 mg left ventricular tissue at maximum speed for 30 seconds in guanidinium thiocyanate-phenol-chloroform extraction (Tri-Reagent, MRC, Cincinnati, OH). The suspension then underwent phase separation by a series of centrifugation steps. In the final step, RNA was precipitated out of the aqueous phase by isopropanol. RNA concentration was then measured with a Nanodrop ND-1000 Spectrophotometer. All RNA samples were diluted to a final concentration of 30 ng/uL and stored at -80^{o}C. 60 ng of RNA were analyzed in triplicate per sample.

qRTPCR

RNA was first reverse transcribed into its complementary DNA by reverse transcriptase (Invitrogen, Carlsbad, CA) and the resulting cDNA was amplified by real-time PCR using the ABI Prism 7100 SDS. On each 96-well plate, select samples were also run in the absence of reverse transcriptase to detect DNA contamination. These samples served as the non-amplified control (NAC). Fluorescence is produced by cleavage of a reporter dye from a quencher dye on a nucleic acid probe that is degraded by Taq polymerase during each cycle of PCR. The number of cycles necessary to reach a fluorescence threshold (C_t) is used to determine the amount of RNA transcripts present in each sample compared to standard amounts of RNA over a log range of concentrations **(Fig. 2.3)**. Data are presented as transcript copy per nanogram of RNA. Primer and probe sequences have been previously published (Harmancey, Wilson et al. 2010) and are listed below:

Glucose Regulated Protein 78 (GRP78)

Forward 5‟-ACCGTCGTATGTGGCCTTCA-3‟

Reverse 5‟-TCCGGGTTGGACGTGAGTT-3‟

Probe 5‟-FAM-CTGATTGGCGATGCGGCC-TAMRA-3‟

Glucose Regulated Protein 94 (GRP94)

Forward 5‟-TGTCAAAGGTGTTGTGGATTCC-3‟

Reverse 5‟-AGAGTTTTGCGGACAAGCTTCT-3‟

Probe 5‟-FAM-TCTCCCCCTCAATGTTTCCCGTGA-TAMRA-3‟

Endoplasmic Reticulum Protein 72 (ERp72)

Forward 5‟-CTTCTAACGATGCTAAGCGGTACA-3‟

Reverse 5‟-CGCCAAAACTGAGTAGCAGTTCT-3‟

Probe 5‟-FAM-CAAGCGCCCCCTGGTGGTTGTA-TAMRA-3‟

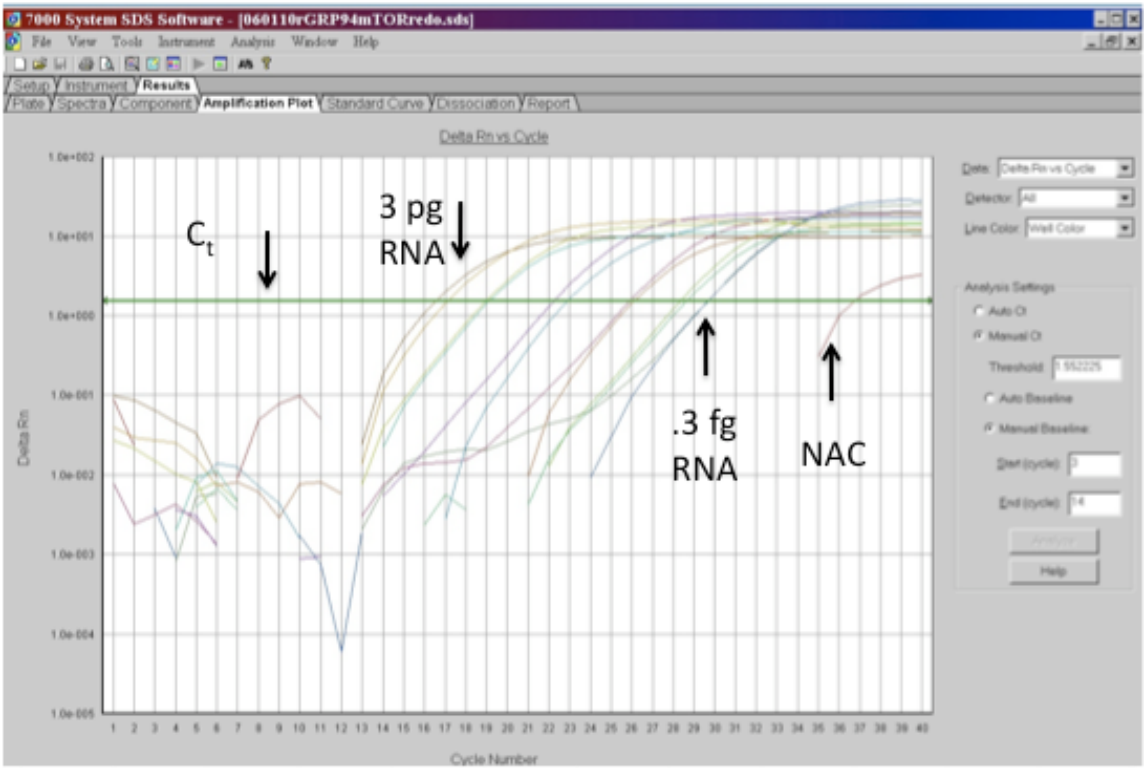

Figure 2.3 Sample Standard Curve Used to Quantify mRNA Transcript levels of ER stress markers. The fluorescent signal for up to 40 cycles of PCR are recorded from standard amounts of mRNA. A non-amplification control (NAC, sample without reverse transcriptase) is run alongside each set of samples.

2.3.6 Statistical Analysis

Two way repeated measures analysis of variance (ANOVA) and Holm-Sidak post hoc test were used to compare cardiac power, rates of glucose uptake, and rates of glucose oxidation between different groups of hearts perfused *ex vivo*. All numerical data were displayed as a mean ± SEM. A $p<0.05$ was considered statistically significant.

CHAPTER 3: LOAD-INDUCED MTOR ACTIVATION IS MEDIATED BY GLUCOSE 6-PHOSPHATE ACCUMULATION

3.1 Introduction

This chapter includes rationale, results, and discussion of the experiments in support of the hypothesis that load-induced mTOR activation is mediated by glucose 6-phosphate accumulation. Hypertension, valvular heart disease, anemia, and prior myocardial infarctions all stress the heart with an increase in workload and can ultimately lead to heart failure. Metabolically, hearts increase their reliance on glucose for energy provision (Goodwin, Taylor et al. 1998) and structurally, hearts hypertrophy when stressed (Dorn and Force 2005). However, the mechanisms that trigger a heart to hypertrophy and ultimately fail under such conditions remain largely unknown. We therefore investigated whether the metabolic remodeling process drives the structural and functional remodeling process in hearts subjected to high workload via mTOR activation.

Load-induced cardiac hypertrophy is largely driven by the mammalian target of rapamycin (mTOR), a major regulator of protein synthesis that is located dowstream of the PI3K-Akt signaling pathway **(Fig. 3.1)**. mTORC1 directly triggers cardiac hypertrophy via activation of p70S6 kinase (p70S6k) and 4E-binding protein 1 (4EBP1), which promote ribosomal biogenesis and CAP-dependent protein translation, respectively.

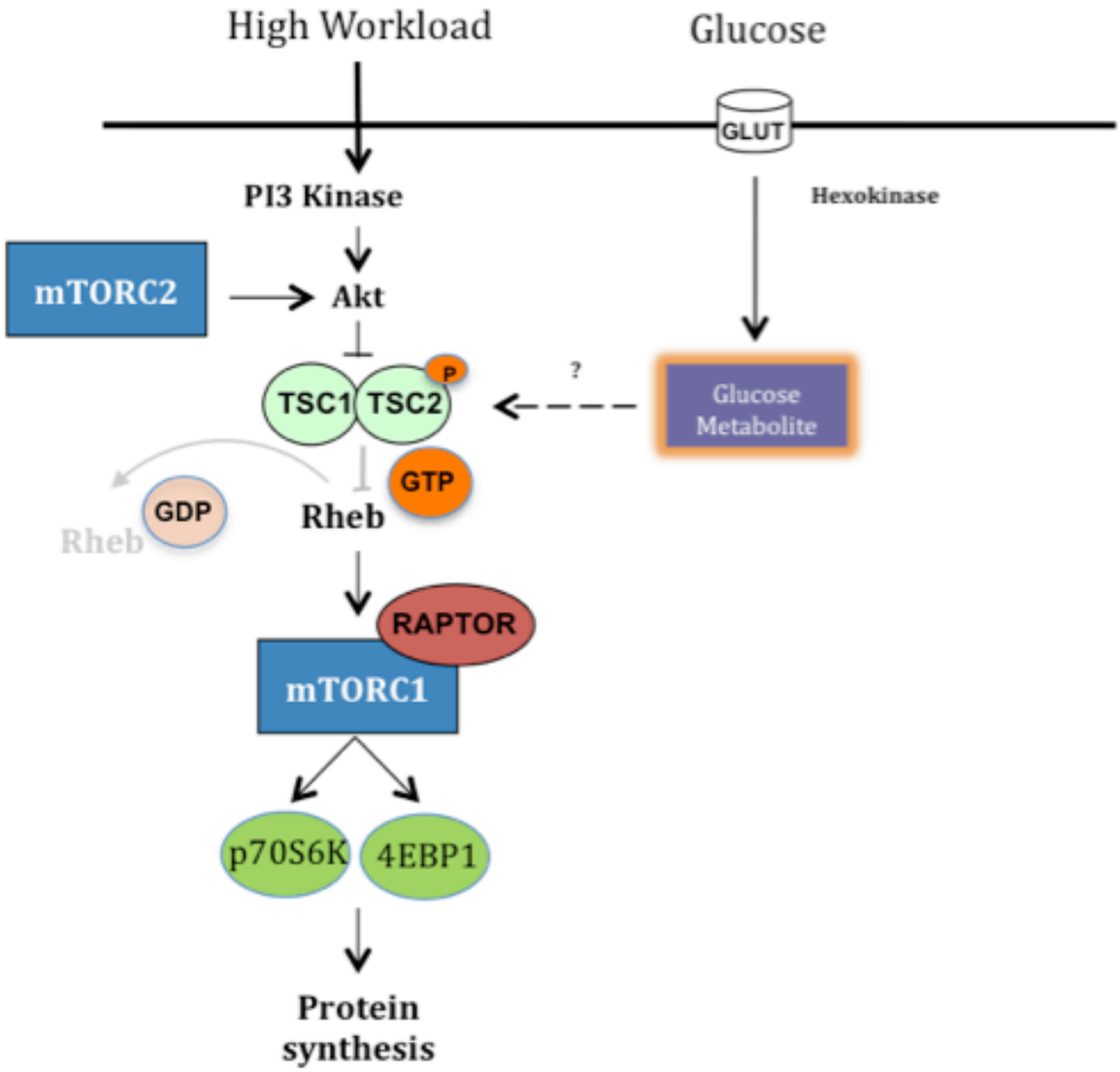

Figure 3.1 Proposed activation of the mTOR signaling pathway by glucose. Load-induced mTOR activation is known to occur via the PI3K-Akt signaling pathway. Whether the heart's increased reliance upon glucose at high workload regulates this signaling pathway is unknown.

mTORC1 plays a critical role in promoting cardiac growth in response to increased workload (Shioi, McMullen et al. 2003). mTOR also couples energy and nutrient abundance to cell growth owing ot the capacity to sense nutrients, stress, and growth factors (Zoncu, Efeyan et al. 2011). It is also known to be activated by nutrients and growth factors (Proud 2002). Whether load-induced mTORC1 activation in the heart is regulated by physiological changes in energy substrate metabolism in the stressed heart was unknown at the beginning of my project. We previously reported that the insulin signaling pathway and mTORC1 can only be activated by the combination of glucose and insulin in rat heart (Sharma, Guthrie et al. 2007). I extended this work and investigated the metabolic, functional and structural consequences of glucose-mediated mTOR signaling in the stressed heart.

The chapter addresses the following four objectives: 1) Determining whether in hearts subjected to increased workload *in vivo*, metabolic remodeling precedes the structural and functional remodeling process. 2) Determining whether load-induced mTOR activation is dependent upon the heart's increased reliance upon glucose at high workload. 3) Elucidating the mechanism by which changes in glucose metabolism modulate phosphorylation (i.e. activation) of proteins along the PI3K/Akt and TSC2/mTOR axis at high workload. 4) Identifying the functional consequences of sustained mTOR activation and determining whether these consequences are preventable.

We investigated whether signals generated by glucose metabolism regulate mTOR activation in the heart when it is subjected to high workload. I tested this hypothesis by first subjecting mice to increased workload *in vivo* and serially monitoring changes in glucose metabolism, contractile function, and structure using PET and MRI imaging. I then assessed mTOR activation in these hearts to determine whether the metabolic or structural changes were associated with changes in mTOR activation. Next, to determine the mechanism by which changes in glucose metabolism regulate mTOR activation *in vivo,* I systematically modulated substrate supply and workload to the heart *ex vivo* and assessed changes in the activation of nearly every major protein involved in the mTOR signaling cascade. Lastly, I investigated whether or not markers of load-induced mTOR activation were metabolically regulated in left ventricular tissue from failing human hearts before and after implantation of an LVAD. My objective was to establish that pathways of protein synthesis are metabolially regulated in the heart and to determine whether any of the findings in animal models are also present in th failing human heart. It was my expectation that these results provide evidence to support the idea that modulation of cardiac metabolism can be used to regulate cardiac growth and contractile function.

3.2 Results

3.2.1. Metabolic Remodeling Accompanies Functional but Precedes Structural Remodeling In Response to Increased Workload *In Vivo*

In order to determine whether enhanced glucose uptake precedes the structural and functional remodeling process in response to increased cardiac workload *in vivo*, mice were serially imaged with FDG-PET and MRI 1 day, 2 weeks, and 4 weeks to transverse aortic constriction (TAC) in the laboratory of our collaborator Bijoy Kundu at the University of Virginia. Transverse end-diastolic FDG-PET images demonstrated a 5-fold increase in the rate of myocardial FDG uptake beginning 1 day after TAC, which further increased (1.5- to 3.2-fold) over 4 weeks **(Fig. 3.2A-B)**. Sham operated animals showed no change in FDG uptake over the same period. The PET images also suggested hypertrophy and an enlargement in LV cavity in the TAC mice, but only at 2 and 4 weeks.

While metabolic remodeling was detected 1 day after TAC, no structural changes were appreciated at this early time point by MRI. There was no significant increase in either the heart weight to body weight ratio (HW/BW) **(Fig. 3.2C)** or end diastolic wall thickness **(Fig. 3.2D)** 1 day after TAC. Both HW/BW and end diastolic wall thickness exhibited a 1.4 fold increase only after 2 and 4 weeks after TAC. There was no significant change in HW/BW or wall thickness over 4 weeks in sham-operated mice.

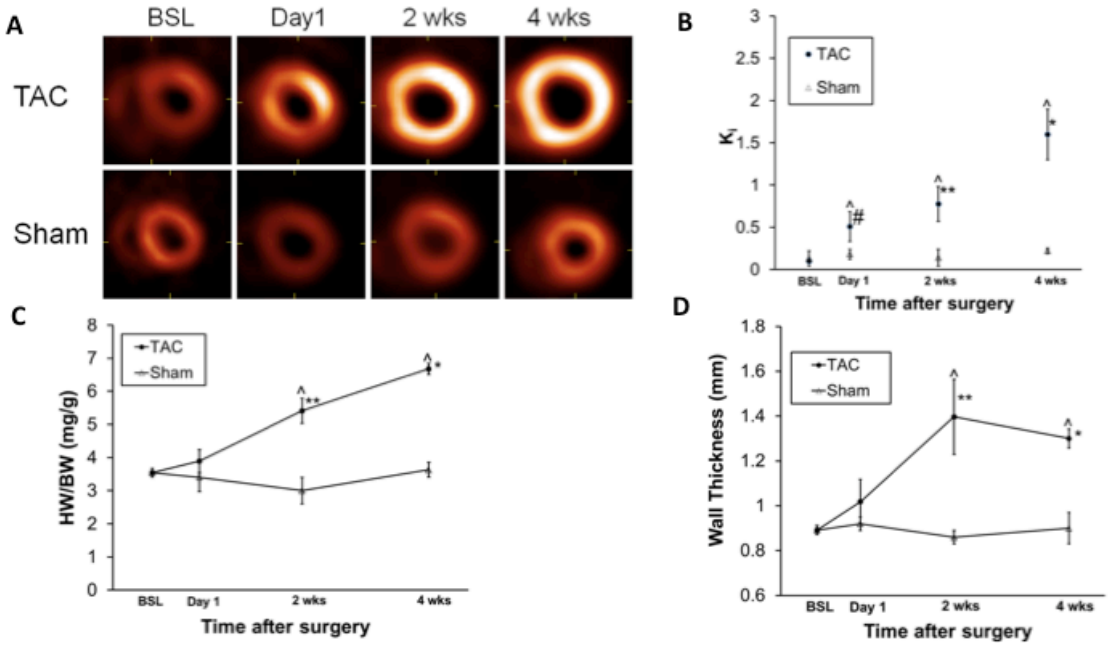

Figure 3.2 Metabolic remodeling precedes structural remodeling in hearts subjected to high workload *in vivo*. (A) 1 day after TAC, there is an increase in FDG uptake prior to any structural changes in the heart. (B) Myocardial FDG uptake (K_i) in TAC mice demonstrates a 5-fold increase in FDG uptake at day 1, and a 1.5- to 3.2-fold increase from day 1 to 4 weeks. Sham operated mice show no significant change in FDG uptake over 4 weeks. (C) Body weight (BW) was recorded and heart weight (HW) was measured using MRI *in vivo*. HW/BW remains unchanged 1 day after TAC, but increases 1.4- and 1.7-fold between day 1 and 4 weeks, respectively. HW/BW shows no significant change over 4 weeks in sham operated mice. (D) End diastolic wall thickness is unchanged 1 day after TAC, but increases about 1.4-fold between day 1 and 4 weeks. Wall thickness shows no significant change over 4 weeks in sham operated mice. n=8 for the TAC and n=5 for the shams. All values are mean ± SD. #$p<0.05$ day 1 vs BSL, *$p<0.001$ vs BSL, day 1, 2 weeks, **$p<0.05$ vs BSL, day 1; ^$p<0.05$ between the TAC and sham groups on the same day. Imaging studies and analysis were completed at our collaborator Bijoy Kundu's laboratory at The University of Virginia Medical School.

In order to determine whether functional changes accompanied the early metabolic or later structural changes in response to high workload, end-diastolic volume (EDV), end-systolic volume (ESV) and ejection fraction (EF) were also assessed by

MRI**.** There were no significant changes in EDV at 1 day after TAC **(Fig. 3.3A)**, but there were increases in ESV **(Fig. 3.3B)** and significant decreases in EF **(Fig. 3.3C)** at the same time point. Both ESV and EDV **(Fig. 3.3A-B)** progressively increased 2 and 4 weeks after TAC, while the EF progressively declined over the same time period. There were no significant changes in EDV, ESV, or EF in sham operated animals over 4 weeks. Collectively, the data support the hypothesis that metabolic changes precede structural changes and accompany functional changes in hearts subjected to increased workload *in vivo*.

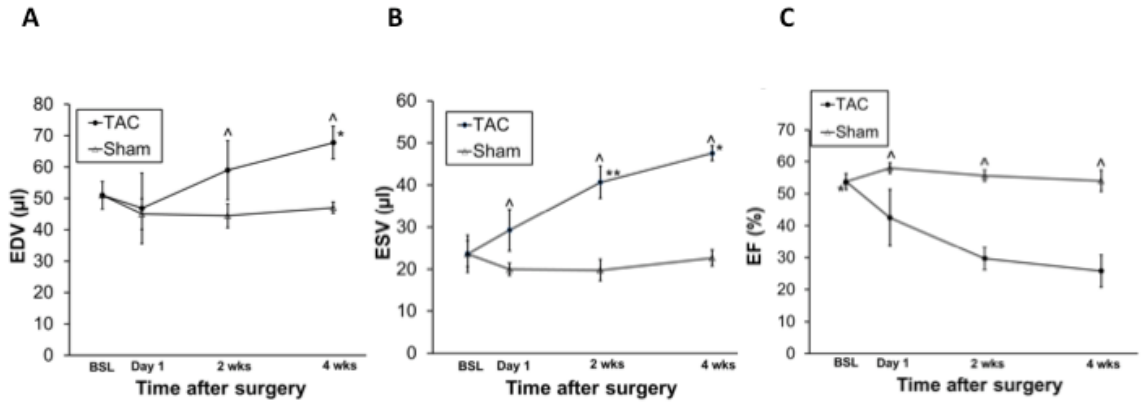

Figure 3.3 Functional changes accompany metabolic changes in response to high workload. (A) End-systolic volume (ESV), (B) end-diastolic volume (EDV), and resultant (C) ejection fractions (EF) were assessed *in vivo* using MRI. An increase in ESV and decline in EF is present 1 day after TAC. Sham operated mice exhibited no significant change in EDV, ESV and EF over 4 weeks. n=8 for TAC group and n=5 for the shams. All data are mean ± SD. In the plot for ESV, *p<0.005 vs BSL and 1d; **p<0.05 vs BSL and 1d. In the plot for EDV, *p<0.01 vs BSL and 1d. In the EF plot, *p<0.05 vs 1 d, 2 wks and 4 weeks; ^p<0.05 between the TAC and sham groups on the same day. Data are from Dr. Kundu's lab at The University of Virginia.

3.2.2. My central hypothesis: Load-Induced mTOR Activation Requires Glucose

Because metabolic changes occur instantaneously in response to increased workload *in vivo* (as seen above already 1 day after TAC), it was difficult to distinguish whether the 'load-induced' changes in contractile function and mTOR activation were in fact metabolically regulated or not. At this point, it remained a distinct possibility that the heart's observed increased reliance upon glucose *in vivo* occurred simultaneously, but independently, to the changes in cardiac growth. In order to determine whether load-induced mTOR activation and contractile dysfunction is regulated by glucose

metabolism, cardiac substrate supply and workload were *independently* modulated *ex vivo*. I performed four sets of matched perfusions: (1) at normal workload (near-physiologic) with acetoacetate plus propionate (control with only non-carbohydrate substrates, NCS) (2) at increased workload (high physiologic) with NCS (control) (3) at normal workload with glucose (at physiologic 5 mM concentration) as the only substrate (4) at increased workload with glucose (5 mM) as the only substrate. A second set of rats were pretreated with mTOR inhibitor rapamycin (PO, 4 mg/kg/day) or vehicle control (propylene glycol) 7 days prior to sacrifice. The hearts were subjected to the same protocols to assess whether changes in cardiac power were in fact due to changes in mTOR activation or not. Cardiac power was assessed and the hearts were freeze-clamped at the end of the perfusion protocol at 60 minutes.

We determined that increased workload (depicted as orange) triggers phosphorylation of upstream PI3K and Akt in all rat hearts irrespective of substrate supply. However, increased workload alone is not sufficient to activate TSC2, mTOR, or its downstream targets. Maximal TSC2, mTOR, p70S6K, and 4EBP1 phosphorylation occurs only in hearts perfused with glucose and subjected to increased workload **(Figure 3.4)**.

Others in the lab had previously demonstrated that 7 day rapamycin pretreatment prior to perfusion effectively inhibits mTOR in the isolated working rat heart (Sharma, Guthrie et al. 2007). I now elucidated its effect on the entire mTOR signaling pathway. Rapamcyin pretreatment did not effect PI3K phosphorylation, but inhibited phosphorylation of Akt, TSC2, mTOR, p70S6K, and 4EBP1 in hearts subjected to increased workload with glucose. Not surprisingly, the mTOR signaling cascade was not

activated in hearts perfused at normal, physiological workload in the presence or absence of glucose (blue).

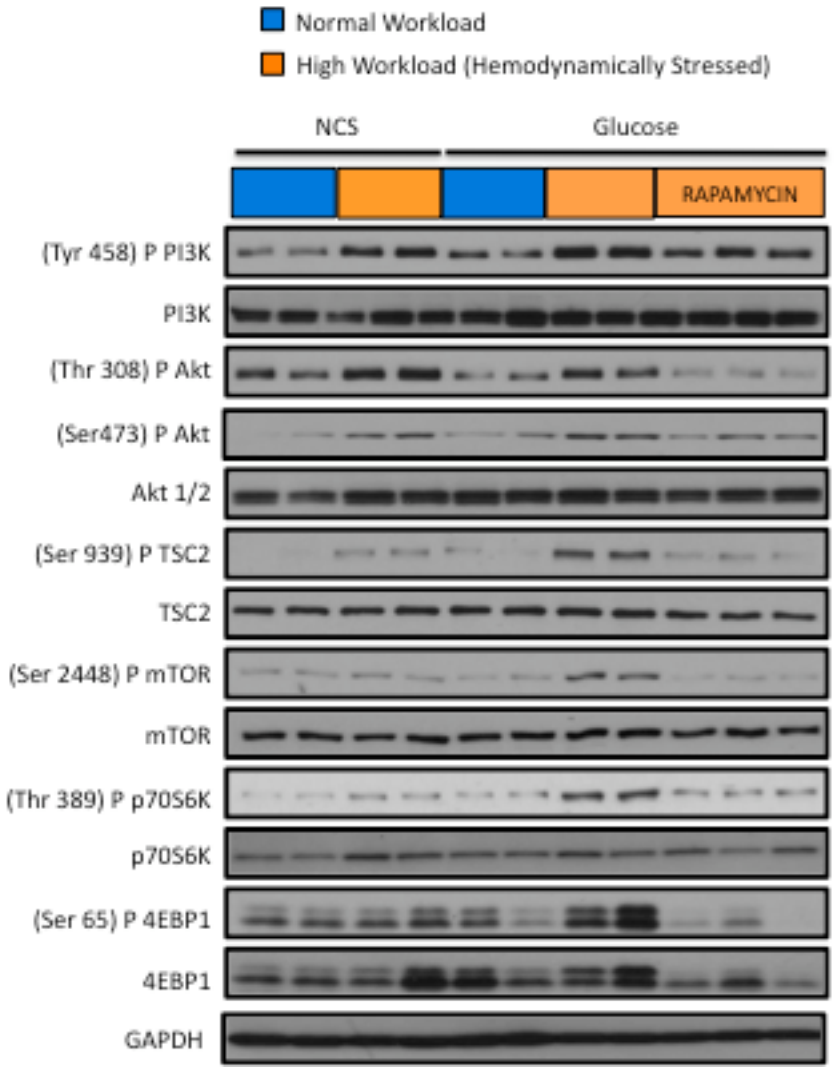

Figure 3.4 In hearts subjected to high workload, glucose activates mTOR. The mTOR signaling pathway was assessed by western blot in isolated working rat hearts perfused as described in **Table 2.2**. Increased phosphorylation of upstream PI3K and AKT were seen in all hearts perfused at high workload. Increased phosphorylation of TSC2, mTOR and p70S6K required glucose at high workload. Rapamycin administration for 7 days (4 mg/kg/day) prior to perfusion inhibited phosphorylation of Akt, TSC2, mTOR, and its downstream targets. The perfusion medium contained no insulin. NCS refers to noncarbohydrate substrates (acetoacetate, 7.5 mM and propionate, 5 mM); Glucose refers to hearts perfused with only glucose (5 mM).

Next I wanted to demonstrate that hearts perfused *ex vivo* with physiological concentrations of glucose, fatty acids, acetoacetate, and propionate (mixed) would demonstrate these same properties, we also assessed the phosphorylation of P70S6K and 4EBP1 in hearts perfused with mixed substrates at normal and high workload. Like hearts perfused with glucose alone, hearts perfused with mixed substrates demonstrated increased phosphorylation of P70S6K and 4EBP1 at high workload **(Fig 3.5)**. This suggested that amongst the substrates that perfuse the heart, glucose alone is sufficient for mTOR activation at high workload.

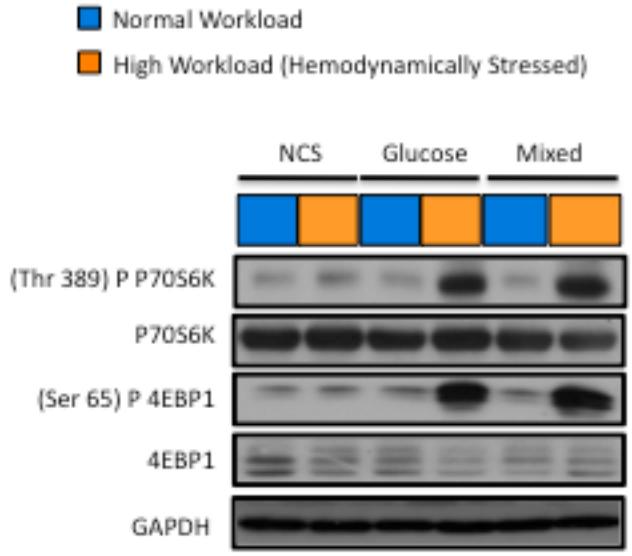

Figure 3.5 In the presence of mixed substrates, mTOR signaling is activated and G6P levels are elevated at high workload. P70S6K and 4EBP1 phosphorylation were increased to the same extent in hearts perfused at high workload with mixed substrates compared to hearts perfused with glucose alone. Data are shown as mean ± SEM, n=5-8. See text and earlier figures for definition of terms. Mixed refers to hearts perfused with a mixture of substrates at physiologic concentrations (glucose at 5 mM, oleate at .4 mM, acetoacetate at 7.5 mM, and propionate at 5 mM).

3.2.3. mTOR Activation Impairs Contractile Function At High Workload

To determine the functional consequence of glucose-mediated mTOR activation, we calculated cardiac power in all perfused hearts **(Figure 3.6)**. Under all conditions, cardiac power was stable both at normal workload and at increased workload, representing the stability of the model. At normal workload, there was no significant difference in cardiac power between hearts perfused with glucose (11.89± 1.3 mW) and hearts perfused with NCS (12.12± 0.83 mW). However, when subjected to increased workload *ex vivo*, hearts perfused with glucose (16.37± 1.5 mW) displayed in a 29% decrease in cardiac power compared to hearts perfused with NCS (18.91± 0.84 mW). Rapamycin pretreatment for 7 days prior to perfusion prevented the decline in contractile function in hearts perfused with glucose at increased workload (20.75± 1.32 mW), suggesting that the decreased cardiac output in hearts perfused with glucose at high workload is mTOR-dependent. The mechanism for this phenomenon is unknown but may relate to the unfolded protein response (see next chapter). Rapamycin had no significant effect on cardiac power in hearts perfused with NCS or in hearts perfused at normal (near-physiological) workload (not shown for clarity).

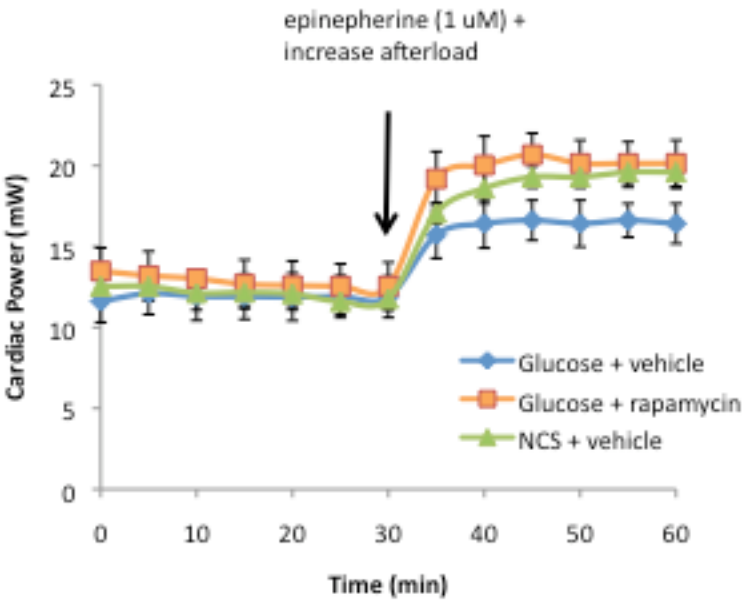

Figure 3.6 In hearts subjected to high workload, cardiac power is impaired when glucose is the only substrate. Rapamycin rescues contractile function. Cardiac power was assessed every 5 minutes throughout each 60 minute perfusion. At normal workload, neither glucose nor rapamycin had an effect on cardiac power. At increased workload, glucose impaired cardiac power. Rapamycin improved contractile function in stressed hearts perfused with glucose. Rapamycin did not change contractile function in hearts perfused with NCS (data not shown for clarity). Data are shown as mean ± SEM, n=5-8, *$p<0.002$ compared to hearts perfused with NCS + vehicle and glucose + rapamycin at high workload.

3.2.4 High Workload Induces A Mismatch Between Rates Of Glucose Uptake And Oxidation

To elucidate the mechanism of glucose-mediated mTOR activation, I assessed rates of glucose uptake and oxidation under all conditions. In vehicle treated rats, rates of glucose uptake (4.2 ± 0.7 μmoles/min/g dry wt) matched rates of glucose oxidation (3.9 ± 0.7 μmoles/min/g dry wt) at normal workload. When subjected to increased workload, rates of glucose uptake (11.5± 0.8 μmoles/min/g dry wt) exceeded rates of glucose oxidation (9.5± 0.6 μmoles/min/g dry wt). Pretreatment with the mTOR inhibitor rapamcyin (4 mg/kg/d) for 7 days prevented this mismatch between glucose uptake and oxidation. Pretreatment of rats with rapamycin reduced rates of glucose uptake (4.4± 0.7 μmoles/min/g dry wt) and glucose oxidation (4.3± 0.7 μmoles/min/g dry wt) when hearts were subjected to increased workload **(Fig. 3.7)**. This observation suggests the following – there is an increase in cardiac efficiency when animals are pre-treated with rapamycin, and the metabolic stress of glucose in the hearts from untreated animals leads to proteotoxicity (discussed below).

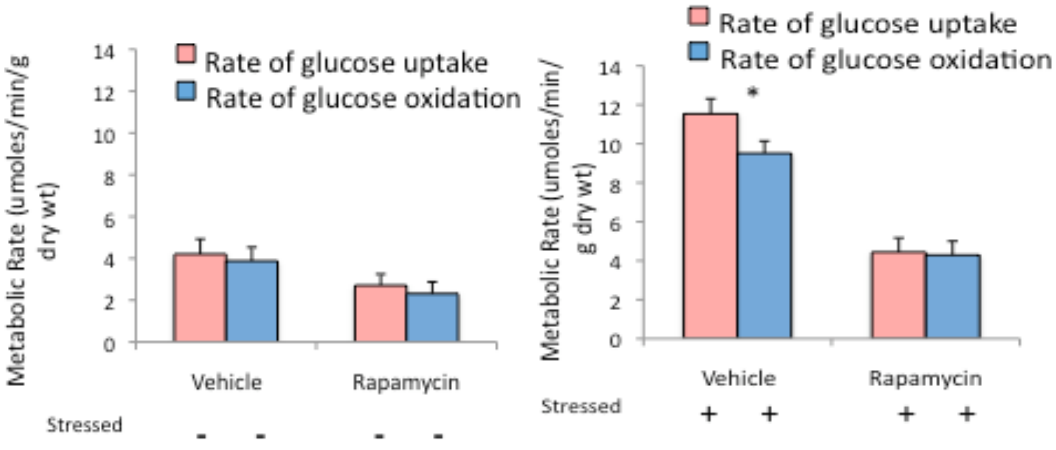

Figure 3.7 Rates of glucose uptake exceed rates of glucose oxidation in response to high workload. Rapamycin corrects this mismatch. Rates of glucose uptake and oxidation were closely coupled at normal workload (in both vehicle and rapamycin treated rats). At high workload, rates of glucose uptake exceeded rates of glucose oxidation in vehicle treated rats. Rapamycin treatment significantly reduced rates of both glucose uptake and oxidation. * $p<0.05$ versus rates of glucose uptake in vehicle treated rats. #$p<.001$ versus metabolic rates in vehicle treated rats.

3.2.5. Glucose 6-Phosphate Accumulates At High Workload as a Consequence of a Mismatch between Rates of Glucose Uptake and Oxidation

Because mTOR activation was associated with a mismatch between glucose uptake and oxidation, we investigated whether the accumulation of glucose or one of its metabolites correlated with mTOR activation. Levels of glucose 6-phosphate (G6P) directly correlated with mTOR activation **(Fig. 3.7-3.8)**. G6P levels were 4.3-fold higher in hearts subjected to an acute increase in workload (4.4± 1.0 nmoles/mg protein) compared to hearts perfused at physiologic workload (1.0± 0.5 nmoles/mg protein). Rapamycin pretreatment blunted G6P levels (0.36± 0.1 nmoles/mg protein) in hearts perfused at increased workload. In contrast, levels of other upstream glycolytic intermediates were unchanged at high workload.

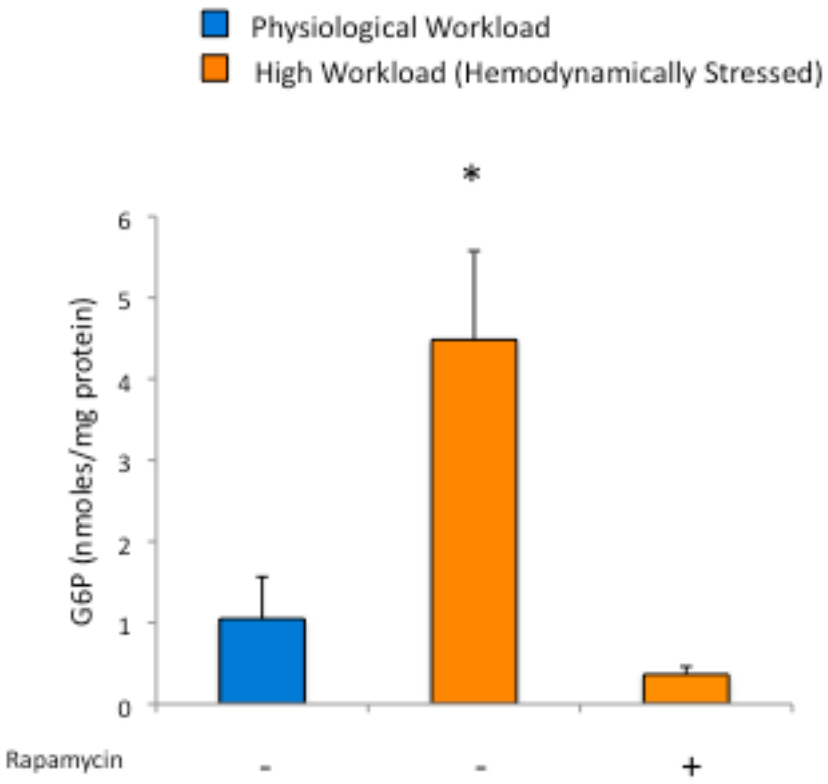

Figure 3.8 G6P accumulates in response to high workload. Cardiac G6P levels were assessed in freeze-clamped hearts. Subjecting hearts to high workload *ex vivo* induced a 4-fold increase in G6P levels, which was reversed with rapamycin treatment. Rapamycin = hearts from animals pretreated with rapamycin for 7 days. See text for further detail.

3.2.6. Accumulation Of Glucose 6-Phosphate Analogue 2-Deoxy-Glucose 6-Phosphate Activates mTOR

To verify whether G6P accumulation was a cause or consequence of mTOR activation in hearts subjected to increased workload, I perfused hearts with the following glucose analogues: (1) 3-O-methylglucose (which is taken up by the cardiomyocyte but not metabolized) and (2) 2-deoxyglucose (which is taken up by the cardiomyocyte, phosphorylated and trapped as a G6P analogue) **(Fig. 3.9)**. Following perfusion, Akt, TSC2, mTOR and p70S6K phosphorylation were assessed in freeze-clamped hearts. At high workload, increased AKT phosphorylation was present when hearts were perfused with both 3-O-methylglucose and 2 DG. However, 3-O-methylglucose was unable to increase phosphorylation of TSC2, mTOR or its downstream target p70S6K in hearts perfused at high workload. However, 2-deoxyglucose phosphorylated TSC2, mTOR and p70s6k to an even greater extent then in hearts perfused with glucose at high workload. mTOR and p70S6K were not phosphorylated in hearts perfused with either glucose analogue at normal workload. Hexose 6-phosphate levels were assessed by enzymatic spectrophotometric analysis and demonstrated that a correlation with mTOR activation in hearts perfused with non-metabolizable glucose analogues, as well **(Fig. 3.10)**. These experiments provide further evidence that G6P is associated with mTORC1 activation in hearts subjected to increased workload.

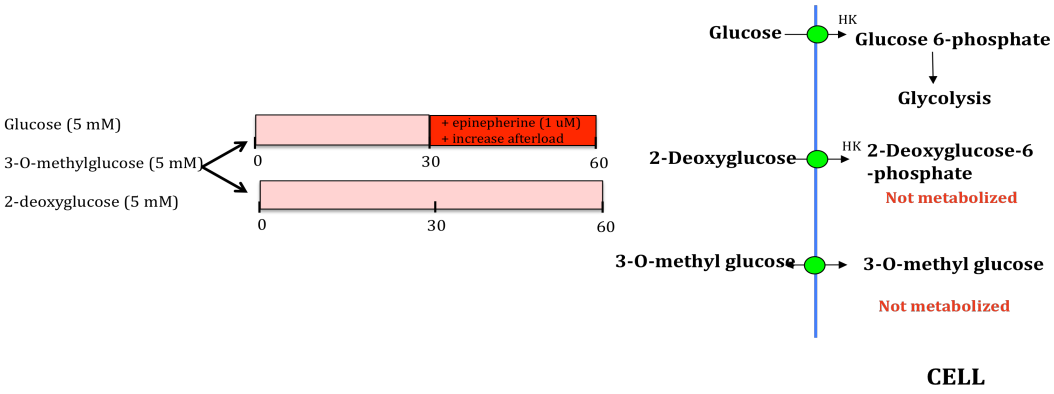

Figure 3.9 Glucose analogues used in isolated working heart perfusions. Hearts were perfused *ex vivo* for either 60 minutes under normal workload (pink) or for 30 minutes under normal workload and subsequently for 30 minutes at high workload (red). Hearts were perfused with either glucose, 2-deoxyglucose (which is phosphorylated by hexokinase and retained in the cardiomyocyte as the G6P analogue, 2-DG 6-P), or 3-O-methylglucose (which cannot be acted upon by hexokinase and remains in the cardiomyocyte as a free glucose analogue). All hearts perfused with glucose analogues were also perfused with acetoacetate (7.5 mM) and propionate (5 mM) for energy provision.

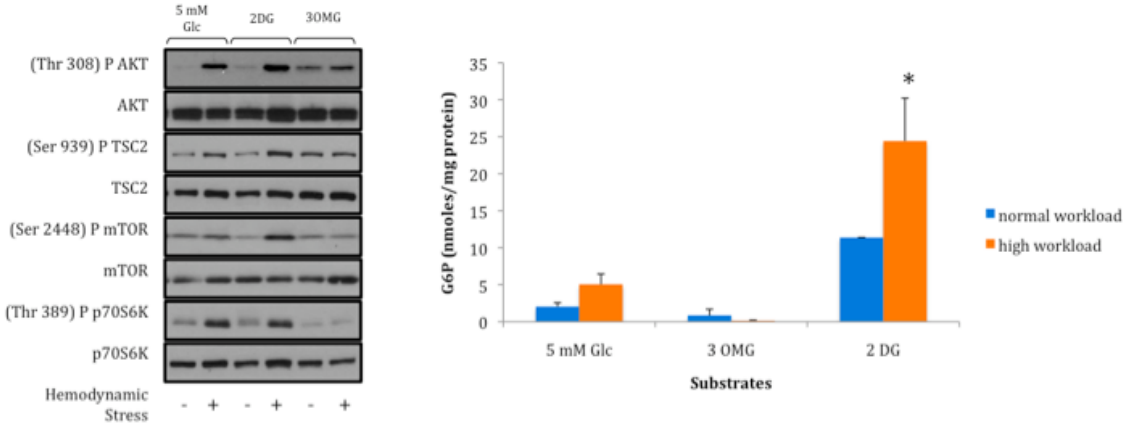

Figure 3.10 Increased phosphorylation of mTOR and p70S6K is associated with increased hexose 6-phosphate levels in hearts perfused with 2DG. Representative western blots of Akt, TSC2, mTOR and p70S6K phosphorylation in hearts perfused with glucose and glucose analogues 2 deoxyglucose (2DG) and 3-O-methylglucose (3OMG) at either normal or high workload. 2DG, but not 3OMG, increased phosphorylation of TSC2, mTOR, and p70S6K at high workload. Hearts perfused with 2DG had significantly increased levels of intracardiac hexose 6-phosphate levels. All hearts perfused with glucose analogues were also perfused with acetoacetate (7.5 mM) and propionate (5 mM) for energy provision.

3.2.7. Glucose 6-Phosphate-dependent mTOR Activation is Mediated By Downregulation of AMPK

Up to this point my data suggest that TSC2 or one of its upstream regulators mediates G6P-dependent mTOR activation in the heart. AMPK is a heterotrimeric enzyme that lies upstream of TSC2 and regulates fuel supply and substrate metabolism in response to the metabolic milieu of the heart. When phosphorylated at Thr 172, AMPK phosphorylates acetyl co-A carboxylase (ACC) at Ser 79, a commonly used marker of AMPK activation, and phosphorylates TSC2 at Ser1387 and RAPTOR at Ser 792 to inhibit mTOR (Young, Cell Metabolism 2008). High glucose-mediated mTOR activation is regulated by a downregulation in AMPK in skeletal muscle (Saha *et al.* Diabetes 2010). I therefore examined changes in AMPK phosphorylation in all perfused hearts. Neither increased workload nor glucose alone was associated with a change in AMPK phosphorylation. However, perfusion at increased workload *with* glucose led to a downregulation of phospho-AMPK (Thr 172), phospho-ACC (Ser 79) and phospho-TSC2 (Ser 1387). Rapamycin treatment prevented the downregulation of AMPK, ACC, and TSC2 phosphorylation. RAPTOR phosphorylation was unchanged with workload or rapamycin treatment **(Fig. 3.11)**.

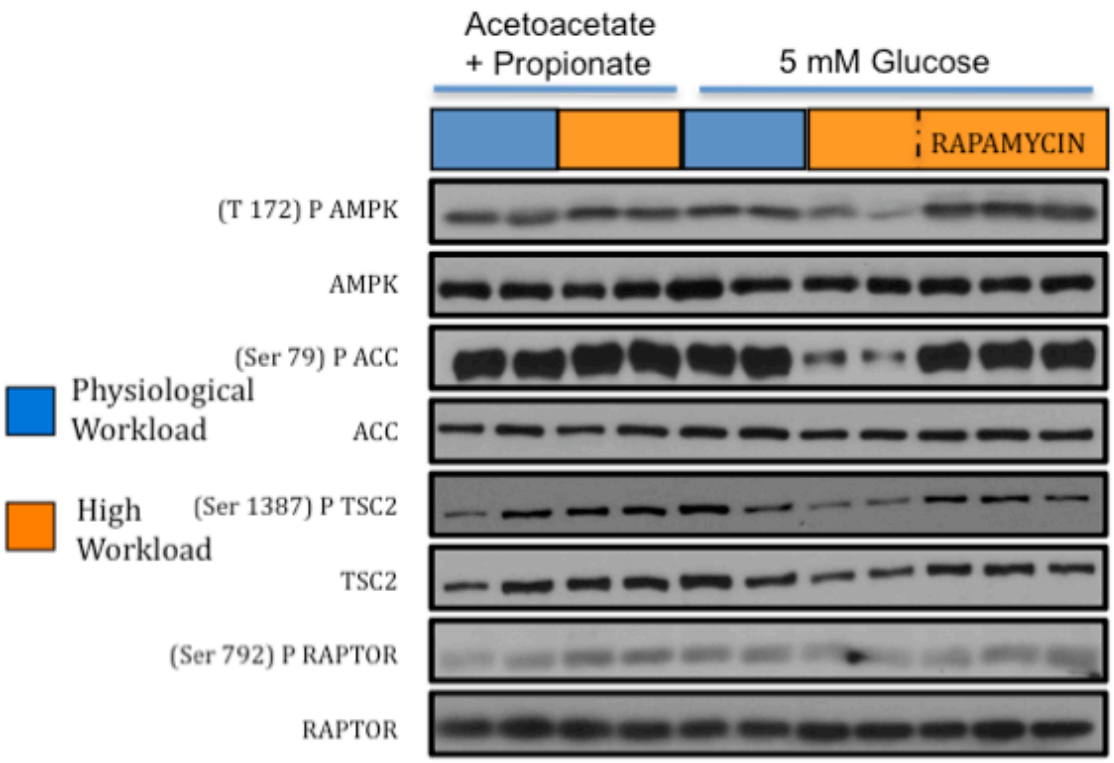

Figure 3.11 G6P-dependent mTOR activation is mediated by AMPK downregulation. (A) Representative western blots demonstrate a reduction in AMPK phosphorylation (T 172) and ACC phosphorylation (Ser 79) in hearts perfused with glucose at high workload.

3.2.8 Metformin Inhibits mTOR Activation and Rescues Contractile Function at High Workload

To confirm whether AMPK downregulation was necessary for glucose-dependent mTOR activation and to determine whether it could be prevented with metformin (AMPK activator) pretreatment, rats were systemically pre-treated with either control (NaCl) or metformin *in vivo* for 7 days (IP, 250 mg/kg/d or 500 mg/kg/d) prior to being perfused with glucose at high workload. Compared to control treatment, metformin prevented AMPK downregulation and inhibited mTOR, p70S6K, and 4EBP1 phosphorylation in a dose-dependent manner **(Fig. 3.12)**. In order to determine whether these effects were due to metformin's systemic effects or direct effects in the heart, I perfused hearts with glucose at high workload in buffer that contained metformin at three doses (5 mM, 7.5 mM, 10 mM). *Ex vivo* perfusion with metformin also prevented AMPK downregulation and inhibited mTOR, p70S6K, and 4EBP1 phosphorylation in a dose-dependent manner in hearts perfused at high workload with glucose **(Fig. 3.12)**.

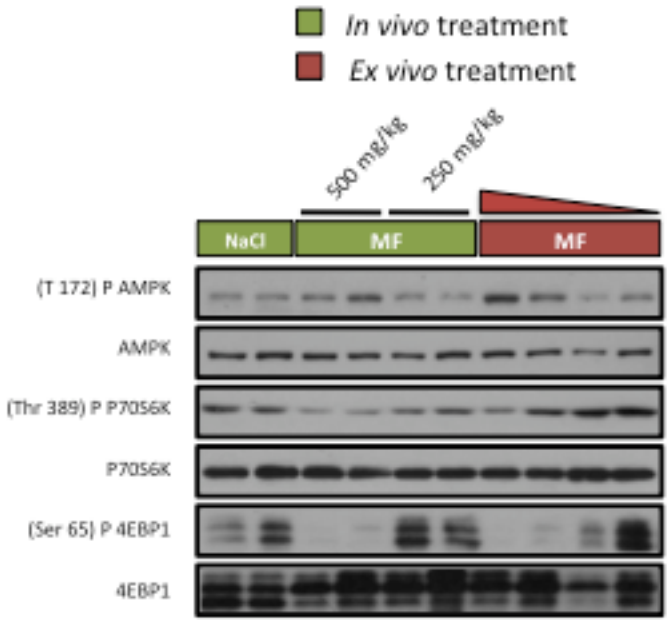

Figure 3.12 G6P-dependent mTOR activation is inhibited by metformin. Both *in vivo* metformin prior to perfusion and *ex vivo* metformin during perfusion increased AMPK phoshphorylation and prevented P70S6K phosphorylation in a dose-dependent manner.

We assessed rates of glucose uptake and oxidation as well as cardiac glucose 6-phosphate levels in these hearts, as well. In unstressed hearts (perfused at normal physiologic workload), systemic *in vivo* metformin treatment did not significantly change rates of glucose uptake or glucose oxidation. In hearts subjected to high workload, *in vivo* metformin treatment did not change rates of glucose uptake (11.7± 1.1 μmoles/min/g dry) but increased rates of glucose oxidation (11.0± 0.7 μmoles/min/g dry) and blunted G6P accumulation compared to vehicle treated animals **(Fig 3.13)**. Metformin improved cardiac power 26% in hearts perfused at increased workload with glucose **(Fig. 3.14)**. Metformin treatment had no effect on mTOR phosphorylation or cardiac power in hearts perfused at physiologic workload.

The major regulator of AMPK is a shift in the AMP:ATP ratio. Therefore, I also assessed AMP, ADP, and AMP levels in all perfused hearts. Surprisingly, I found no significant change in their levels under any perfusion condition **(Table 3.1)**.

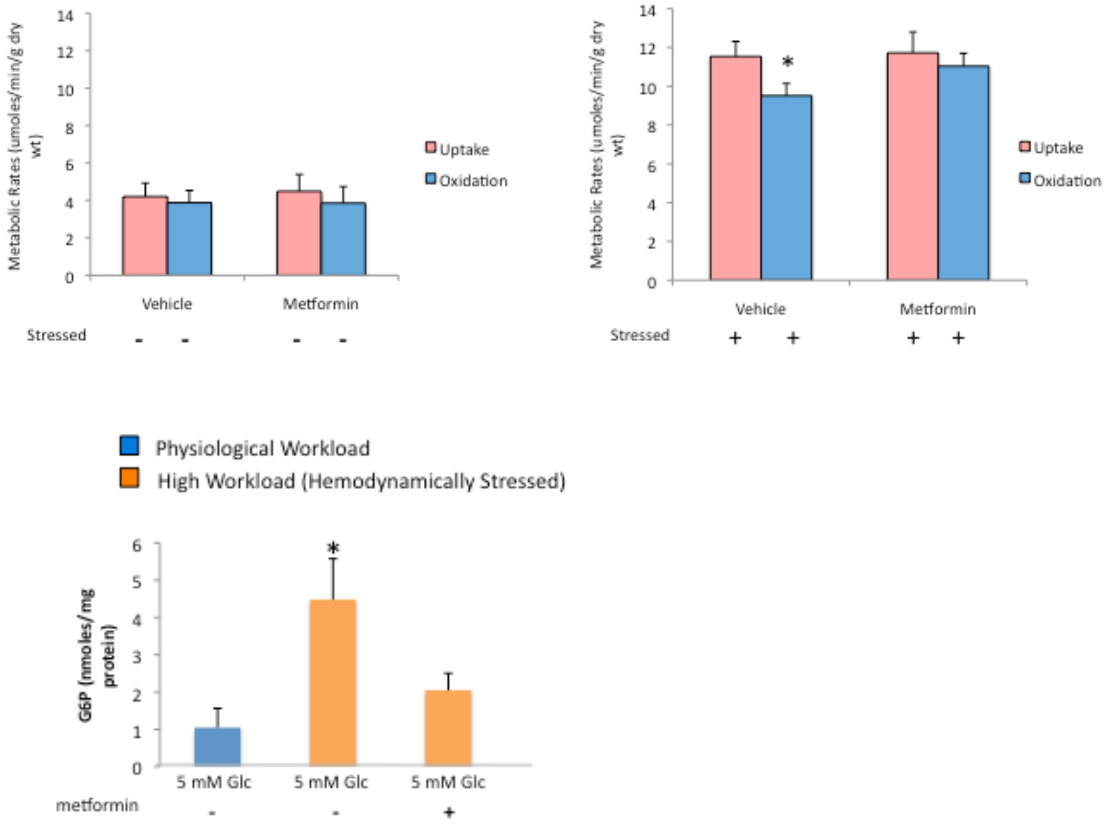

Figure 3.13 Metformin treatment corrects the mismatch between rates of glucose uptake and oxidation at high workload and blunuts G6P accumulation. Rates of glucose uptake and oxidation were closely coupled at normal workload (in both vehicle and metformin treated rats). At high workload (stressed), metformin corrected the mismatch between rates of glucose uptake and oxidation (top). G6P accumulation was reduced in hearts perfused at high workload with glucose after metformin treatment (bottom). * $p<0.05$ versus rates of glucose uptake in vehicle treated rats. #$p<.001$ versus metabolic rates in vehicle treated rats.

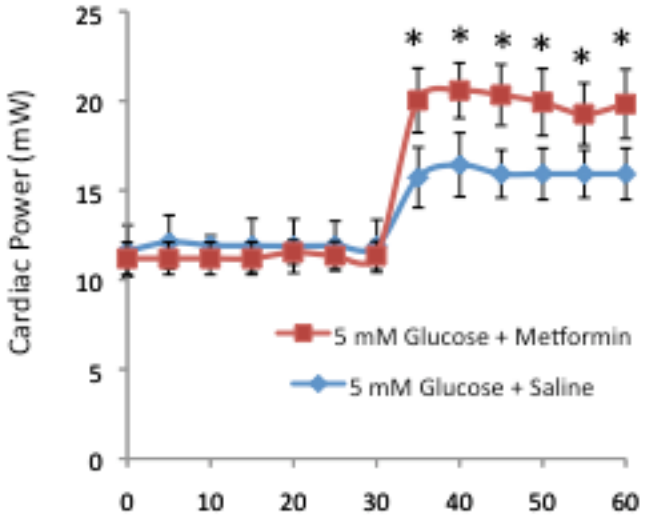

Figure 3.14 Metformin treatment improves cardiac power at high workload. Contractile performance in the isolated working rat heart perfused with glucose in the presence and absence of metformin treatment. n=5-8; *p<0.05

	Perfused at low workload with:				Perfused at high workload with:				
	AcAc + P	Glucose	3OMG	2DG	AcAc + P	Glucose		3OMG	2DG
						Veh	Rapa		
ATP	278.95±28.8	270.72±29.4	288.06±14.6	286.07±15.3	296.02±13.4	302.85±31.8	285.31±28.5	292.69±21.6	281.53±19.0
ADP	34.22±4.8	36.31±3.8	40.77±3.6	36.99±2.8	37.32±.8	38.06±5.2	41.67±3.6	38.54±4.6	38.74±3.7
AMP	33.47±3.4	26.93 ± 4.6	29.65 ± 4.1	26.79 ± 3.2	28.63 ± 3.3	29.74±1.4	33.36±4.0	33.11±2.9	27.09±3.6

Table 3.1 Cardiac ATP, ADP, and AMP levels in ex vivo perfused hearts. Data are presented as nmoles/mg protein. AcAc+P (Acetoacetate+Propionate); 3OMG (3-O-Methylglucose); 2DG (2-Deoxy-glucose); Veh (Vehicle); Rapa (Rapamycin); ATP (adenosine triphosphate); ADP (adensoine diphosphate); AMP (adenosine monophosphate). All data are presented as mean ± SEM in units of µmol/mg protein. n=5-7

3.2.9 Glucose Phosphorylation Modulates mTOR Activation *in vivo* (TAC and ACSL-/- mice)

To determine whether changes in glucose metabolism led to G6P accumulation in mouse hearts subjected to increased workload *in vivo*, I assessed cardiac G6P accumulation and mTOR activation in mice that were sacrificed one day and two weeks after transverse aortic constriction (TAC). We selected hearts at one day (before significant structural and functional changes) and two weeks (after significant structural and functional changes) after TAC in order to check the validity of our hypothesis that metabolic changes precede, trigger, and sustain structural and functional changes in hearts subjected to increased workload *in* vivo. Cardiac G6P levels are 2.3-fold and 4.6-fold higher compared to sham-operated animals 1 day and 2 weeks after TAC, respectively **(Fig. 3.15)**. Both P70S6K and 4EBP1 phosphorylation were significantly increased both 1 day and 2 weeks after TAC compared to sham-operated mice **(Fig 3.16)**.

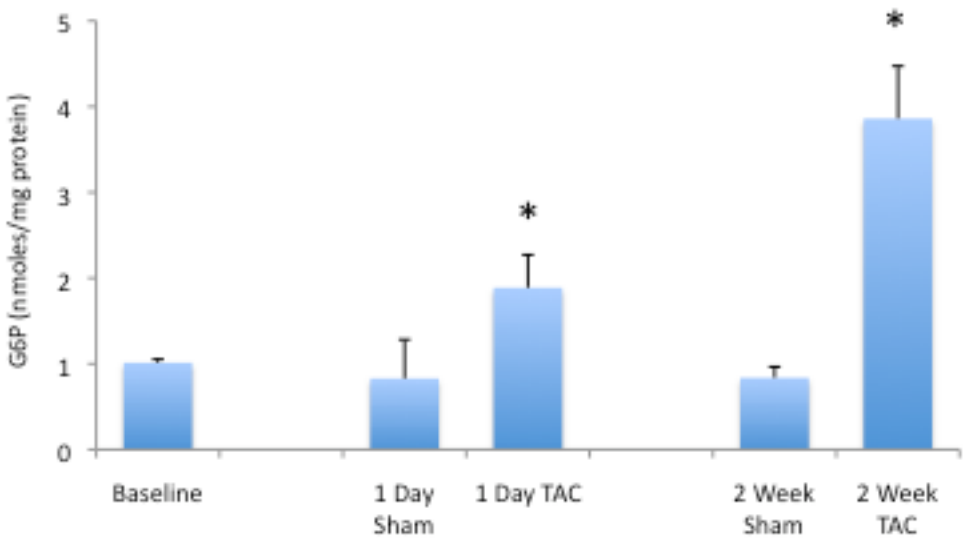

Figure 3.15 Early metabolic changes are associated with G6P accumulation in hearts subjected to high workload *in vivo*. Intracardiac G6P levels are 2.3-fold and 4.6-fold higher compared to sham-operated animals 1 day and 2 weeks after TAC, respectively. n=5-8; *p<0.05

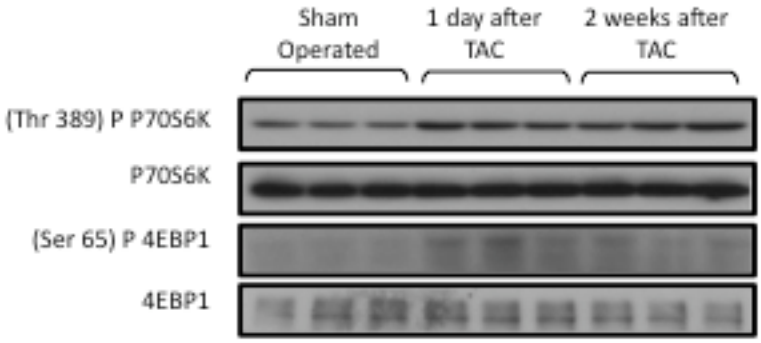

Figure 3.16 Early metabolic changes are associated with mTOR activation in hearts subjected to high workload *in vivo*. Representative western blots demonstrate an increase in p70S6K and 4EBP1 phosphorylation 1 day and 2 weeks after TAC. n=8 for the TAC and n=5 for the sham operated mice. *p<.002

Next, I tested my hypothesis in a genetic model that was metabolically similar to the pressure overload-induced hypertrophied heart by using the cardiac specific long-chain acyl coenzyme A synthetase (ACSL) -/- mouse. ACSL is necessary to activate fatty acids to their acyl coenzyme A counterparts before they can be oxidized. Accordingly, mice hearts lacking ACSL have marked reductions in fatty acid oxidation and rely primarily on carbohydrate metabolism for energy provision (Ellis, Mentock et al. 2011). As already observed in the *ex vivo* hearts subjected to increased workload, hearts from ACSL -/- mice demonstrate a downregulation of AMPK and an activation of mTOR in the absence of any increased mechanical load placed on the heart (Ellis, Mentock et al. 2011). Moreover, the changes in AMPK signaling are independent of any change in the AMP/ATP ratio, as well. We assessed G6P accumulation in these mouse hearts and demonstrated that G6P accumulation was associated with mTOR activation in this mouse model, as well **(Fig 3.17)**.

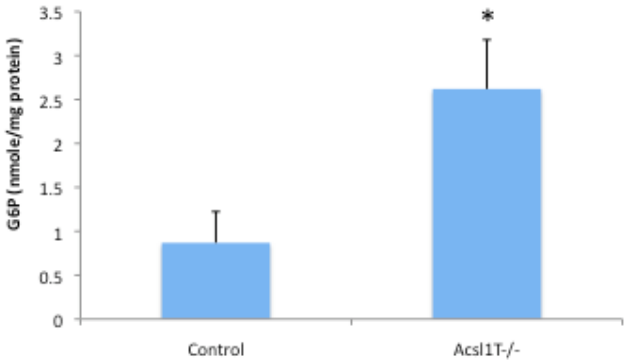

Figure 3.17 G6P accumulation correlates with mTOR activation in the ACSL -/- mouse. Intracardiac G6P levels are 2.5-fold higher in ACSL -/- mice compared to WT mice. N=5. Data are presented as mean ± SEM.

3.2.10 Mechanically unloading failing human hearts with a left ventricular assist device (LVAD) reduces Glucose 6-Phosphate levels and mTOR Activation

When the human heart is subjected to sustained increases in workload it ultimately fails. Changes in substrate energy have been observed in failing human hearts metabolism (Razeghi, Young et al. 2001; Kato, Niizuma et al. 2010), but the effect of mechanical unloading on intermediary glucose metabolism and mTOR signaling is not known. In order to gain insight into whether 'load-induced' cardiac growth is governed by G6P accumulation in the failing human heart, I obtained cardiac tissue from Dr. O.H. Frazier and his team at the Texas Heart Institute during LVAD implantation and again during explantation from 11 non-diabetic patients with idiopathic dilated cardiomyopathy and assessed the tissue for changes in G6P concentration and mTOR activation. G6P levels significantly decreased after mechanical unloading **(Fig. 3.18A-B)** as did phosphorylation of p70S6K and 4EBP1 **(Fig. 3.18C)**.

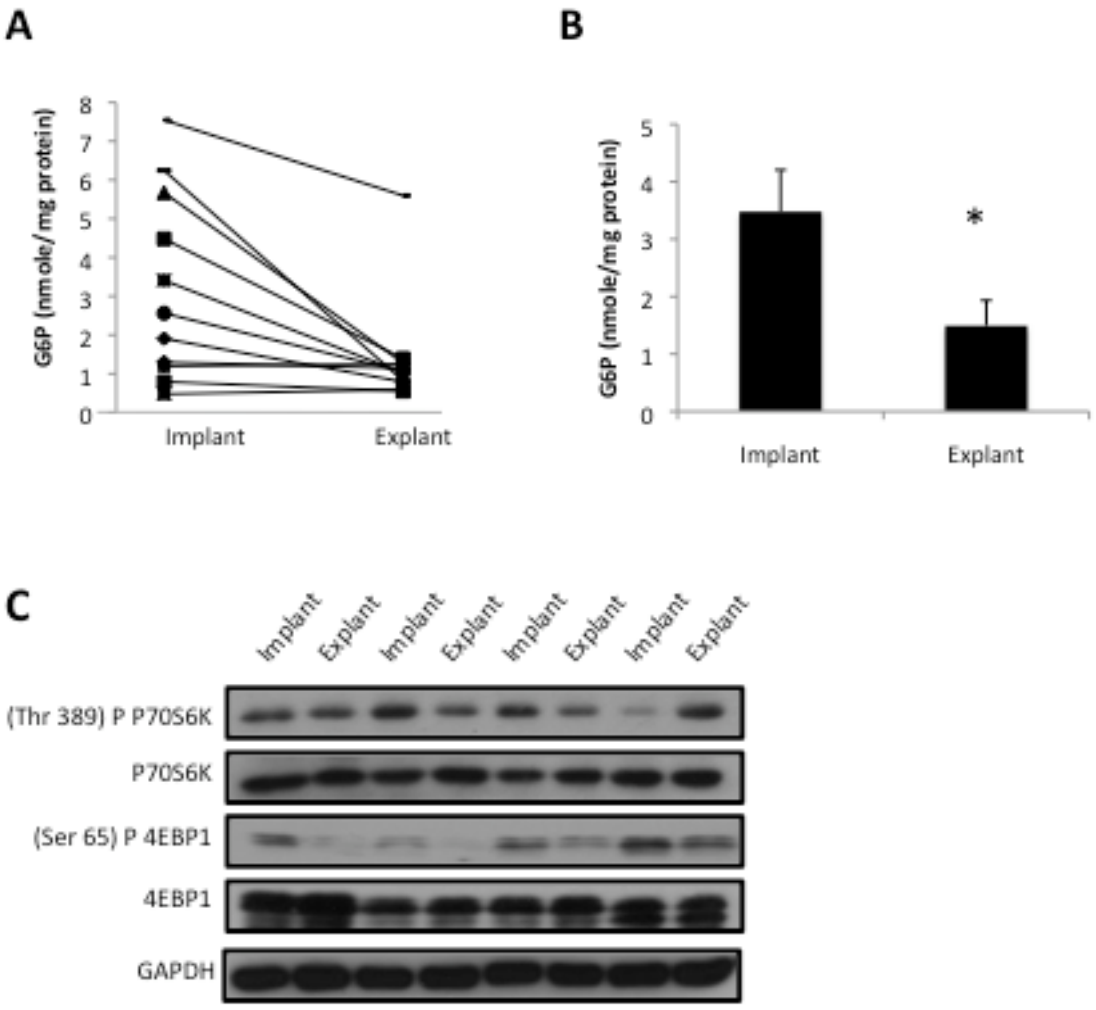

Figure 3.18 Mechanical Unloading of Failing Human Hearts Reduces G6P accumulation and mTOR activation. (**A)** Intracardiac G6P levels in each patient with idiopathic dilated cardiomyopathy before after mechanical unloading. **(B)** Average G6P levels demonstrate a dramatic reduction at time of explant from LVAD. **(C)** Representative western blots demonstrate a reduction in mTOR downstream targets P70S6K and 4EBP1 in failing human hearts after mechanical unloading. n=11 paired samples. Panel A traces individual patients. Panel B shows mean ± SEM* $p < 0.05$

3.3 Discussion

Hemodynamic stress induces instant quantitative and qualitative changes in the use of energy providing substrates (Goodwin, Taylor et al. 1998). The structural and functional response to increased workload has been extensively studied in the murine transverse aortic constriction (TAC) model (Rockman, Ross et al. 1991). How the metabolic response to increased workload regulates these changes has previously not been investigated.

I interrogated the consequences of these early metabolic changes and demonstrated that signals generated by glucose metabolism are associated with mTOR activation and impaired contractile function. The main findings are: 1) In hearts subjected to increased workload *in vivo*, metabolic remodeling precedes structural remodeling of the heart and accompanies load-induced mTOR activation and contractile dysfunction. 2) Doubling the workload *ex vivo* increases rates of myocardial glucose uptake beyond the heart's oxidative capacity, resulting in G6P accumulation, which mediates load-induced mTOR activation. 4) Correcting the mismatch between glucose uptake and oxidation in the stressed heart with mTOR inhibitor rapamcyin or AMPK activator metformin prevents G6P accumulation and rescues contractile function in hearts subjected to increased workload. 5) In the failing human heart, mechanical unloading decreases levels of G6P as well as phosphorylation of p70S6K and 4EBP1. This makes it likely that G6P induced changes in mTOR activation and ER stress are of clinical relevance for the failing human heart.

While the normal heart primarily oxidizes fatty acids (Bing, Siegel et al. 1954), increased energy requirements of hearts subjected to high workload are met by the oxidation of carbohydrates (Goodwin, Taylor et al. 1998). The classic explanation for this phenomenon is based on the fact that the heart oxidizes the most efficient substrate for a given situation (Taegtmeyer, Hems et al. 1980). Specifically, it can be reasoned that at a high workload the heart would prefer to utilize glucose since it generates more moles of ATP per O_2 consumed compared to fatty acids (Korvald, Elvenes et al. 2000). I asked myself the question: what if changes in substrate utilization regulate more than just energy provision?

It is already known that aside from merely providing energy for cell function, glucose metabolites regulate gene expression in the liver and pancreatic β-cell (Girard, Ferre et al. 1997; Schuit, Huypens et al. 2001) and that long-chain fatty acids are ligand activators of PPARα in the heart (Finck and Kelly 2007). The lab initially had asked the question: could glucose-driven metabolic gene expression also occur in the heart? Previous work demonstrated that changes in glucose metabolism *are* linked to transcriptional changes in gene expression in the heart (Young, Yan et al. 2007). More specifically, we recently suggested that the metabolite G6P mediates activation of transcription factor carbohydrate responsive binding protein (Li, Chen et al. 2010). This work was conducted in parallel with our studies showing that glucose metabolism is required for insulin-dependent mTOR activation in the heart (Sharma, Guthrie et al. 2007). I now provide new evidence that load-induced mTOR activation and contractile dysfunction is mediated by G6P, as well.

My mechanistic studies *ex vivo* stemmed from our observations made in mice subjected to an increase in workload *in vivo*. Compared to hearts from sham-operated mice, hearts from banded mice demonstrated enhanced glucose uptake, G6P accumulation, mTOR activation and contractile dysfunction one day after TAC prior to the presence of structural changes. When increased workload was sustained via TAC for up to 4 weeks, increasing cardiac hypertrophy (assessed by our collaborators with cardiac MRI and confirmed by us with HW/BW measurements) directly correlated with continued increases in FDG retention and G6P accumulation, which suggested that metabolic remodeling precedes and potentially triggers and sustains structural remodeling of the heart.

Previous studies have largely ignored whether cardiac substrate metabolism can regulate 'load-induced' hypertrophy and contractile dysfunction (Shioi, McMullen et al. 2003; McMullen, Sherwood et al. 2004; Zhang, Contu et al. 2010). In order to address this issue I utilized the isolated working heart model. The isolated working rat heart allows a dynamic minute-by-minute assessment of metabolism and function and permits us to assess intracellular metabolite concentrations and activation of the major regulatory proteins along the mTOR signaling cascade at the end of the perfusion. The *ex vivo* isolated working heart model also provided us complete control over workload, substrate concentration and hormone supply. My findings *ex vivo* demonstrated that an acute increase in workload alone is *not* sufficient to activate mTOR in the absence of glucose. Only in the presence of glucose did hearts subjected to high workload demonstrate increased phosphorylation of mTOR and its downstream targets p70S6K and 4EBP1, suggesting that 'load-induced' hypertrophic signaling through mTORC1 *is* in fact

substrate-dependent. More specifically, our data suggested mTORC1 is activated by the metabolic signal G6P, which accumulates at increased workload when rates of glucose uptake exceed the heart's oxidative capacity.

TSC is the primary critical signaling node upstream of mTORC1 regulated by differential phosphorylation on numerous TSC2 serine and threonine residues (Huang and Manning 2008). I dissected the load and substrate-dependence of mTORC1 signaling in the heart and determined that increased workload alone triggers PI3K, Akt, and minimal Akt-dependent phosphorylation of TSC2 at Ser939 phosphorylation, both in the presence and absence of glucose. However, complete load-induced mTORC1 activation required not only Akt-dependent phosphorylation of TSC2 at Ser939 but also a downregulation of AMPK-dependent phosphorylation of TSC2 at Ser1387 (Shaw, Bardeesy et al. 2004), which occured with G6P accumulation. Indeed, AMPK activation with metformin, both *in vivo* and *ex vivo*, prevented G6P-mediated mTOR activation at increased workload in a dose-dependent manner.

In skeletal muscle, high levels of glucose activate mTOR in an AMPK-dependent manner by modulating redox state (Saha, Xu et al. 2010). In the heart, the redox state does not change with workload (Taegtmeyer 1985). Indeed, lactate levels and lactate-to-pyruvate ratio were unchanged in hearts perfused with glucose at high workload indicating no significant changes in the cytosolic state, and presumably, the nuclear redox state (NAD^+-to-NADH ratio). However, like in skeletal muscle, AMPK downregulation by glucose in the heart occurs independent of the energy state, which is consistent with previous work that has demonstrated no change in the energy charge of the heart with increased workload both *ex vivo* (Taegtmeyer 1985) (Neely, Denton et al.

1972) and *in vivo* (Balaban, Kantor et al. 1986). AMPK is activated by the AMP/ATP ratio in the heart (Young, Li et al. 2005). However, studies have also suggested that metabolites such as long-chain fatty acids can activate AMPK *without* accompanying changes in AMP and ATP levels in skeletal muscle (Clark, Carling et al. 2004).

In the genetically modified ACSL -/- mouse, which preferentially upregulates cardiac glucose metabolism (like a heart subjected to increased workload), G6P levels are elevated, AMPK is downregulated, mTOR signaling is activated, and hearts hypertrophy independent of change in the AMP/ATP ratio, as well (Ellis, Mentock et al. 2011). Taken together, our studies highlight that 'load-induced' mTOR activation is mediated by changes in glucose metabolism.

The two major isoforms of transporters that shuttle glucose into the cardiomyocyte are GLUT1 (glucose transporter responsible for basal glucose transport independent of insulin) and GLUT4 (glucose transporter responsible for insulin-mediated glucose transport into the cardiomyocyte). Interestingly, hearts overexpressing GLUT1 hypertrophy (Liao, Jain et al. 2002) as do hearts deficient in GLUT4 likely secondary to compensatory GLUT1 overexpression (Abel, Kaulbach et al. 1999). These data support our hypothesis that non-insulin mediated glucose uptake likely plays a major role in mediating cardiac growth. Glucose uptake is increased in both models, which gives indirect support to my hypothesis. Neither group assessed the role of intermediary metabolite accumulation or mTOR activation in their models.

Enhanced glucose uptake in the heart has been associated with contractile dysfunction and deemed 'glucotoxic' by increasing flux through the hexosamine

biosynthetic pathway, dysregulating protein glycosylation, and producing reactive oxygen species (Ren and Davidoff 1997; Modesti, Bertolozzi et al. 2005). Interestingly, genetically modified mice that take up excess glucose but also demonstrate enhanced glycolytic flux are, however, protected from glucotoxicity (Liao, Jain et al. 2002; Taegtmeyer, McNulty et al. 2002). Taken together, these data support our hyopthesis that intermediary glucose metabolite (G6P) accumulation may be imposing a metabolic stress on the heart and contributing to contractile dysfunction in an mTOR-dependent manner.

Rapamycin pretreatment rescued G6P-mediated cardiac dysfunction at increased workload. Rapamycin is well known for its ability to bind and disrupt the mTOR complexes (Yip, Murata et al. 2010). I now provide compelling evidence that its metabolic effects on the heart may mediate its inhibition of mTOR and its downstream targets, as well. Prolonged rapamycin treatment inhibits mTORC2 assembly, which prevents phosphorylation of Akt (Sarbassov, Ali et al. 2006), a known regulator of glucose uptake in the heart (Cong, Chen et al. 1997). Therefore, not surprisingly, I observed that rapamycin administration reduced Akt phosphorylation and blunted rates of glucose uptake at increased workload. In doing so, rapamycin prevented the mismatch between glucose uptake and oxidation, depleted intracardiac G6P, inhibited the phoshporylation of mTOR and its downstream targets, and improved contractile function at high workload.

Interestingly, rapamycin improved cardiac power despite lowering rates of myocardial glucose uptake and oxidation to levels nearly equivalent to hearts beating against a normal workload may seem paradoxical. One may ask: how can the heart

perform better when it is oxidizing less substrate? From an energetic perspective, the data suggests that the increased energy requirements of hearts subjected to high workload, which are met by the oxidation of carbohydrates, may no longer be necessary in hearts of rats treated with rapamycin. I will expand upon the mechanism in the next chapter. The improvement in cardiac power observed in rapamycin treated rats also gives credence to the hypothesis that the hypertrophic process may not be necessary to maintain systolic function in hearts subjected to increased workload (Hill, Karimi et al. 2000).

While metformin is known to improve cardiac function in murine models of heart failure (Gundewar, Calvert et al. 2009; Yin, van der Horst et al. 2011), its ability to alleviate contractile dysfunction in hearts subjected to increased workload has yet to be studied. I demonstrate that when administered directly to the heart *ex vivo* or systemically *in vivo*, metformin enhances the heart's capacity to oxidize glucose, reduces intracardiac G6P levels, inhibits mTOR activation and improves contractile function in a dose-dependent manner. Therefore, I propose that like rapamycin, metformin metabolically protects hearts subjected to increased workload and in doing so may account for improving survival in diabetic patients with heart failure (Aguilar, Chan et al. 2011). Whereas metformin decreases substrate supply to the heart by lowering circulating nonesterified free fatty acids, inhibiting hepatic gluconeogenesis, improving peripheral glucose uptake, and improving energy homeostasis (Wang, Zhang et al. 2011), insulin sensitizers, such as thiazolidinediones (TZDs) increase substrate uptake to the insulin-responsive heart. Despite decreasing circulating free fatty acid levels, TZDs therefore further flood the metabolically overloaded heart as we have previously

demonstrated by measuring rates of substrate utilization in the *ex vivo* perfused heart (Golfman, Wilson et al. 2005). It is possible that this contributes to explaining the increased risk of heart failure and adverse cardiac events associated with their use (Dormandy, Charbonnel et al. 2005) (Lincoff, Wolski et al. 2007; Graham, Ouellet-Hellstrom et al. 2010).

Our studies also implicate a critical role for dysregulated glucose metabolism in cardiac growth signaling in human heart failure. I observed a significant decrease in G6P accumulation in human heart failure tissue samples after LVAD support (as was seen in our rodent hearts treated with rapamycin and metformin). We have previously observed a trend for decreased myocardial glycogen content in failing human hearts after mechanical unloading (Razeghi and Taegtmeyer 2004) and more recently, proteomic analysis has revealed an upregulation of proteins involved in glycolysis, energy, and oxidative metabolism in LVAD supported patients (de Weger, Schipper et al. 2011). Moreover, our finding that markers of mTOR activation are downregulated following LVAD support is also consistent with studies by Baba *et al.* that reported decreased myocyte size and decreased activity of Akt with mechanical unloading (Baba, Stypmann et al. 2003). Taken together, these studies suggest that *mechanical* unloading with LVAD may also metabolically unload the heart by promoting a re-coupling of glucose uptake and oxidation, preventing intermediary metabolite accumulation, and conserving energy in the failing heart in an mTOR-dependent manner. To date, no reliable marker exists to predict which patients will benefit most from LVAD placement. Unfortunately, in our 11 patient samples there is no data available on cardiac ejection fraction at time of explantation. However, it is tempting to speculate that a metabolic parameter, such as

cardiac G6P levels, could be useful in identifying which patients would benefit most from LVAD placement. Due to the difficulty in obtaining myocardial tissue samples and assessing substrate flux in humans, it remains difficult to more accurately assess the effects of mechanical unloading on myocardial energetics and glucose utilization in the heart.

In conclusion, in this chapter I have demonstrated that metabolic remodeling precedes, triggers, and sustains structural remodeling of the heart. Specifically, I have identified that dysregulated glucose metabolism (uptake in excess of oxidation) and subsequent G6P accumulation mediate load-induced mTOR activation and contractile dysfunction. Our study highlights the importance of intermediary metabolism as a rich source of signals for cardiac growth and demonstrate the potential to reduce internal work and improve cardiac efficiency by targeting the metabolic axis in load-induced heart disease.

CHAPTER 4: SUSTAINED mTOR ACTIVATION INDUCES ENDOPLASMIC RETICULUM STRESS

4.1 Introduction

While the previous chapter detailed the upstream metabolic regulation of 'load-induced' mTOR signaling, this chapter focuses on its downstream consequences. Stated otherwise, it seeks to answer the question: why does sustained mTOR activation lead to contractile dysfunction both *in vivo* and *ex vivo*? Phosphorylation of mTOR and its downstream targets triggers protein synthesis by promoting mRNA translation and ribosomal biogenesis (Mayer and Grummt 2006) and inhibiting protein degradative processes such as autophagy (Kroemer, Marino et al. 2010) and the ubiquitin proteasome system (Depre, Wang et al. 2006; Depre, Powell et al. 2010).

Normal contractile function of the cardiomyocyte requires all synthesized proteins to be properly folded (Sanbe, Osinska et al. 2005). Molecular chaperones located in the endoplasmic reticulum (ER) ensure the proper folding of many proteins by identifying hydrophobic segments of misfolded or unfolded proteins and refolding them into functioning proteins. In doing so, the ER is able to prevent the formation of toxic protein aggregates in the unstressed heart (Ron and Walter 2007). Mice expressing mutant molecular chaperone proteins develop cardiomyopathy secondary to the accumulation of protein aggregates (Maloyan, Osinska et al. 2009). Fortunately, with the notable exception of cardiac amyloidosis, not many primary protein-folding disorders have been identified. However, proteotoxicity in the stressed heart may be more common that generally assumed and it may be metabolically regulated.

In the *in vivo* hemodynamically stressed heart, activation of mTOR drives protein synthesis and floods the ER with unfolded and misfolded proteins beyond its protein folding capacity leading to ER stress (Okada, Minamino et al. 2004). Histological examination has clearly demonstrated marked development of the ER in hypertrophic and failing hearts (Ferrans, Jones et al. 1975). I, therefore, explored whether increased glucose uptake (and subsequent accumulation of intermediary metabolites of glucose such as G6P) induces contractile dysfunction by generating ER stress in the stressed heart. Contractile dysfunction in cardiac hypertrophy and heart failure has been linked to elevated glucose uptake in numerous humans and animal models (Bishop and Altschuld 1970; Taegtmeyer and Overturf 1988; Zhang, Duncker et al. 1995) in an insulin-independent manner (Allard, Wambolt et al. 2000). However, it has yet to be studied whether the mechanism involves dysregulated protein synthesis. In yeast, a number of the molecular chaperones that assist in protein folding in the ER are responsive to glucose and appropriately named glucose-regulated proteins (Groenendyk, Sreenivasaiah et al. 2010).

The two main objectives of the experiments conducted in this chapter were to: 1) Determining whether sustained mTOR activation leads to ER stress in the heart in a substrate-dependent manner. 2) Identifying whether the ER stress response can be targeted to improve contractile function in the stressed heart. Specifically, I tested the hypothesis that signals generated by glucose metabolism impair contractile function via mTOR-mediated ER stress in the heart. I tested this hypothesis by first assessing cardiac power and ER stress in hearts subjected to high workload and perfused with glucose in order to confirm that G6P-mediated mTOR activation is associated with ER stress and

contractile dysfunction. Next, I alleviated ER stress pharmacologically by adding 4-Phenylbutyrate (4PBA) to the perfusate in order to determine whether relieving ER stress improves cardiac function despite continued G6P-mediated mTOR activation. Lastly, I assessed whether rapamycin pretreatment can prevent ER stress and improve cardiac function in hearts subjected to high workload. These experiments were meant to establish changes in glucose metabolism, and subsequent G6P accumulation, as a regulator of ER stress and contractile function in hearts subjected to high workload and determine whether it is possible to pharmacologically prevent G6P-mediated ER stress.

4.2 Results

4.2.1 Load-induced ER Stress Requires Glucose and mTOR Activation

Because of mounting evidence that dysregulated mTOR activation induces ER stress (Ozcan, Ozcan et al. 2008), I elucidated whether the induction of ER stress was responsible for the decline in cardiac power in hearts perfused with glucose at high workload. Transcription of the ER chaperones *GRP78, GRP94, and ERp72* are increased when a cell exhibits ER stress. Neither high workload with NCS nor glucose at normal workload increased markers of ER stress **(Fig. 4.1A)**. However, perfusion at high workload with glucose as the only substrate induced a 1.9-fold increase in *GRP78*, 1.8-fold increase in *GRP94*, and a 1.6-fold increase in *ERP72* mRNA expression compared

to hearts perfused with NCS at normal workload **(Fig. 4.1A).** It was also associated with an increase in GRP78 protein level **(Fig. 4.1B).** Because prolonged ER stress causes cellular damage and induces apoptosis I also assessed levels of GADD153/CHOP, a marker of ER-associated apoptosis. GADD153/CHOP protein levels were unchanged under all untreated conditions suggesting the absence of apoptosis **(Fig. 4.1B).** I used thapsigargin as a positive control for ER stress. Thapsigargin is a non-competitive inhibitor of SERCA2a (sarco-endoplasmic reticulum calcium ATP-ase) that raises cytosolic calcium and inhibits the fusion of autophagosomes with lysosomes.

Besides for unfolded and misfolded proteins, ischemia is a known trigger of the ER stress response. In order to determine whether ischemia was contributing to the imposition of ER stress in hearts perfused with glucose at high workload, I assessed lactate release. Lactate release did not significantly change with high workload or with rapamycin treatment **(Fig 4.2)**.

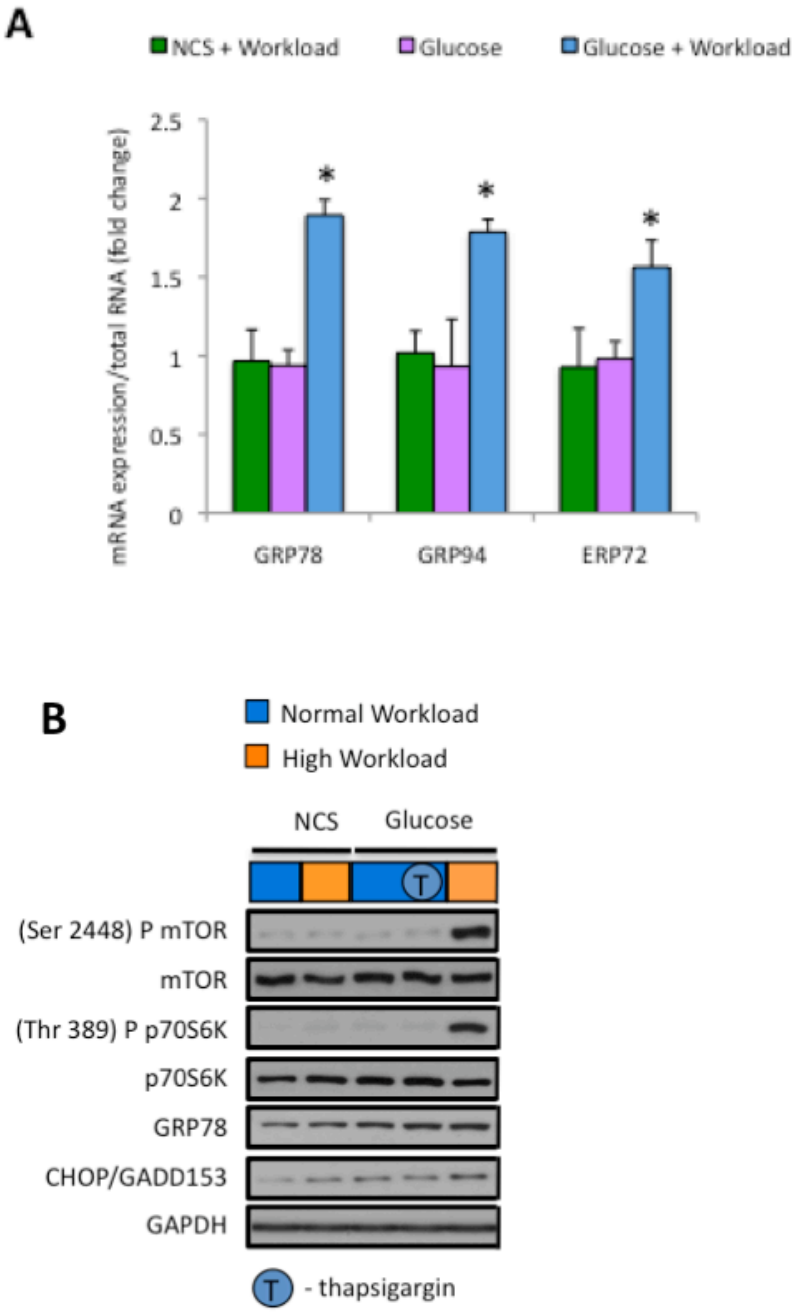

Figure 4.1 Hearts perfused with glucose at high workload show evidence for ER stress. (A) qRT-PCR analysis of ER stress markers in isolated working rat hearts. Data is presented as fold change in ER stress markers compared to hearts perfused with NCS at normal workload. Hearts perfused with glucose at high workload undergo a nearly two-fold increase in markers of ER stress. (B) Representative western blots demonstrate increased GRP78 protein level in hearts perfused with glucose at high workload. n=5-8, *$p<0.05$ compared to hearts perfused with NCS at normal high workload and glucose at normal workload

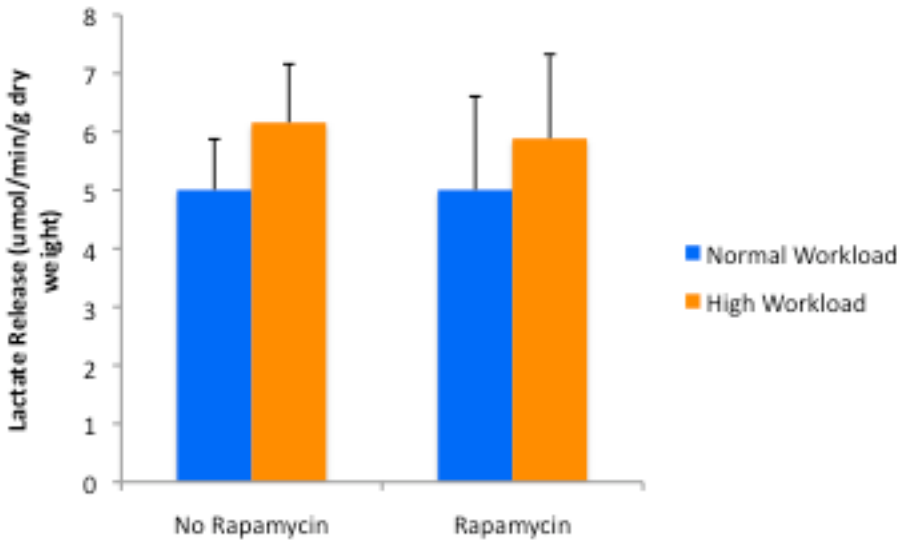

Figure 4.2 Lactate release is unchanged with workload or rapamycin treatment in isolated working hearts perfused with glucose. Lactate release was assessed in coronary effluent samples drawn every 5 minutes throughout the perfusion. Data are presented as mean ± SEM under each condition. n=5-8 for each group

4.2.2 Pretreatment with Rapamycin or Metformin Inhibits ER Stress and Prevent Contractile Dysfunction at High Workload

In order to determine whether ER stress was a consequence of mTOR activation, I assessed markers of ER stress in hearts of animals treated with either AMPK-activator metformin or mTOR-inhibitor rapamycin prior to being perfused with glucose at high workload. Increases in *GRP78, GRP94, ERp72* mRNA expression and GRP78 protein level were prevented in hearts subjected to high workload in animals pretreated with rapamycin or metformin treatment prior to perfusion **(Fig. 4.3A-B).**

To determine whether ER stress contributed to the decline in cardiac power in hearts perfused with glucose at increased workload, perfusions were repeated in the presence of the ER stress-relieving agent phenylbutyrate (PBA). PBA reduced mRNA expression levels of *GRP78, GRP94, and ERp72* **(Fig. 4.3A)**, reduced protein level of GRP78 **(Fig. 4.3B)**, and was associated with a 27% increase in cardiac power in hearts perfused at increased workload with glucose **(Fig. 4.3C).** Taken together, these data suggest that ER stress is, at least partially responsible for the decline in contractile function associated with G6P-mediated mTOR activation. PBA had no effect on cardiac power at normal workload. PBA also had no effect on G6P accumulation, mTOR or p70S6K phosphorylation **(Fig. 4.3D)**. Hearts perfused at normal workload with ER stress inducing agent thapsigargin, an inhibitor of SERCA2a, were used as a positive control.

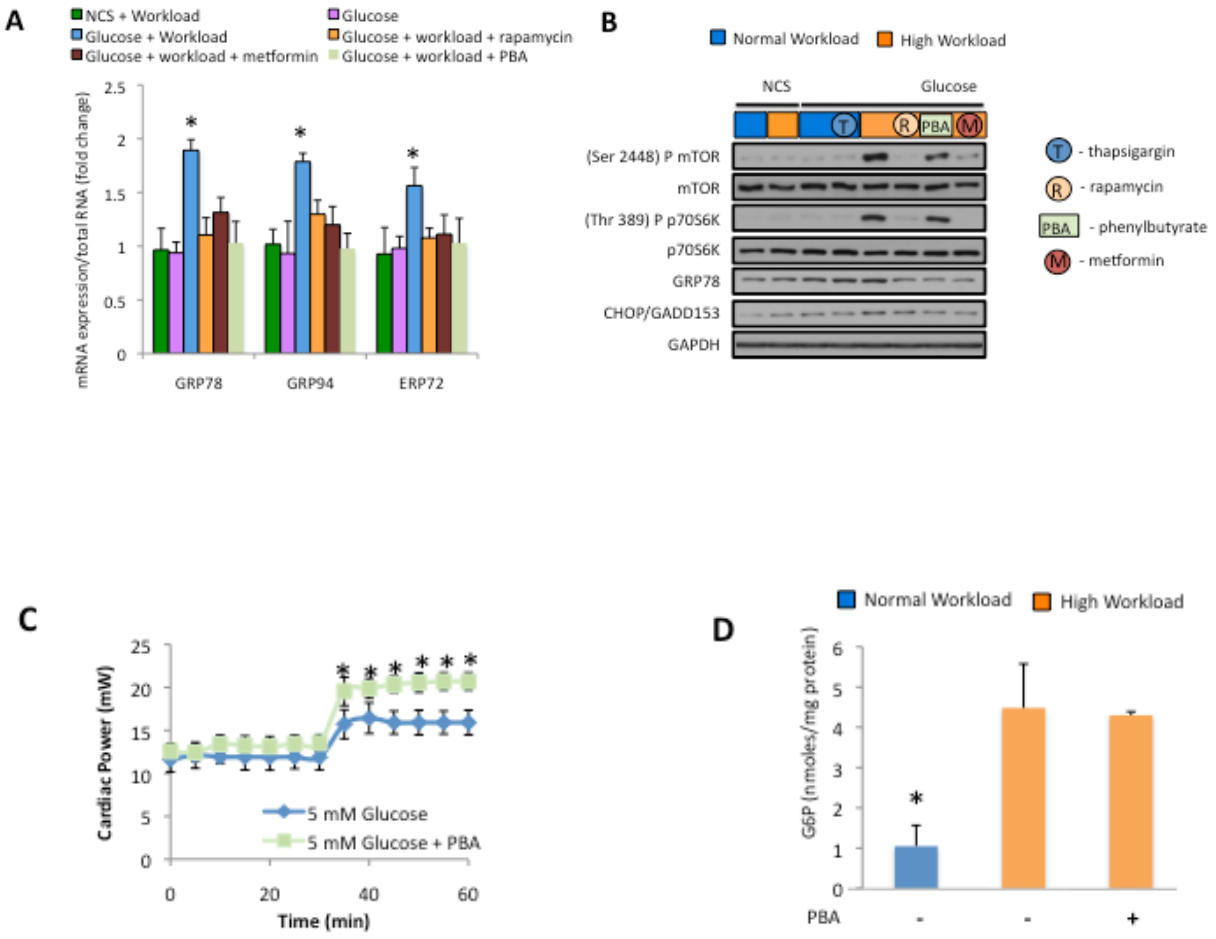

Figure 4.3 ER Stress is relieved with rapamyin, metformin, and PBA. Relief of ER stress improves contractile function in hearts perfused with glucose at high workload. (A) qRT-PCR analysis of ER stress in isolated working rat hearts. Data is presented as fold change in ER stress markers compared to hearts perfused with NCS at normal workload. Hearts perfused with glucose at high workload undergo a nearly two-fold increase in markers of ER stress, which is alleviated by rapamycin, metformin, and phenylbutyrate (PBA). (B) Representative western blots demonstrate an inhibition of mTOR signaling and GRP78 protein level in hearts treated with rapamycin or metformin. Hearts treated directly with ER stress reliever PBA exhibited a decrease in GRP78 protein level independent of changes in mTOR signaling. Taken together, these data suggest that the induction of ER stress is downstream of mTOR activation and prevented by rapamycin and metformin treatment. (C) Cardiac power in the isolated working rat heart perfused with glucose in the presence and absence of PBA. PBA improved cardiac power at high workload. (D) G6P accumulation in isolated working rat hearts freeze clamped at the end of the perfusion protocol. n=5-8. Data are presented as mean ± SEM * $p< 0.05$

Next we performed microarray analyses to delineate whether systemic pretreatment with either rapamycin or metformin or phenylbutyrate addition to the perfusion medium could transcriptionally activate other genes responsible for contractile function in stressed hearts perfused with glucose. Cluster analysis showed no significant clusters of genes similarly regulated by all three treatment groups **(Fig. 4.4A)**. The number of genes differentially regulated by each treatment group are listed in **Fig. 4.4B** and the fold-change of the four genes downregulated by each of the three treatments is listed in **Fig. 4.4C**. One gene has yet to be identified and the other three genes (Scgb1a1, Sp6, and Bpifa1) are not known to be associated with any changes in glucose metabolism or protein turnover. Scgb1a1, the gene that encodes uteroglobin, has no physiological role known in either rodents or humans and is named for its role in binding progesterone in uterus of rabbits. Sp6 encodes a transcription factor with no known role in the heart. The Bpifa1 gene is expressed in the nasopharynx during the inflammatory response. Although this approach does not capture potential changes in changes that could occur at the post-translational level with all three treatments, these results support the hypothesis that an alternative mechanism is unlikely to be responsible for improving contractile function in stressed hearts perfused with glucose.

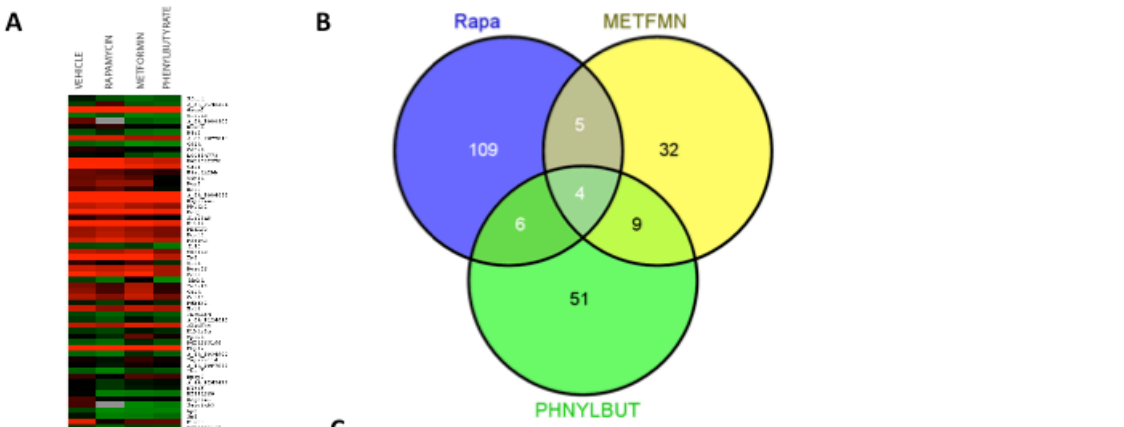

C

Gene	Rapamycin/control (fold change)	Metformin/control (fold change)	Phenylbutyrate/control (fold change)	P – value
Scgb1a1	0.361355809	0.400072503	0.425702374	5.00E-06
Sp6	0.162732919	0.182382835	0.244720497	0.0055877
Bpifa1	0.064809636	0.132029915	0.140646515	0.0073049
Unindentified	0.130385289	0.143870403	0.1617338	0.0041784

Figure 4.4 Transcriptome analysis of stressed hearts treated with rapamycin, metformin, and phenylbutyrate (A) Representative heat map of microarray analyses of rat hearts treated with rapamycin, metformin, or phenylbutyrate prior to being perfused with glucose at high workload (B) Venn diagram of the number of genes identified that are differentially regulated by each treatment. (C) Genes regulated by phenylbutyrate, metformin, and rapamycin treatment. Scgb1a1 (Secretoglobin, family 1A, member 1 (uteroglobin)), Sp6 (Sp6 transcription factor), Bpifa1 (BPI fold containing family A, member 1) n=3 rats per group. Rapa, pretreated with rapamycin; METFMN, pretreated with metformin; PHNYLBUT, phenylbutryrate added to the perfusion medium.

4.2.3 Markers of ER Stress are Downregulated in Failing Human Hearts Following Mechanical Unloading with LVAD

In order to investigate whether changes in cardiac glucose metabolism were accompanied by changes in ER stress, ER chaperones GRP78, GRP94, and ERp72 were assessed. Protein levels of GRP78, GRP94, and ERp72 were decreased after mechanical unloading with LVAD in the same group of patients described before **(Fig. 4.4)**.

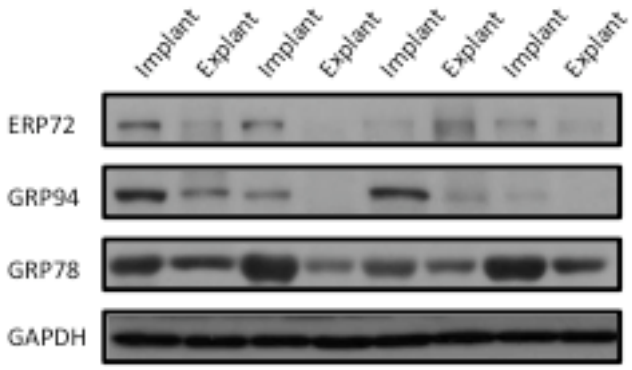

Figure 4.5. Mechanically unloading failing human hearts reduces markers of ER stress. Representative western blots demonstrate a reduction in markers of ER stress (ERP72, GRP94, GRP78) in failing human hearts after mechanical unloading, as well. n=11 paired samples.

4.2.4 Role of Autophagy in G6P-mediated mTOR activation

Protein quality control is highly regulated by autophagy in an mTOR-dependent manner. I therefore wanted to know the whether markers of autophagy were dynamically regulated with acute changes in workload and whether pretreatment with rapamycin could prevent these changes. At the protein level, no changes were appreciated in hearts of animals treated with rapamycin treatment prior to perfusion at high workload with glucose **(Fig. 4.6)**. The autophagic process is very time-dependent and an assessment of LC3 localization into discrete punctate cytoplasmic dots (seen by immunofluoresence) or protein levels of LCIII and Beclin at earlier and later time-points would be necessary to confirm whether or not autophagy is regulated by glucose-dependent mTOR activation.

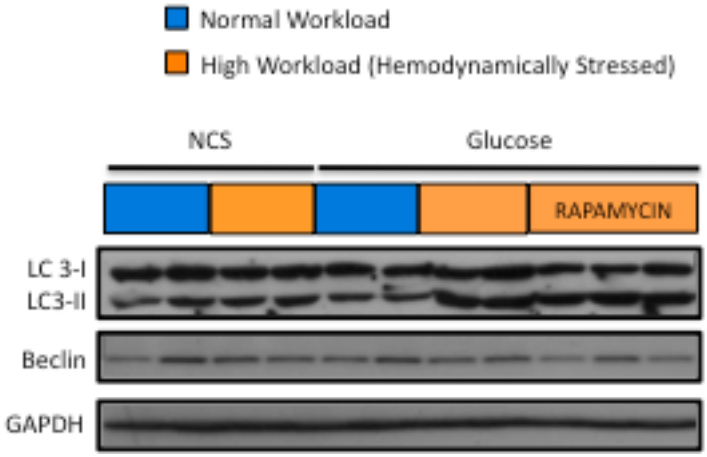

Figure 4.6 Markers of autophagy are unchanged with rapamycin treatment in hearts stressed with an acute increase in workload. Markers of autophagy (LC3, Beclin) were unchanged by rapamycin treatment prior to being subjected to high workload in ex vivo isolated working hearts as described in **Table 2.2**. NCS refers to hearts perfused with the non-carbohydrate substrates acetoacetate (7.5 mM) and propionate (5 mM), glucose refers to the hearts perfused with glucose as the only substrate.

4.3 Discussion

In hearts subjected to high workload, mTOR activation is associated with cardiac hypertrophy and contractile dysfunction (Shioi, McMullen et al. 2003). Even in *Drosophila*, dTOR (drosophila TOR) overactivity is associated with cardiac dysfunction and decreased lifespan (Topisirovic and Sonenberg 2010). Sustained mTOR activation synthesizes proteins beyond the folding capacity of the endoplasmic reticulum (ER), and induces ER stress (Glembotski 2008). By evaluating the ER chaperone expression as a marker of ER stress, I demonstrate that load-induced ER stress in the heart is metabolically regulated. Transcriptional activation of genes regulating the ER stress response is significantly increased in hearts subjected to high workload only when perfused with glucose (which leads to G6P accumulation and contractile dysfunction). Although the mechanism by which ER stress causes contractile dysfunction has yet to be defined, I suspect that it involves a perturbation of normal calcium handling. Contractile dysfunction in isolated rodent hearts perfused with high concentrations of glucose is associated with the presence of abnormal calcium transients (Tang, Cheng et al. 2010). Because the ER regulates calcium flux and excitation-contraction coupling, it is conceivable that G6P-mediated ER stress is responsible for impairing contractile function by inducing abnormal calcium transients. Specifically, I suggest a critical role for ER chaperone GRP78, which is involved in calcium transport from the ER to the mitochondria (Dudek, Benedix et al. 2009). In our studies, GRP78 gene expression and

protein levels were dynamically upregulated with even an acute increase in workload for 30 min in the presence of glucose. Direct relief of ER stress with chemical chaperone PBA rescued contractile function in hearts perfused with glucose at high workload. PBA is already approved by the U.S. Food and Drug Administration for urea cycle disorders and safely used in clinical trials to treat cystic fibrosis (Rubenstein and Zeitlin 1998). It may have therapeutic benefit in load-induced heart disease, as well.

Rapamycin pretreatment also rescues G6P-mediated ER stress and cardiac dysfunction at increased workload. By blunting rates of glucose uptake at increased workload and preventing the mismatch between glucose uptake and oxidation, it depletes intracardiac G6P, inhibits mTOR, and prevents the imposition of ER stress.

However, rapamycin treatment also improves cardiac power despite lowering rates of myocardial glucose uptake and oxidation to unstressed levels. From an energetic perspective, this suggests that the increased energy requirements of hearts subjected to high workload, which are met by the oxidation of carbohydrates, may largely be responsible for fueling protein turnover and protein quality control ("internal work"). Protein turnover utilizes roughly 15-20% of a cell's energy in the resting state (Waterlow 1984), and at least 3 times more energy during times of growth (Laurent and Millward 1980) (Lane and Martin 2010). It is, therefore, tempting to speculate that the energy conserved by rapamycin's inhibition of protein synthesis and ER stress improves cardiac efficiency and contributes to its ability to reverse load-induced cardiac dysfunction (Shioi, McMullen et al. 2003; McMullen, Sherwood et al. 2004; Marin, Keith et al. 2011). Furthermore, the improvement in cardiac power observed in rapamycin treated rats gives credence to the hypothesis that the hypertrophic process may not be necessary

to maintain systolic function in hearts subjected to increased workload (Hill, Karimi et al. 2000). Our results offer a new perspective on the energy cost of protein synthesis and protein quality control.

Metformin has been shown to inhibit ER stress in isolated mouse aortas from mice fed an athrogenic diet (Dong, Zhang et al. 2010) and in cardiomyocytes subjected to ER stress by reperfusion after hypoxia (Yeh, Chen et al. 2010). While metformin is known to improve cardiac function in murine models of heart failure (Gundewar, Calvert et al. 2009; Yin, van der Horst et al. 2011) its ability to alleviate ER stress in hearts subjected to increased workload has yet to be studied. I demonstrate that metformin inhibits G6P-mediated mTOR activation in a dose-dependent manner and protects against load-induced ER stress. When administered systemically, metformin also improves the oxidative capacity of the heart, blunts G6P accumulation, and improves cardiac function. Therefore, I propose that like rapamycin, metformin metabolically protects hearts subjected to increased workload and in doing so may account for improving survival in diabetic patients with heart failure (Aguilar, Chan et al. 2011).

Indeed, markers of ER stress are upregulated in failing human hearts (Okada, Minamino et al. 2004). I now report that in hearts from a cohort of 11 non-diabetic patients with idiopathic heart failure, mechanical unloading with an LVAD reduces intracardiac G6P levels and protein levels of ER stress markers. Our studies in the rodent heart implicate a critical role for dysregulated glucose metabolism and toxic intermediary metabolite accumulation in the induction of ER stress. Similarly, I observed a significant decrease in G6P accumulation after LVAD support. We have previously observed a trend for decreased myocardial glycogen content in failing human

hearts after mechanical unloading (Razeghi and Taegtmeyer 2004) and more recently, proteomic analysis has revealed an upregulation of proteins involved in glycolysis, energy, and oxidative metabolism in LVAD supported patients (de Weger, Schipper et al. 2011). Taken together, these studies support our findings and suggest that mechanical unloading promotes a re-coupling of glucose uptake and oxidation, prevents intermediary metabolite accumulation, and conserves energy in the failing heart by reducing ER stress. Due to the difficulty in obtaining myocardial tissue samples and assessing substrate flux in humans, it remains difficult to more accurately assess the effects of mechanical unloading on myocardial energetics and glucose utilization in the heart.

When supplied with excess substrate by high fat feeding, mice become insulin resistant and skeletal muscle, liver and adipocytes all undergo ER stress (Li, Huang et al. 2012) (Gregor and Hotamisligil 2007; Deldicque, Cani et al. 2010). Oral administration of ER stress relieving agent 4-phenyl butyric acid (PBA) to obese mice restores systemic insulin sensitivity, normalizes serum glucose levels, resolves fatty liver disease, and enhances insulin action in liver, muscle, and adipose tissues (Ozcan, Yilmaz et al. 2006). Taken together, these data support our conclusions that excess substrate supply may lead to cellular dysfunction by inducing ER stress. Moreover, direct relief of ER stress may have therapeutic potential both systemically and in the heart (Engin and Hotamisligil 2010). Interestingly, FDA-approved tyrosine kinase inhibitors imatinib and sunitinib have recently been found to have ER stress relieving properties, as well, and both have prevented and reversed obese mice from developing diabetes and heart failure (Louvet, Szot et al. 2008; Han, Lerner et al. 2009).

In a cohort of 11 morbidly obese patients (BMI 51.3 ± 3.0 kg/m^2), markers of ER stress were elevated in both adipose tissue and liver. Moreover, one year after gastric bypass surgery (which forces caloric restriction and a significant reduction in exogenous fuel supply to the body), markers of ER stress such as GRP78 were reduced in adipose tissue and liver, which directly correlated with reversal of insulin resistance (Gregor, Yang et al. 2009). In the heart, both diet-induced weight loss and weight-loss surgery lead to a reduction in left ventricular mass, regression of cardiac hypertrophy, and improvement in midwall fractional shortening (Rider, Francis et al. 2009; Algahim, Lux et al. 2010; Owan, Avelar et al. 2011). By reducing substrate supply to the heart, it is plausible that the beneficial cardiovascular effects may be mediated by regulating glucose metabolism, mTOR activation, and ER stress in the heart.

4.4 Limitations

I am the first to admit that my studies are not without limitations. First, there are significant differences between the human and rodent heart that are worth mentioning. The human heart rate and ejection fraction is significantly less than that of the rodent heart. Also, acute increases in workload via aortic banding *in vivo* or doubling afterload *ex vivo* may not accurately mimic the chronic, low levels of hemodynamic stress induced by pathological stimuli that induce cardiac hypertrophy. Moreover, while it is plausible that abnormal calcium handling by the sarcoplasmic reticulum may be responsible for ER stress induced contractile dysfunction in the rodent heart, it is less clear whether the

same mechanism would exist in the human heart. Calicum handling in rodents relies much more heavily on transport through the sarcoplasmic reticulum than the human heart, which seems to rely more heavily on transsarcolemmal calcium transport (Berenji, Drazner et al. 2005). In spite of these limitations and because the structural, functional, and metabolic changes that occur in the rodent heart mimic those of the human heart, I believe the work in this dissertation has identified glucose metabolism (and specifically glucose 6-phosphate) as a dynamic regulator of myocardial protein synthesis, ER stress and possibly also protein turnover as well as expanded the role of energy substrate metabolism from simply being a provider of ATP to a regulator of cardiac protein synthesis and growth as well.

SUMMARY OF RESULTS AND PERSPECTIVE

The heart is a dynamic organ with an enormous capacity to respond to stress. The heart also remodels metabolically and structurally before it goes into heart failure. The question I began to address in my dissertation tried to fill an important gap in the current knowledge of cardiac physiology: Does the early metabolic remodeling process *regulate* the structural and functional remodeling process in the heart? In a series of different experimental strategies I provided evidence in support of our hypothesis that metabolic remodeling (which is potentially reversible) regulates functional and structural remodeling (which is largely irreversible) and discovered that it is both deleterious and preventable.

With help from collaborators at the University of Virginia, we first quantitatively demonstrated *in vivo* that enhanced glucose uptake in the heart accompanies load-induced contractile dysfunction prior to the presence of structural changes. Stated otherwise, metabolic remodeling precedes structural remodeling of the heart and accompanies load-induced contractile dysfunction. Before beginning my dissertation project, numerous studies had quite convincingly provided evidence that load-induced mTOR signaling mediates cardiac growth (Shioi, McMullen et al. 2003; McMullen, Sherwood et al. 2004; Zhang, Contu et al. 2010). However, every study largely ignored the fact that changes in workload are accompanied by instantaneous changes in cardiac substrate metabolism (Goodwin, Taylor et al. 1998), which could be contributing to regulating 'load-induced' hypertrophy and contractile dysfunction as well. Indeed, my findings in the isolated working heart *ex vivo* demonstrate that an acute increase in workload is *not* sufficient to activate mTOR in the absence of glucose, suggesting that 'load-induced' hypertrophic signaling through mTORC1 is glucose-dependent. A

number of genetically engineered mouse hearts that take up glucose in excess of its oxidative capacity also hypertrophy and provide evidence in support of our hypothesis, as well (Domenighetti, Danes et al. 2010; Ellis, Mentock et al. 2011; Liu, Yu et al. 2011).

More specifically, I propose that mTORC1 is activated by the metabolic signal G6P. I dissected the load and substrate-dependence of mTORC1 signaling in the heart *ex vivo* and determined that doubling the workload alone triggers PI3K, Akt, and minimal Akt-dependent phosphorylation of TSC2 at Ser939 phosphorylation, both in the presence and absence of glucose. However, complete 'load-induced' mTORC1 activation and contractile dysfunction requires not only Akt-dependent phosphorylation of TSC2 at Ser939 but also a downregulation of AMPK-dependent phosphorylation of TSC2 at Ser1387 (Shaw, Bardeesy et al. 2004), which occurs with G6P accumulation (in hearts perfused *with glucose* as the only substrate at high workload).

In order to determine the consequences of G6P-dependent mTOR activation, I focused my attention on the role of endoplasmic retiticulum (ER) stress. When subjected to hemodynamic stress (continued pumping against high workload), increased rates of protein synthesis flood the ER with unfolded and misfolded proteins beyond its capacity to cope with the load, which leads to ER stress (Glembotski 2008). Whether increased glucose uptake and accumulation as G6P causes contractile dysfunction by generating ER stress remains unknown. I therefore investigated whether when subjected to high workload, the metabolic remodeling process (increased reliance upon glucose) contributes to a decline in cardiac function by generating ER stress.

Indeed, it does. Expression levels of three early response markers of ER stress (GRP78, ERp72, and GRP94) all correlated with G6P-mediated mTOR activation and contractile dysfunction *ex vivo*. Furthermore, both rapamycin and metformin pretreatment, which inhibited G6P-mediated mTOR activation and rescued contractile function, also prevented the upregulation of markers of ER stress at both the transcriptional and translational level. Similarly, pharmacologic alleviation of ER stress with chemical chaperone 4-Phenylbutyrate (4PBA) improved cardiac function, as well. Alleviation of ER stress improved contractile function despite elevated G6P levels, however, suggesting that the induction of ER stress is downstream of G6P-mediated mTOR activation. Taken together, these data suggested that G6P-mediated mTOR activation leads to ER stress and impairs contractile function in hearts subjected to high workload.

I believe my findings also shed new light on the energetic cost of protein turnover in the stressed heart. Rather unexpectedly, rapamycin treatment improved cardiac power despite lowering rates of myocardial glucose uptake and oxidation to unstressed levels. From an energetic perspective, this suggests that the increased energy requirements of hearts subjected to high workload, which are met by the oxidation of carbohydrates, may largely be responsible for fueling protein turnover and protein quality control ("internal work"). Protein turnover utilizes roughly 15-20% of a cell's energy in the resting state (Waterlow 1984), and at least 3 times more energy during times of growth (Laurent and Millward 1980). It is, therefore, tempting to speculate that the energy conserved by rapamycin's inhibition of protein synthesis and ER stress improves cardiac efficiency and contributes to its ability to reverse load-induced cardiac

dysfunction (Shioi, McMullen et al. 2003; Sancak, Peterson et al. 2008; Marin, Keith et al. 2011). Furthermore, the improvement in cardiac power observed in rapamycin treated rats gives credence to the hypothesis that the hypertrophic process may not be necessary to maintain systolic function in hearts subjected to increased workload (Hill, Karimi et al. 2000). Our results offer a new perspective on the energy cost of protein synthesis and protein quality control.

My studies have also demonstrated a novel mechanism that contributes to the improvement in contractile function known to occur in the stressed heart with metformin treatment. Metformin has been shown to inhibit ER stress in isolated mouse aortas from mice fed an athrogenic diet (Dong, Zhang et al. 2010) and in cardiomyocytes subjected to ER stress by reperfusion after hypoxia (Yeh, Chen et al. 2010). While metformin is known to improve cardiac function in murine models of heart failure (Gundewar, Calvert et al. 2009; Yin, van der Horst et al. 2011), its ability to alleviate ER stress in hearts subjected to increased workload had previously not been studied. I demonstrate that metformin inhibits G6P-mediated mTOR activation in a dose-dependent manner and protects against load-induced ER stress. When administered systemically, metformin also improves the oxidative capacity of the heart, blunts G6P accumulation, and improves cardiac function. Therefore, I propose that like rapamycin, metformin metabolically protects hearts subjected to increased workload and in doing so may account for improved survival in diabetic patients with heart failure (Aguilar, Chan et al. 2011). These data may have wide implications outside of cardiovascular disease, as well. Metformin is associated with increased survival in various types of cancer although the mechanism remains unknown (Dowling, Goodwin, et al. 2011). Its well-studied effects

of activating AMPK, reducing plasma insulin levels, and inhibiting hepatic gluconeogenesis likely reduce G6P accumulation and subsequent mTOR activation.

Next, one must consider the possible clinical relevance of my findings. Despite the recent advances in cardiovascular medicine, the majority of patients with heart disease still progress to end-stage heart failure, for which treatment is largely limited to cardiac transplantation. As the need for transplantable hearts continues to far exceed the supply of available organs, left ventricular assist devices (LVADs) are implanted with increased frequency. Although initially meant to serve as a 'bridge to transplantation', and not necessarily as destination therapy, many patients experienced functional improvement without requiring a heart transplantation but the mechanism remains largely unknown. Transcriptional analysis of metabolic genes revealed a reversal of the failing human heart to the fetal gene program (Razeghi, Young et al. 2001) and a partial reversal after implantation of an LVAD (Razeghi, Young et al. 2002). However, proteomic analysis has now shown an upregulation of proteins involved in glycolysis, energy, and oxidative metabolism in LVAD supported patients (de Weger, Schipper et al. 2011). Taken together, these data suggest improved metabolic capacity with LVAD implantation. Both the mTOR signaling pathway and markers of ER stress are also upregulated in the hypertrophied and failing human heart. I have found that in hearts from a cohort of 11 patients with idiopathic heart failure, mechanical unloading with a left ventricular assist device (LVAD) reduces protein levels of ER stress markers. Moreover, consistent with our data that implicate a critical role for dysregulated glucose metabolism and intermediary metabolite accumulation in the induction of ER stress, I observed a significant decrease in G6P accumulation after LVAD support. These studies

suggest that mechanical unloading may promote a re-coupling of rates of glucose uptake and oxidation prevent intermediary metabolite accumulation and contribute to a reduction of ER stress in the failing heart.

However, a number of important questions remain. This is a common feature of all novel research. The first question is: What is the exact molecular mechanism by which G6P modulates TSC2 to promote mTOR activation? Two probable mechanisms by which G6P may regulate TSC2 include: 1) modulation of one or several kinases that act on TSC2 or 2) allosteric regulation of TSC2 itself. The generation and transfection into of constructs containing mutated phosphorylation sites into stressed cardiomyocytes would help determine whether G6P modulates TSC2 or one of its upstream kinases. Phosphorylation site mutations on TSC2 have been used previously to investigate mTORC1 activation (Huang and Manning 2008). It is plausible that G6P promotes the phosphorylation of TSC2 or one of its upstream kinases in a manner similar to its ability to control the phosphorylation state of glycogen synthase (Huang, Wilson et al. 1997). Radiolabeled binding assays can determine whether G6P promotes mTOR activation by directly binding itself to TSC2 or one of its upstream kinases by pulling down the candidate kinases from rat heart lysates by immunoprecipitation, incubating with uniformly labeled [^{14}C]-G6P, and assaying for radioactivity. This approach has previously been used to identify novel binding of proteins in the Akt/mTOR pathway to small non-protein molecules such as microfilaments (Zhu, Rosenblatt et al. 2011).

The second question is: By which mechanism does ER stress causes contractile dysfunction? I suspect the mechanism involves a perturbation of proper calcium cycling in and out of the cardiomyocytes specialized ER, the sarcoendoplasmic (SR) reticulum.

The SR is a known regulator of calcium flux and excitation-contraction coupling in the cardiomyocyte. Indeed, contractile dysfunction in rodent hearts perfused with high concentrations of glucose has already been associated with the presence of abnormal calcium (Hu, Belke et al. 2005). It is conceivable that this may have been mediated by ER stress. Moreover, mice with cardiac overexpression of the SR Ca^{2+} transporter (sarco/endoplasmic reticulum Ca^{2+}-ATPase, SERCA) demonstrate improved cardiac function compared to wild type mice when subjected to aortic banding (Suarez, Gloss et al. 2004). Assessing glucose metabolism, mTOR activation, and markers of ER stress in these mice would help determine the exact mechanism by which ER stress induces contractile dysfunction in hearts subjected to high workload.

The third question is: How can the new knowledge on a metabolic signal driving another signaling pathway be leveraged to devise new therapeutic targets for the treatment of heart failure. This is perhaps the most challenging question for a young physician-scientist. The metabolic management of heart failure is the subject of reviews (Osterholt, Sen et al. 2012), clinical studies(Wallhaus, Taylor et al. 2001), and of meta-analyses (Zhang, Lu et al. 2012). It is my hope that my work has laid the cornerstone for a new paradigm, just as Rudolph Schoenheimer wrote when he discovered the dynamic state of body constituents (Schoenheimer, 1942): “The new results imply that not only the fuel, but also the structural materials are in a steady state of flux. The classical picture must thus be replaced by one which takes account of the dynamic state of body structure” (page 64).

Conclusion

My findings demonstrate that metabolic remodeling precedes, triggers, and sustains structural remodeling of the heart. Specifically, I identify dysregulated glycolytic homeostasis as a novel regulator of contractile function, mTOR activation, and ER stress in response to increased cardiac workload. The study highlights the importance of intermediary metabolism, not only as energy providing substrates, but also as signals for driving cardiac growth. In doing so, it underscores the need to better metabolically protect patients with heart failure and sheds light on the metabolic effects of mechanically unloading the failing human heart. I believe these results have wide-ranging implications for load-induced heart disease and based on the new findings, I speculate that targeting metabolism offers therapeutic promise in treating cardiovascular disease.

Bibliography

1. Abel, E. D., H. C. Kaulbach, R. Tian, J. C. Hopkins, J. Duffy, T. Doetschman, T. Minnemann, M. E. Boers, E. Hadro, C. Oberste-Berghaus, W. Quist, B. B. Lowell, J. S. Ingwall and B. B. Kahn (1999). "Cardiac hypertrophy with preserved contractile function after selective deletion of GLUT4 from the heart." J Clin Invest 104(12): 1703-1714.
2. Aguilar, D., W. Chan, B. Bozkurt, K. Ramasubbu and A. Deswal (2011). "Metformin use and mortality in ambulatory patients with diabetes and heart failure." Circ Heart Fail 4(1): 53-58.
3. Alexander, A., S. L. Cai, J. Kim, A. Nanez, M. Sahin, K. H. MacLean, K. Inoki, K. L. Guan, J. Shen, M. D. Person, D. Kusewitt, G. B. Mills, M. B. Kastan and C. L. Walker (2010). "ATM signals to TSC2 in the cytoplasm to regulate mTORC1 in response to ROS." Proc Natl Acad Sci U S A 107(9): 4153-4158.
4. Algahim, M. F., T. R. Lux, J. G. Leichman, A. F. Boyer, C. C. Miller, 3rd, S. T. Laing, E. B. Wilson, T. Scarborough, S. Yu, B. Snyder, C. Wolin-Riklin, U. G. Kyle and H. Taegtmeyer (2010). "Progressive regression of left ventricular hypertrophy two years after bariatric surgery." Am J Med 123(6): 549-555.
5. Allard, M. F., R. B. Wambolt, S. L. Longnus, M. Grist, C. P. Lydell, H. L. Parsons, B. Rodrigues, J. L. Hall, W. C. Stanley and G. P. Bondy (2000). "Hypertrophied rat hearts are less responsive to the metabolic

and functional effects of insulin." Am J Physiol Endocrinol Metab 279(3): E487-493.

6. Andersen, J. B., B. C. Rourke, V. J. Caiozzo, A. F. Bennett and J. W. Hicks (2005). "Physiology: postprandial cardiac hypertrophy in pythons." Nature 434(7029): 37-38.

7. Asakura, M. and M. Kitakaze (2009). "Global gene expression profiling in the failing myocardium." Circ J 73(9): 1568-1576.

8. Baba, H. A., J. Stypmann, F. Grabellus, P. Kirchhof, A. Sokoll, M. Schafers, A. Takeda, M. J. Wilhelm, H. H. Scheld, N. Takeda, G. Breithardt and B. Levkau (2003). "Dynamic regulation of MEK/Erks and Akt/GSK-3beta in human end-stage heart failure after left ventricular mechanical support: myocardial mechanotransduction-sensitivity as a possible molecular mechanism." Cardiovasc Res 59(2): 390-399.

9. Balaban, R. S., H. L. Kantor, L. A. Katz and R. W. Briggs (1986). "Relation between work and phosphate metabolite in the in vivo paced mammalian heart." Science 232(4754): 1121-1123.

10. Belke, D. D., S. Betuing, M. J. Tuttle, C. Graveleau, M. E. Young, M. Pham, D. Zhang, R. C. Cooksey, D. A. McClain, S. E. Litwin, H. Taegtmeyer, D. Severson, C. R. Kahn and E. D. Abel (2002). "Insulin signaling coordinately regulates cardiac size, metabolism, and contractile protein isoform expression." J Clin Invest 109(5): 629-639.

11. Benes, J., L. Kazdova, Z. Drahota, J. Houstek, D. Medrikova, J. Kopecky, N. Kovarova, M. Vrbacky, D. Sedmera, H. Strnad, M. Kolar,

J. Petrak, O. Benada, P. Skaroupkova, L. Cervenka and V. Melenovsky (2011). "Effect of metformin therapy on cardiac function and survival in a volume-overload model of heart failure in rats." Clin Sci (Lond) 121(1): 29-41.

12. Berenji, K., M. H. Drazner, B. A. Rothermel and J. A. Hill (2005). "Does load-induced ventricular hypertrophy progress to systolic heart failure?" Am J Physiol Heart Circ Physiol 289(1): H8-H16.

13. Berr, S. S., R. J. Roy, B. A. French, Z. Yang, W. Gilson, C. M. Kramer and F. H. Epstein (2005). "Black blood gradient echo cine magnetic resonance imaging of the mouse heart." Magn Reson Med 53(5): 1074-1079.

14. Bing, R. J., A. Siegel, I. Ungar and M. Gilbert (1954). "Metabolism of the human heart. II. Studies on fat, ketone and amino acid metabolism." Am J Med 16(4): 504-515.

15. Bing, R. J., L. D. Vandam, F. Gregoire, J. C. Handelsman, W. T. Goodale and J. E. Eckenhoff (1947). "Catheterization of the coronary sinus and middle cardiac vein in man." Proc Exp Biol Med 66: 239-245.

16. Bishop, S. P. and R. A. Altschuld (1970). "Increased glycolytic metabolism in cardiac hypertrophy and congestive failure." Am J Physiol 218(1): 153-159.

17. Blobel, G. (2000). "Protein targeting." Biosci Rep 20(5): 303-344.

18. Bradford, M. M. (1976). "A rapid and sensitive method for the quantitation of microgram quantities of protein utilizing the principle of protein-dye binding." Anal Biochem 72: 248-254.

19. Budanov, A. V. and M. Karin (2008). "p53 target genes sestrin1 and sestrin2 connect genotoxic stress and mTOR signaling." Cell 134(3): 451-460.

20. Cardenas, M. E., N. S. Cutler, M. C. Lorenz, C. J. Di Como and J. Heitman (1999). "The TOR signaling cascade regulates gene expression in response to nutrients." Genes Dev 13(24): 3271-3279.

21. Clark, H., D. Carling and D. Saggerson (2004). "Covalent activation of heart AMP-activated protein kinase in response to physiological concentrations of long-chain fatty acids." Eur J Biochem 271(11): 2215-2224.

22. Cong, L. N., H. Chen, Y. Li, L. Zhou, M. A. McGibbon, S. I. Taylor and M. J. Quon (1997). "Physiological role of Akt in insulin-stimulated translocation of GLUT4 in transfected rat adipose cells." Mol Endocrinol 11(13): 1881-1890.

23. Crespo, J. L. and M. N. Hall (2002). "Elucidating TOR signaling and rapamycin action: lessons from Saccharomyces cerevisiae." Microbiol Mol Biol Rev 66(4): 579-591.

24. de Weger, R. A., M. E. Schipper, E. Siera-de Koning, P. van der Weide, M. F. van Oosterhout, R. Quadir, H. Steenbergen-Nakken, J. R. Lahpor, N. de Jonge and N. Bovenschen (2011). "Proteomic profiling of the

human failing heart after left ventricular assist device support." J Heart Lung Transplant 30(5): 497-506.

25. Deldicque, L., P. D. Cani, A. Philp, J. M. Raymackers, P. J. Meakin, M. L. Ashford, N. M. Delzenne, M. Francaux and K. Baar (2010). "The unfolded protein response is activated in skeletal muscle by high-fat feeding: potential role in the downregulation of protein synthesis." Am J Physiol Endocrinol Metab 299(5): E695-705.

26. Depre, C., S. R. Powell and X. Wang (2010). "The role of the ubiquitin-proteasome pathway in cardiovascular disease." Cardiovasc Res 85(2): 251-252.

27. Depre, C., G. L. Shipley, W. Chen, Q. Han, T. Doenst, M. L. Moore, S. Stepkowski, P. J. Davies and H. Taegtmeyer (1998). "Unloaded heart in vivo replicates fetal gene expression of cardiac hypertrophy." Nat Med 4(11): 1269-1275.

28. Depre, C., Q. Wang, L. Yan, N. Hedhli, P. Peter, L. Chen, C. Hong, L. Hittinger, B. Ghaleh, J. Sadoshima, D. E. Vatner, S. F. Vatner and K. Madura (2006). "Activation of the cardiac proteasome during pressure overload promotes ventricular hypertrophy." Circulation 114(17): 1821-1828.

29. Doenst, T., G. W. Goodwin, A. M. Cedars, M. Wang, S. Stepkowski and H. Taegtmeyer (2001). "Load-induced changes in vivo alter substrate fluxes and insulin responsiveness of rat heart in vitro." Metabolism 50(9): 1083-1090.

30. Doiron, B., M. H. Cuif, R. Chen and A. Kahn (1996). "Transcriptional glucose signaling through the glucose response element is mediated by the pentose phosphate pathway." J Biol Chem 271: 5321-5324.

31. Domenighetti, A. A., V. R. Danes, C. L. Curl, J. M. Favaloro, J. Proietto and L. M. Delbridge (2010). "Targeted GLUT-4 deficiency in the heart induces cardiomyocyte hypertrophy and impaired contractility linked with Ca(2+) and proton flux dysregulation." J Mol Cell Cardiol 48(4): 663-672.

32. Dong, Y., M. Zhang, S. Wang, B. Liang, Z. Zhao, C. Liu, M. Wu, H. C. Choi, T. J. Lyons and M. H. Zou (2010). "Activation of AMP-activated protein kinase inhibits oxidized LDL-triggered endoplasmic reticulum stress in vivo." Diabetes 59(6): 1386-1396.

33. Dormandy, J. A., B. Charbonnel, D. J. Eckland, E. Erdmann, M. Massi-Benedetti, I. K. Moules, A. M. Skene, M. H. Tan, P. J. Lefebvre, G. D. Murray, E. Standl, R. G. Wilcox, L. Wilhelmsen, J. Betteridge, K. Birkeland, A. Golay, R. J. Heine, L. Koranyi, M. Laakso, M. Mokan, A. Norkus, V. Pirags, T. Podar, A. Scheen, W. Scherbaum, G. Schernthaner, O. Schmitz, J. Skrha, U. Smith and J. Taton (2005). "Secondary prevention of macrovascular events in patients with type 2 diabetes in the PROactive Study (PROspective pioglitAzone Clinical Trial In macroVascular Events): a randomised controlled trial." Lancet 366(9493): 1279-1289.

34. Dorn, G. W., 2nd and T. Force (2005). "Protein kinase cascades in the regulation of cardiac hypertrophy." J Clin Invest 115(3): 527-537.

35. Dowling, R., Goodwin P., and V. Stambolic (2011). "Understanding the benefit of metformin use in cancer treatment." BMC Medicine 7015(9): 33.

36. Dudek, J., J. Benedix, S. Cappel, M. Greiner, C. Jalal, L. Muller and R. Zimmermann (2009). "Functions and pathologies of BiP and its interaction partners." Cell Mol Life Sci 66(9): 1556-1569.

37. Eizirik, D. L., A. K. Cardozo and M. Cnop (2008). "The role for endoplasmic reticulum stress in diabetes mellitus." Endocr Rev 29(1): 42-61.

38. Ellis, J. M., S. M. Mentock, M. A. Depetrillo, T. R. Koves, S. Sen, S. M. Watkins, D. M. Muoio, G. W. Cline, H. Taegtmeyer, G. I. Shulman, M. S. Willis and R. A. Coleman (2011). "Mouse cardiac acyl coenzyme a synthetase 1 deficiency impairs Fatty Acid oxidation and induces cardiac hypertrophy." Mol Cell Biol 31(6): 1252-1262.

39. Engin, F. and G. S. Hotamisligil (2010). "Restoring endoplasmic reticulum function by chemical chaperones: an emerging therapeutic approach for metabolic diseases." Diabetes Obes Metab 12 Suppl 2: 108-115.

40. Ferrans, V. J., M. Jones, B. J. Maron and W. C. Roberts (1975). "The nuclear membranes in hypertrophied human cardiac muscle cells." Am J Pathol 78(3): 427-460.

41. Finck, B. N. and D. P. Kelly (2007). "Peroxisome proliferator-activated receptor gamma coactivator-1 (PGC-1) regulatory cascade in cardiac physiology and disease." Circulation 115(19): 2540-2548.

42. Garza, L., Y. W. Aude and J. F. Saucedo (2002). "Can we prevent in-stent restenosis?" Curr Opin Cardiol 17(5): 518-525.

43. Girard, J., P. Ferre and F. Foufelle (1997). "Mechanisms by which carbohydrates regulate expression of genes for glycolytic and lipogenic enzymes." Annu Rev Nutr 17: 325-352.

44. Glembotski, C. C. (2008). "The role of the unfolded protein response in the heart." J Mol Cell Cardiol 44(3): 453-459.

45. Golfman, L. S., C. R. Wilson, S. Sharma, M. Burgmaier, M. E. Young, P. H. Guthrie, M. Van Arsdall, J. V. Adrogue, K. K. Brown and H. Taegtmeyer (2005). "Activation of PPARgamma enhances myocardial glucose oxidation and improves contractile function in isolated working hearts of ZDF rats." Am J Physiol Endocrinol Metab 289(2): E328-336.

46. Goodwin, G. W., D. M. Cohen and H. Taegtmeyer (2001). "[5-3H]glucose overestimates glycolytic flux in isolated working rat heart: role of the pentose phosphate pathway." Am J Physiol Endocrinol Metab 280(3): E502-E508.

47. Goodwin, G. W., C. S. Taylor and H. Taegtmeyer (1998). "Regulation of energy metabolism of the heart during acute increase in heart work." J Biol Chem 273(45): 29530-29539.

48. Graham, D. J., R. Ouellet-Hellstrom, T. E. MaCurdy, F. Ali, C. Sholley, C. Worrall and J. A. Kelman (2010). "Risk of acute myocardial infarction, stroke, heart failure, and death in elderly Medicare patients treated with rosiglitazone or pioglitazone." JAMA 304(4): 411-418.

49. Gregor, M. F. and G. S. Hotamisligil (2007). "Thematic review series: Adipocyte Biology. Adipocyte stress: the endoplasmic reticulum and metabolic disease." J Lipid Res 48(9): 1905-1914.

50. Gregor, M. F., L. Yang, E. Fabbrini, B. S. Mohammed, J. C. Eagon, G. S. Hotamisligil and S. Klein (2009). "Endoplasmic reticulum stress is reduced in tissues of obese subjects after weight loss." Diabetes 58(3): 693-700.

51. Groenendyk, J., P. K. Sreenivasaiah, H. Kim do, L. B. Agellon and M. Michalak (2010). "Biology of endoplasmic reticulum stress in the heart." Circ Res 107(10): 1185-1197.

52. Grossman, W., D. Jones and L. P. McLaurin (1975). "Wall stress and patterns of hypertrophy in the human left ventricle." J Clin Invest 56(1): 56-64.

53. Gundewar, S., J. W. Calvert, S. Jha, I. Toedt-Pingel, S. Y. Ji, D. Nunez, A. Ramachandran, M. Anaya-Cisneros, R. Tian and D. J. Lefer (2009). "Activation of AMP-activated protein kinase by metformin improves left ventricular function and survival in heart failure." Circ Res 104(3): 403-411.

54. Gunther, S. and W. Grossman (1979). "Determinants of ventricular function in pressure-overload hypertrophy in man." Circulation 59(4): 679-688.

55. Han, D., A. G. Lerner, L. Vande Walle, J. P. Upton, W. Xu, A. Hagen, B. J. Backes, S. A. Oakes and F. R. Papa (2009). "IRE1alpha kinase activation modes control alternate endoribonuclease outputs to determine divergent cell fates." Cell 138(3): 562-575.

56. Haq, S., G. Choukroun, Z. B. Kang, H. Ranu, T. Matsui, A. Rosenzweig, J. D. Molkentin, A. Alessandrini, J. Woodgett, R. Hajjar, A. Michael and T. Force (2000). "Glycogen synthase kinase-3beta is a negative regulator of cardiomyocyte hypertrophy." J Cell Biol 151(1): 117-130.

57. Harmancey, R., C. R. Wilson, N. R. Wright and H. Taegtmeyer (2010). "Western diet changes cardiac acyl-CoA composition in obese rats: a potential role for hepatic lipogenesis." J Lipid Res 51(6): 1380-1393.

58. Hill, J. A., M. Karimi, W. Kutschke, R. L. Davisson, K. Zimmerman, Z. Wang, R. E. Kerber and R. M. Weiss (2000). "Cardiac hypertrophy is not a required compensatory response to short-term pressure overload." Circulation 101(24): 2863-2869.

59. Hill, J. A. and E. N. Olson (2008). "Cardiac plasticity." N Engl J Med 358(13): 1370-1380.

60. Holmes, F. L. (1992). Between Biology and Medicine: The Formation of Intermediary Metabolism. Berkeley, CA, University of California at Berkeley.

61. Horecker, B. L. and A. H. Mehler (1955). "Carbohydrate metabolism." Annu Rev Biochem 24: 207-274.

62. Hotamisligil, G. S. (2010). "Endoplasmic reticulum stress and the inflammatory basis of metabolic disease." Cell 140(6): 900-917.

63. Howell, J. J. and B. D. Manning (2011). "mTOR couples cellular nutrient sensing to organismal metabolic homeostasis." Trends Endocrinol Metab 22(3): 94-102.

64. Hu, Y., D. Belke, J. Suarez, E. Swanson, R. Clark, M. Hoshijima and W. H. Dillmann (2005). "Adenovirus-mediated overexpression of O-GlcNAcase improves contractile function in the diabetic heart." Circ Res 96(9): 1006-1013.

65. Huang, D., W. A. Wilson and P. J. Roach (1997). "Glucose-6-P control of glycogen synthase phosphorylation in yeast." J Biol Chem 272(36): 22495-22501.

66. Huang, J. and B. D. Manning (2008). "The TSC1-TSC2 complex: a molecular switchboard controlling cell growth." Biochem J 412(2): 179-190.

67. Huang, S. and P. J. Houghton (2003). "Targeting mTOR signaling for cancer therapy." Curr Opin Pharmacol 3(4): 371-377.

68. Huber, D., J. Grimm, R. Koch and H. P. Krayenbuehl (1981). "Determinants of ejection performance in aortic stenosis." Circulation 64(1): 126-134.

69. Hwang, Y. C., M. Kaneko, S. Bakr, H. Liao, Y. Lu, E. R. Lewis, S. Yan, S. Ii, M. Itakura, L. Rui, H. Skopicki, S. Homma, A. M. Schmidt, P. J. Oates, M. Szabolcs and R. Ramasamy (2004). "Central role for aldose reductase pathway in myocardial ischemic injury." FASEB J 18(11): 1192-1199.

70. Inoki, K., M. N. Corradetti and K. L. Guan (2005). "Dysregulation of the TSC-mTOR pathway in human disease." Nat Genet 37(1): 19-24.

71. Inoki, K., Y. Li, T. Xu and K. L. Guan (2003). "Rheb GTPase is a direct target of TSC2 GAP activity and regulates mTOR signaling." Genes Dev 17(15): 1829-1834.

72. Kato, T., S. Niizuma, Y. Inuzuka, T. Kawashima, J. Okuda, Y. Tamaki, Y. Iwanaga, M. Narazaki, T. Matsuda, T. Soga, T. Kita, T. Kimura and T. Shioi (2010). "Analysis of metabolic remodeling in compensated left ventricular hypertrophy and heart failure." Circ Heart Fail 3(3): 420-430.

73. Katz, J. and A. Dunn (1967). "Glucose-2-*t* as a tracer for glucose metabolism." Biochemistry 6: 1-5.

74. Koren, M. J., R. B. Devereux, P. N. Casale, D. D. Savage and J. H. Laragh (1991). "Relation of left ventricular mass and geometry to morbidity and mortality in uncomplicated essential hypertension." Ann Intern Med 114(5): 345-352.

75. Korvald, C., O. P. Elvenes and T. Myrmel (2000). "Myocardial substrate metabolism influences left ventricular energetics in vivo." Am J Physiol Heart Circ Physiol 278(4): H1345-1351.

76. Krayenbuehl, H. P., O. M. Hess, M. Ritter, E. S. Monrad and H. Hoppeler (1988). "Left ventricular systolic function in aortic stenosis." Eur Heart J 9 Suppl E: 19-23.

77. Krebs, H. A., Johnson, W. A. (1937). "The role of citric acid in intermediary metabolism in animal tissues." Enzymologia 4: 148-156.

78. Kroemer, G., G. Marino and B. Levine (2010). "Autophagy and the integrated stress response." Mol Cell 40(2): 280-293.

79. Kunz, J., R. Henriquez, U. Schneider, M. Deuter-Reinhard, N. R. Movva and M. N. Hall (1993). "Target of rapamycin in yeast, TOR2, is an essential phosphatidylinositol kinase homolog required for G1 progression." Cell 73(3): 585-596.

80. Lane, N. and W. Martin (2010). "The energetics of genome complexity." Nature 467(7318): 929-934.

81. Laplante, M. and D. M. Sabatini (2009). "mTOR signaling at a glance." J Cell Sci 122(Pt 20): 3589-3594.

82. Laurent, G. J. and D. J. Millward (1980). "Protein turnover during skeletal muscle hypertrophy." Fed Proc 39(1): 42-47.

83. Lee, S. H., N. Doliba, M. Osbakken, M. Oz and D. Mancini (1998). "Improvement of myocardial mitochondrial function after hemodynamic support with left ventricular assist devices in patients with heart failure." J Thorac Cardiovasc Surg 116(2): 344-349.

84. Levy, D., R. J. Garrison, D. D. Savage, W. B. Kannel and W. P. Castelli (1990). "Prognostic implications of echocardiographically determined

left ventricular mass in the Framingham Heart Study." N Engl J Med 322(22): 1561-1566.

85. Li, J., J. Huang, J. S. Li, H. Chen, K. Huang and L. Zheng (2012). "Accumulation of endoplasmic reticulum stress and lipogenesis in the liver through generational effects of high fat diets." J Hepatol 56(4): 900-907.

86. Li, M. V., W. Chen, R. N. Harmancey, A. M. Nuotio-Antar, M. Imamura, P. Saha, H. Taegtmeyer and L. Chan (2010). "Glucose-6-phosphate mediates activation of the carbohydrate responsive binding protein (ChREBP)." Biochem Biophys Res Commun 395(3): 395-400.

87. Liao, R., M. Jain, L. Cui, J. D'Agostino, F. Aiello, I. Luptak, S. Ngoy, R. M. Mortensen and R. Tian (2002). "Cardiac-specific overexpression of GLUT1 prevents the development of heart failure attributable to pressure overload in mice." Circulation 106(16): 2125-2131.

88. Liao, Y., S. Takashima, Y. Asano, M. Asakura, A. Ogai, Y. Shintani, T. Minamino, H. Asanuma, S. Sanada, J. Kim, H. Ogita, H. Tomoike, M. Hori and M. Kitakaze (2003). "Activation of adenosine A1 receptor attenuates cardiac hypertrophy and prevents heart failure in murine left ventricular pressure-overload model." Circ Res 93(8): 759-766.

89. Lincoff, A. M., K. Wolski, S. J. Nicholls and S. E. Nissen (2007). "Pioglitazone and risk of cardiovascular events in patients with type 2 diabetes mellitus: a meta-analysis of randomized trials." JAMA 298(10): 1180-1188.

90. Liu, L., S. Yu, R. S. Khan, G. P. Ables, K. G. Bharadwaj, Y. Hu, L. A. Huggins, J. W. Eriksson, L. K. Buckett, A. V. Turnbull, H. N. Ginsberg, W. S. Blaner, L. S. Huang and I. J. Goldberg (2011). "DGAT1 deficiency decreases PPAR expression and does not lead to lipotoxicity in cardiac and skeletal muscle." J Lipid Res 52(4): 732-744.

91. Long, X., S. Ortiz-Vega, Y. Lin and J. Avruch (2005). "Rheb binding to mammalian target of rapamycin (mTOR) is regulated by amino acid sufficiency." J Biol Chem 280(25): 23433-23436.

92. Louvet, C., G. L. Szot, J. Lang, M. R. Lee, N. Martinier, G. Bollag, S. Zhu, A. Weiss and J. A. Bluestone (2008). "Tyrosine kinase inhibitors reverse type 1 diabetes in nonobese diabetic mice." Proc Natl Acad Sci U S A 105(48): 18895-18900.

93. Maloyan, A., H. Osinska, J. Lammerding, R. T. Lee, O. H. Cingolani, D. A. Kass, J. N. Lorenz and J. Robbins (2009). "Biochemical and mechanical dysfunction in a mouse model of desmin-related myopathy." Circ Res 104(8): 1021-1028.

94. Mann, D. L. (1999). "Mechanisms and models in heart failure: A combinatorial approach." Circulation 100(9): 999-1008.

95. Margulies, K. B., S. Matiwala, C. Cornejo, H. Olsen, W. A. Craven and D. Bednarik (2005). "Mixed messages: transcription patterns in failing and recovering human myocardium." Circ Res 96(5): 592-599.

96. Marin, T. M., K. Keith, B. Davies, D. A. Conner, P. Guha, D. Kalaitzidis, X. Wu, J. Lauriol, B. Wang, M. Bauer, R. Bronson, K. G.

Franchini, B. G. Neel and M. I. Kontaridis (2011). "Rapamycin reverses hypertrophic cardiomyopathy in a mouse model of LEOPARD syndrome-associated PTPN11 mutation." J Clin Invest 121(3): 1026-1043.

97. Mathew, J., P. Sleight, E. Lonn, D. Johnstone, J. Pogue, Q. Yi, J. Bosch, B. Sussex, J. Probstfield and S. Yusuf (2001). "Reduction of cardiovascular risk by regression of electrocardiographic markers of left ventricular hypertrophy by the angiotensin-converting enzyme inhibitor ramipril." Circulation 104(14): 1615-1621.

98. Mayer, C. and I. Grummt (2006). "Ribosome biogenesis and cell growth: mTOR coordinates transcription by all three classes of nuclear RNA polymerases." Oncogene 25(48): 6384-6391.

99. McClain, D. A. (2002). "Hexosamines as mediators of nutrient sensing and regulation in diabetes." Diabetes Complications 16(1): 72-80.

100. McMullen, J. R., M. C. Sherwood, O. Tarnavski, L. Zhang, A. L. Dorfman, T. Shioi and S. Izumo (2004). "Inhibition of mTOR signaling with rapamycin regresses established cardiac hypertrophy induced by pressure overload." Circulation 109(24): 3050-3055.

101. Modesti, A., I. Bertolozzi, T. Gamberi, M. Marchetta, C. Lumachi, M. Coppo, F. Moroni, T. Toscano, G. Lucchese, G. F. Gensini and P. A. Modesti (2005). "Hyperglycemia activates JAK2 signaling pathway in human failing myocytes via angiotensin II-mediated oxidative stress." Diabetes 54(2): 394-401.

102. Molkentin, J. D. and G. W. Dorn (2001). "Cytoplasmic signaling pathyways that regulate cardiac hypertrophy." Annu Rev Physiol 63: 391-426.

103. Nascimben, L., J. S. Ingwall, B. H. Lorell, I. Pinz, V. Schultz, K. Tornheim and R. Tian (2004). "Mechanisms for increased glycolysis in the hypertrophied rat heart." Hypertension 44(5): 662-667.

104. Neely, J. R., R. M. Denton, P. J. England and P. J. Randle (1972). "The effects of increased heart work on the tricarboxylate cycle and its interactions with glycolysis in the perfused rat heart." Biochem J 128(1): 147-159.

105. Neely, J. R., H. Liebermeister and H. E. Morgan (1967). "Effect of pressure development on membrane transport of glucose in isolated rat heart." Am J Physiol 212(4): 815-822.

106. Neubauer, S. (2007). "The failing heart--an engine out of fuel." N Engl J Med 356(11): 1140-1151.

107. Nguyen, V. T., K. A. Mossberg, T. J. Tewson, W. H. Wong, R. W. Rowe, G. M. Coleman and H. Taegtmeyer (1990). "Temporal analysis of myocardial glucose metabolism by 2-[18F]fluoro-2-deoxy-D-glucose." Am J Physiol 259(4 Pt 2): H1022-1031.

108. Nishimura, M. and K. Uyeda (1995). "Purification and characterization of a novel xylulose 5-phosphate-activated protein phosphatase catalyzing dephosphorylation of fructose-6-phosphate,2-kinase:fructose-2,6-bisphosphatase." J Biol Chem 270(44): 26341-26346.

109. Okada, K., T. Minamino, Y. Tsukamoto, Y. Liao, O. Tsukamoto, S. Takashima, A. Hirata, M. Fujita, Y. Nagamachi, T. Nakatani, C. Yutani, K. Ozawa, S. Ogawa, H. Tomoike, M. Hori and M. Kitakaze (2004). "Prolonged endoplasmic reticulum stress in hypertrophic and failing heart after aortic constriction: possible contribution of endoplasmic reticulum stress to cardiac myocyte apoptosis." Circulation 110(6): 705-712.

110. Osterholt, M., S. Sen, V. Dilsizian and H. Taegtmeyer (2012). "Targeted metabolic imaging to improve the management of heart disease." JACC Cardiovasc Imaging 5(2): 214-226.

111. Owan, T., E. Avelar, K. Morley, R. Jiji, N. Hall, J. Krezowski, J. Gallagher, Z. Williams, K. Preece, N. Gundersen, M. B. Strong, R. C. Pendleton, N. Segerson, T. V. Cloward, J. M. Walker, R. J. Farney, R. E. Gress, T. D. Adams, S. C. Hunt and S. E. Litwin (2011). "Favorable changes in cardiac geometry and function following gastric bypass surgery: 2-year follow-up in the Utah obesity study." J Am Coll Cardiol 57(6): 732-739.

112. Ozcan, U., L. Ozcan, E. Yilmaz, K. Duvel, M. Sahin, B. D. Manning and G. S. Hotamisligil (2008). "Loss of the tuberous sclerosis complex tumor suppressors triggers the unfolded protein response to regulate insulin signaling and apoptosis." Mol Cell 29(5): 541-551.

113. Ozcan, U., E. Yilmaz, L. Ozcan, M. Furuhashi, E. Vaillancourt, R. O. Smith, C. Z. Gorgun and G. S. Hotamisligil (2006). "Chemical

chaperones reduce ER stress and restore glucose homeostasis in a mouse model of type 2 diabetes." Science 313(5790): 1137-1140.

114. Powell, J. D. and G. M. Delgoffe (2010). "The mammalian target of rapamycin: linking T cell differentiation, function, and metabolism." Immunity 33(3): 301-311.

115. Proud, C. G. (2002). "Regulation of mammalian translation factors by nutrients." Eur J Biochem 269: 5338-5349.

116. Rajabi, M., C. Kassiotis, P. Razeghi and H. Taegtmeyer (2007). "Return to the fetal gene program protects the stressed heart: a strong hypothesis." Heart Fail Rev 12(3-4): 331-343.

117. Razeghi, P., T. J. Myers, O. H. Frazier and H. Taegtmeyer (2002). "Reverse remodeling of the failing human heart with mechanical unloading. Emerging concepts and unanswered questions." Cardiology 98(4): 167-174.

118. Razeghi, P. and H. Taegtmeyer (2004). "Activity of the Akt/GSK-3beta pathway in the failing human heart before and after left ventricular assist device support." Cardiovasc Res 61(1): 196-197; author reply 198-199.

119. Razeghi, P., M. E. Young, J. L. Alcorn, C. S. Moravec, O. H. Frazier and H. Taegtmeyer (2001). "Metabolic gene expression in fetal and failing human heart." Circulation 104(24): 2923-2931.

120. Razeghi, P., M. E. Young, J. Ying, C. Depre, I. P. Uray, J. Kolesar, G. L. Shipley, C. S. Moravec, P. J. Davies, O. H. Frazier and H. Taegtmeyer (2002). "Downregulation of metabolic gene expression in failing human

heart before and after mechanical unloading." Cardiology 97(4): 203-209.

121. Ren, J. and A. J. Davidoff (1997). "Diabetes rapidly induces contractile dysfunctions in isolated ventricular myocytes." Am J Physiol 272(1 Pt 2): H148-158.

122. Rider, O. J., J. M. Francis, M. K. Ali, S. E. Petersen, M. Robinson, M. D. Robson, J. P. Byrne, K. Clarke and S. Neubauer (2009). "Beneficial cardiovascular effects of bariatric surgical and dietary weight loss in obesity." J Am Coll Cardiol 54(8): 718-726.

123. Riquelme, C. A., J. A. Magida, B. C. Harrison, C. E. Wall, T. G. Marr, S. M. Secor and L. A. Leinwand (2011). "Fatty acids identified in the Burmese python promote beneficial cardiac growth." Science 334(6055): 528-531.

124. Rockman, H., R. Ross, A. Harris, K. Knowlton, M. Steinhelper, L. Field, J. Ross and K. Chien (1991). "Segregation of atrial-specific and inducible expression of an atrial natriuretic factor transgene in an in vivo murine model of cardiac hypertrophy." Proc Natl Acad Sci USA 88: 8277-8281.

125. Roger, V. L., A. S. Go, D. M. Lloyd-Jones, R. J. Adams, J. D. Berry, T. M. Brown, M. R. Carnethon, S. Dai, G. de Simone, E. S. Ford, C. S. Fox, H. J. Fullerton, C. Gillespie, K. J. Greenlund, S. M. Hailpern, J. A. Heit, P. M. Ho, V. J. Howard, B. M. Kissela, S. J. Kittner, D. T. Lackland, J. H. Lichtman, L. D. Lisabeth, D. M. Makuc, G. M. Marcus,

A. Marelli, D. B. Matchar, M. M. McDermott, J. B. Meigs, C. S. Moy, D. Mozaffarian, M. E. Mussolino, G. Nichol, N. P. Paynter, W. D. Rosamond, P. D. Sorlie, R. S. Stafford, T. N. Turan, M. B. Turner, N. D. Wong and J. Wylie-Rosett (2011). "Heart disease and stroke statistics--2011 update: a report from the American Heart Association." Circulation 123(4): e18-e209.

126. Rohde, J., J. Heitman and M. E. Cardenas (2001). "The TOR kinases link nutrient sensing to cell growth." J Biol Chem 276(13): 9583-9586.

127. Ron, D. and P. Walter (2007). "Signal integration in the endoplasmic reticulum unfolded protein response." Nat Rev Mol Cell Biol 8(7): 519-529.

128. Rose, E. A., A. C. Gelijns, A. J. Moskowitz, D. F. Heitjan, L. W. Stevenson, W. Dembitsky, J. W. Long, D. D. Ascheim, A. R. Tierney, R. G. Levitan, J. T. Watson, P. Meier, N. S. Ronan, P. A. Shapiro, R. M. Lazar, L. W. Miller, L. Gupta, O. H. Frazier, P. Desvigne-Nickens, M. C. Oz and V. L. Poirier (2001). "Long-term use of a left ventricular assist device for end-stage heart failure." N Engl J Med 345(20): 1435-1443.

129. Rubenstein, R. C. and P. L. Zeitlin (1998). "A pilot clinical trial of oral sodium 4-phenylbutyrate (Buphenyl) in deltaF508-homozygous cystic fibrosis patients: partial restoration of nasal epithelial CFTR function." Am J Respir Crit Care Med 157(2): 484-490.

130. Saha, A. K., X. J. Xu, E. Lawson, R. Deoliveira, A. E. Brandon, E. W. Kraegen and N. B. Ruderman (2010). "Downregulation of AMPK accompanies leucine- and glucose-induced increases in protein synthesis and insulin resistance in rat skeletal muscle." Diabetes 59(10): 2426-2434.

131. Sanbe, A., H. Osinska, C. Villa, J. Gulick, R. Klevitsky, C. G. Glabe, R. Kayed and J. Robbins (2005). "Reversal of amyloid-induced heart disease in desmin-related cardiomyopathy." Proc Natl Acad Sci U S A 102(38): 13592-13597.

132. Sancak, Y., L. Bar-Peled, R. Zoncu, A. L. Markhard, S. Nada and D. M. Sabatini (2010). "Ragulator-Rag complex targets mTORC1 to the lysosomal surface and is necessary for its activation by amino acids." Cell 141(2): 290-303.

133. Sancak, Y., T. R. Peterson, Y. D. Shaul, R. A. Lindquist, C. C. Thoreen, L. Bar-Peled and D. M. Sabatini (2008). "The Rag GTPases bind raptor and mediate amino acid signaling to mTORC1." Science 320(5882): 1496-1501.

134. Sandler, H. and H. T. Dodge (1963). "Left Ventricular Tension and Stress in Man." Circ Res 13: 91-104.

135. Sandler, H., H. T. Dodge, R. E. Hay and C. E. Rackley (1963). "Quantitation of valvular insufficiency in man by angiocardiography." Am Heart J 65: 501-513.

136. Sarbassov, D. D., S. M. Ali, S. Sengupta, J. H. Sheen, P. P. Hsu, A. F. Bagley, A. L. Markhard and D. M. Sabatini (2006). "Prolonged rapamycin treatment inhibits mTORC2 assembly and Akt/PKB." Mol Cell 22(2): 159-168.

137. Schmelzle, T. and M. N. Hall (2000). "TOR, a central controller of cell growth." Cell 103(2): 253-262.

138. Schuit, F. C., P. Huypens, H. Heimberg and D. G. Pipeleers (2001). "Glucose sensing in pancreatic beta-cells: a model for the study of other glucose-regulated cells in gut, pancreas, and hypothalamu." Diabetes 50(1): 1-11.

139. Sengupta, S., T. R. Peterson and D. M. Sabatini (2010). "Regulation of the mTOR complex 1 pathway by nutrients, growth factors, and stress." Mol Cell 40(2): 310-322.

140. Sharma, S., P. H. Guthrie, S. S. Chan, S. Haq and H. Taegtmeyer (2007). "Glucose phosphorylation is required for insulin-dependent mTOR signalling in the heart." Cardiovasc Res 76: 71-80.

141. Shaw, R. J., N. Bardeesy, B. D. Manning, L. Lopez, M. Kosmatka, R. A. DePinho and L. C. Cantley (2004). "The LKB1 tumor suppressor negatively regulates mTOR signaling." Cancer Cell 6(1): 91-99.

142. Shioi, T., J. R. McMullen, O. Tarnavski, K. Converso, M. C. Sherwood, W. J. Manning and S. Izumo (2003). "Rapamycin attenuates load-induced cardiac hypertrophy in mice." Circulation 107(12): 1664-1670.

143. Steenman, M., Y. W. Chen, M. Le Cunff, G. Lamirault, A. Varro, E. Hoffman and J. J. Leger (2003). "Transcriptomal analysis of failing and nonfailing human hearts." Physiol Genomics 12(2): 97-112.

144. Suarez, J., B. Gloss, D. D. Belke, Y. Hu, B. Scott, T. Dieterle, Y. K. Kim, M. L. Valencik, J. A. McDonald and W. H. Dillmann (2004). "Doxycycline inducible expression of SERCA2a improves calcium handling and reverts cardiac dysfunction in pressure overload-induced cardiac hypertrophy." Am J Physiol Heart Circ Physiol 287(5): H2164-2172.

145. Taegtmeyer, H. (1985). "On the role of the purine nucleotide cycle in the isolated working rat heart." J Mol Cell Cardiol 17(10): 1013-1018.

146. Taegtmeyer, H. (1994). "Energy metabolism of the heart: from basic concepts to clinical applications." Curr Prob Cardiol 19: 57-116.

147. Taegtmeyer, H., L. Golfman, S. Sharma, P. Razeghi and M. van Arsdall (2004). "Linking gene expression to function: metabolic flexibility in the normal and diseased heart." Ann N Y Acad Sci 1015: 202-213.

148. Taegtmeyer, H., R. Hems and H. A. Krebs (1980). "Utilization of energy-providing substrates in the isolated working rat heart." Biochem J. 3: 186-194

149. Taegtmeyer, H., P. McNulty and M. E. Young (2002). "Adaptation and maladaptation of the heart in diabetes: Part I: general concepts." Circulation 105(14): 1727-1733.

150. Taegtmeyer, H. and M. L. Overturf (1988). "Effects of moderate hypertension on cardiac function and metabolism in the rabbit." Hypertension 11: 416-426.

151. Taegtmeyer, H. and M. L. Overturf (1988). "Effects of moderate hypertension on cardiac function and metabolism in the rabbit." Hypertension 11(5): 416-426.

152. Takagi, H., Y. Matsui and J. Sadoshima (2007). "The role of autophagy in mediating cell survival and death during ischemia and reperfusion in the heart." Antioxid Redox Signal 9(9): 1373-1381.

153. Tang, W. H., W. T. Cheng, G. M. Kravtsov, X. Y. Tong, X. Y. Hou, S. K. Chung and S. S. Chung (2010). "Cardiac contractile dysfunction during acute hyperglycemia due to impairment of SERCA by polyol pathway-mediated oxidative stress." Am J Physiol Cell Physiol 299(3): C643-653.

154. Tee, A. R., R. Anjum and J. Blenis (2003). "Inactivation of the tuberous sclerosis complex-1 and -2 gene products occurs by phosphoinositide 3-kinase/Akt-dependent and -independent phosphorylation of tuberin." J Biol Chem 278(39): 37288-37296.

155. Terai, K., Y. Hiramoto, M. Masaki, S. Sugiyama, T. Kuroda, M. Hori, I. Kawase and H. Hirota (2005). "AMP-activated protein kinase protects cardiomyocytes against hypoxic injury through attenuation of endoplasmic reticulum stress." Mol Cell Biol 25(21): 9554-9575.

156. Thuerauf, D. J., H. Hoover, J. Meller, J. Hernandez, L. Su, C. Andrews, W. H. Dillmann, P. M. McDonough and C. C. Glembotski (2001). "Sarco/endoplasmic reticulum calcium ATPase-2 expression is regulated by ATF6 during the endoplasmic reticulum stress response: intracellular signaling of calcium stress in a cardiac myocyte model system." J Biol Chem 276(51): 48309-48317.

157. Thuerauf, D. J., M. Marcinko, N. Gude, M. Rubio, M. A. Sussman and C. C. Glembotski (2006). "Activation of the unfolded protein response in infarcted mouse heart and hypoxic cultured cardiac myocytes." Circ Res 99(3): 275-282.

158. Topisirovic, I. and N. Sonenberg (2010). "Cell biology. Burn out or fade away?" Science 327(5970): 1210-1211.

159. Vinnakota, K. C. and J. B. Bassingthwaighte (2004). "Myocardial density and composition: a basis for calculating intracellular metabolite concentrations." Am J Physiol Heart Circ Physiol 286(5): H1742-1749.

160. Wallhaus, T. R., M. Taylor, T. R. DeGrado, D. C. Russell, P. Stanko, R. J. Nickles and C. K. Stone (2001). "Myocardial free fatty acid and glucose use after carvedilol treatment in patients with congestive heart failure." Circulation 103(20): 2441-2446.

161. Wang, X. F., J. Y. Zhang, L. Li, X. Y. Zhao, H. L. Tao and L. Zhang (2011). "Metformin improves cardiac function in rats via activation of AMP-activated protein kinase." Clin Exp Pharmacol Physiol 38(2): 94-101.

162. Waterlow, J. C. (1984). "Protein turnover with special reference to man." Q J Exp Physiol 69(3): 409-438.

163. Watson, L. J., H. T. Facundo, G. A. Ngoh, M. Ameen, R. E. Brainard, K. M. Lemma, B. W. Long, S. D. Prabhu, Y. T. Xuan and S. P. Jones (2010). "O-linked beta-N-acetylglucosamine transferase is indispensable in the failing heart." Proc Natl Acad Sci U S A 107(41): 17797-17802.

164. Wheeler, T. J., R. D. Fell and M. A. Hauck (1994). "Translocation of two glucose transporters in heart: effects of rotenone, uncouplers, workload, palmitate, insulin and anoxia." Biochim Biophys Acta 1196: 191-200.

165. Wisneski, J. A., E. W. Gertz, R. A. Neese and M. Mayr (1987). "Myocardial metabolism of free fatty acids. Studies with 14C-labeled substrates in humans." J Clin Invest 79(2): 359-366.

166. Wollenberger, A. and W. Schulze (1961). "Mitochondrial alterations in the myocardium of dogs with aortic stenosis." J Biophys Biochem Cytol 10: 285.

167. Yeh, C. H., T. P. Chen, Y. C. Wang, Y. M. Lin and S. W. Fang (2010). "AMP-activated protein kinase activation during cardioplegia-induced hypoxia/reoxygenation injury attenuates cardiomyocytic apoptosis via reduction of endoplasmic reticulum stress." Mediators Inflamm 2010: 130636.

168. Yin, M., I. C. van der Horst, J. P. van Melle, C. Qian, W. H. van Gilst, H. H. Sillje and R. A. de Boer (2011). "Metformin improves cardiac

function in a nondiabetic rat model of post-MI heart failure." Am J Physiol Heart Circ Physiol 301(2): H459-468.

169. Yip, C. K., K. Murata, T. Walz, D. M. Sabatini and S. A. Kang (2010). "Structure of the human mTOR complex I and its implications for rapamycin inhibition." Mol Cell 38(5): 768-774.

170. Young, L. H., J. Li, S. J. Baron and R. R. Russell (2005). "AMP-activated protein kinase: a key stress signaling pathway in the heart." Trends Cardiovasc Med 15(3): 110-118.

171. Young, M. E., Z. Yan, P. Razeghi, R. C. Cooksey, P. H. Guthrie, S. M. Stepkowski, D. A. McClain, R. Tian and H. Taegtmeyer (2007). "Proposed regulation of gene expression by glucose in rodent heart." Gene Reg Systems Biol 1: 251-262.

172. Yusuf, S., P. Sleight, J. Pogue, J. Bosch, R. Davies and G. Dagenais (2000). "Effects of an angiotensin-converting-enzyme inhibitor, ramipril, on cardiovascular events in high-risk patients. The Heart Outcomes Prevention Evaluation Study Investigators." N Engl J Med 342(3): 145-153.

173. Zeng, Z., D. Sarbassov dos, I. J. Samudio, K. W. Yee, M. F. Munsell, C. Ellen Jackson, F. J. Giles, D. M. Sabatini, M. Andreeff and M. Konopleva (2007). "Rapamycin derivatives reduce mTORC2 signaling and inhibit AKT activation in AML." Blood 109(8): 3509-3512.

174. Zhang, D., R. Contu, M. V. Latronico, J. Zhang, R. Rizzi, D. Catalucci, S. Miyamoto, K. Huang, M. Ceci, Y. Gu, N. D. Dalton, K. L. Peterson,

K. L. Guan, J. H. Brown, J. Chen, N. Sonenberg and G. Condorelli (2010). "MTORC1 regulates cardiac function and myocyte survival through 4E-BP1 inhibition in mice." J Clin Invest 120(8): 2805-2816.

175. Zhang, J., D. J. Duncker, X. Ya, Y. Zhang, T. Pavek, H. Wei, H. Merkle, K. Ugurbil, A. H. From and R. J. Bache (1995). "Effect of left ventricular hypertrophy secondary to chronic pressure overload on transmural myocardial 2-deoxyglucose uptake. A 31P NMR spectroscopic study." Circulation 92(5): 1274-1283.

176. Zhang, L., Y. Lu, H. Jiang, A. Sun, Y. Zou and J. Ge (2012). "Additional use of trimetazidine in patients with chronic heart failure: a meta-analysis." J Am Coll Cardiol 59(10): 913-922.

177. Zhu, Q. S., K. Rosenblatt, K. L. Huang, G. Lahat, R. Brobey, S. Bolshakov, T. Nguyen, Z. Ding, R. Belousov, K. Bill, X. Luo, A. Lazar, A. Dicker, G. B. Mills, M. C. Hung and D. Lev (2011). "Vimentin is a novel AKT1 target mediating motility and invasion." Oncogene 30(4): 457-470.

178. Zimmer, H. G. (1992). "The oxidative pentose phosphate pathway in the heart: Regulation, physiological significance, and clinical implications." Basic Res Cardiol 87: 303-316.

179. Zoncu, R., A. Efeyan and D. M. Sabatini (2011). "mTOR: from growth signal integration to cancer, diabetes and ageing." Nat Rev Mol Cell Biol 12(1): 21-35.

VITA

Shiraj Sen was born in Houston, Texas on July 21, 1983, the son of Subrata Sen and Pramila Sen. After completing high school at William P. Clements High School in Sugar Land, Texas in 2001, he entered the University of Texas at Austin. He received the degree of Bachelor of Arts with a major in the Plan II Honors Program in May, 2005. In June of 2005, he entered the MD/PhD Program at The University of Texas Medical School at Houston. He completed three years of medical school before beginning his PhD studies at The University of Texas Health Science Center at Houston Graduate School of Biomedical Sciences. He will graduate in May 2012 and begin internal medicine residency at The University of Texas Southwestern in July 2012.

Permanent address:
17430 Marigold Drive

Sugar Land, TX 77479